Analysis of transcriptomic changes that occur following loss of DARPP-32 expression in breast cancer

Sarah Storr PhD

Submitted to the University of Nottingham

for the degree of MRes Bioinformatics, 2022

1 Contents

2 Abstract 4

3 Introduction 6

3.1 The discovery of DARPP-32 7

3.2 DARPP-32 and gastric cancer 8

3.3 DARPP-32 and breast cancer 9

3.4 DARPP-32 and lung cancer 11

3.5 DARPP-32 in other tumour types 11

3.6 Summary 12

4 Hypothesis 13

5 Objectives 14

5.1 Objective 1 14

5.2 Objective 2 14

5.3 Objective 3 14

6 Methods 15

6.1 DARPP-32 knockdown and treatments 15

6.2 RNA-Seq 15

6.3 Quality control 16

6.4 Pseudoalignment and quantification 16

6.5 Differential transcript expression 17

6.6 Gene overrepresentation analysis 17

6.7 METABRIC data 18

7 Results 20

7.1 DARPP-32 knockdown 20

7.2 Quality control 21

7.3 DESeq2 22

7.4 DARPP-32 signalling partners in DARPP-32 knockdown cells 36

7.5 DARPP-32 signalling partners and E2 stimulation 37

7.6 DARPP-32 signalling partners and PKA inhibition 43

7.7 Pathway analyses 46

7.8 Alternate pathway assessments 57

7.9 Correlations between signalling partners and DARPP-32 in breast cancer 57

7.10 Associations between signalling partners and patient survival 59

8 Discussion 62

9 Conclusion 69

10 Future work 70

11 References 71
12 Acknowledgements 78
13 Appendix 79
13.1 Appendix 1 79
13.2 Appendix 2 80
13.3 Appendix 3 81

2 Abstract

Background

Breast cancer is the most common cancer in the UK, with >55,000 new cases per annum and >11,500 deaths, with metastasis the major cause of mortality. Since the early 1990s, the incidence of breast cancer has increased by 18% in the UK with cases predicted to rise 2% between 2014 and 2035. The molecular basis that underpins cancer progression and metastasis is complex and presents an important research challenge. Dopamine and cAMP-regulated protein phosphatase (DARPP-32) is a central signalling switch in the brain and the consequence of altered phosphorylation has been extensively studied. In breast cancer, we have demonstrated that low expression of DARPP-32 is associated with poor clinical outcome of patients; however, the mechanism by which DARPP-32 exerts this effect remains unclear.

Methods

DARPP-32 expression was reduced in oestrogen receptor positive luminal B breast cancer cells (T47D) using siRNA, and both DARPP-32 knockdown T47D cells, negative control siRNA treated control T47D cells were subject to stimulation with estradiol17β (E2) or inhibition of protein kinase A (PKA) with PKA inhibitor fragment (6-22) amide prior to RNA sequencing. A bioinformatics pipeline of Trim Galore, Kallisto, DESeq2 was utilised and pathway overrepresentation analysis was performed using Qiagen Ingenuity Pathway Analysis software.

Results

A reduction in DARPP-32 expression resulted in the differential expression of 202 transcripts, with the top 10 downregulated genes being *CLN8*, *GRAMD2B*, *HNRNPC*, *ZCCHC7*, *CMIP*, *OSBPL2*, *TSEN34*, *MAN2C1*, *NDUFS1*, and *MAP2* and the top 10 upregulated genes being *KBTBD11*, *ZNF230*, *BCL2L11*, *ZNF227*, *VKORC1L1*, *C19orf25*, *TSEN35*, *SART3*, *AAGAB* and *CHEK2*. 42641 differentially expressed transcripts were identified following E2 stimulation of DARPP-32 knockdown cells, 40065 differentially expressed transcripts were identified when control cells were stimulated with E2, and 193 differentially expressed transcripts were identified when DARPP-32 knockdown cells were compared with control cells, when both were subject to E2 stimulation. When DARPP-32 knockdown cells and control cells were both treated with E2, the top 10 downregulated genes were *BCLAF1*, *NEDD4L*, *MAGEA3*, *RBCK1*, *PTBP1*, *GON7*, *PBX3*, *TXLNA*, and *METTL8* and the top 10 upregulated genes were *CTDSPL*, *ARMC1*, *FGFR3*, *G3BP1*, *TNRC6A*, *EIF3L*, *CDKN1C*, *PUF60*, *BMPR1B*, and *SLC16A7.*

When a PKA inhibitor was used to treat DARPP-32 knockdown cells and/or control cells, 1155 differentially expressed transcripts were identified in DARPP-32 knockdown cells when treated with PKAi, 1704 differentially expressed transcripts were identified when control cells were treated with PKAi, and 181 differentially identified transcripts were identified when DARPP-32 knockdown cells were compared with control cells, when both were subject to PKA inhibition.

Conclusions

The transcriptomic changes resultant from DARPP-32 knockdown in ER positive breast cancer cells have been determined, with and without E2 stimulation and PKA inhibition. These changes identify that DARPP-32 functions as an important partner in many cancer-associated signalling pathways that have been linked with poor prognosis and clinical outcome of breast cancer patients.

3 Introduction

Breast cancer is the most common cancer in the UK, with >55,000 new cases per annum. Since the early 1990s, the incidence of breast cancer has increased by 18% in the UK with cases predicted to rise 2% between 2014 and 2035. In the UK, there are >11,500 deaths per annum, with metastasis the major cause of mortality (Cancer Research UK). Breast cancer is a heterogeneous disease, with many genes involved in modulating cell growth, death, differentiation, and response to anti-cancer treatments. Whilst many genes have been associated with the prognosis of breast cancer, expression of some genes have a direct implication on the clinical management of breast cancer; a classic exemplar of this is oestrogen receptor (ER), occurring in 70% of breast cancers. Patients with ER positive tumours can receive hormone therapies, including selective ER modulators (i.e., tamoxifen), selective ER downregulators (i.e., fulvestrant), and aromatase inhibitors (i.e. anastrozole, letrozole, exemestane). ER is a member of the nuclear receptor superfamily and functions as a transcription factor capable of binding oestrogen response elements and is responsible for the regulation of the expression of genes involved in cell division; over three quarters of all breast cancers express ER (reviewed in (1)). In the ER positive breast cancer cell line, MCF-7 thousands of unique ER binding sites have been identified (2, 3). In addition to direct regulation of gene expression, ER can regulate gene expression through binding other DNA-binding transcription factors within the nucleus (reviewed in (4)).

Clinical management tools are also available for ER positive (and human epidermal growth factor receptor-2 (HER2 or *ERBB2*) negative) patients, such as the Oncotype DX Recurrence Score that utilises a 21 gene signature to predict a patient's response to chemotherapy, or PAM50 (Prosigna), that utilises a 50 gene signature. Gene expression profiling to understand breast cancer heterogeneity has detailed six principal molecular phenotypes, luminal subtype A, luminal subtype B, luminal subtype C, basal-like, *ERBB2* overexpressing, and normal breast-like, with distinct clinical outcomes in a seminal publication from 2001 (5); luminal subgroups are largely ER positive.

The molecular basis that underpins cancer progression and metastasis is complex and presents an important research challenge. Research from our group has identified that DARPP-32 (dopamine and cAMP regulated phosphoprotein 32kDa), also known as phospho-protein phosphatase regulatory subunit 1B and encoded by *PPP1R1B* is an important biomarker in breast cancer at both the protein and mRNA level in large cohorts of patients (6); it is unclear how DARPP-32 is able to modulate cancer cell behaviour.

3.1 The discovery of DARPP-32

DARPP-32 was originally described in a series of publications nearly 40 years ago, expressed in dopamine innervated brain regions and being highly concentrated in the basal ganglia (7-9). Initially DARPP-32 was described as a potent inhibitor of protein-phosphatase-1 (PP-1) (10); and this was quickly demonstrated to be dependent on the phosphorylation status of DARPP-32 (11), mediated through cyclic adenosine monophosphate (cAMP)-dependent protein kinase (PKA). cAMP is an influential second messenger with a myriad of important roles in cellular function and pathology; cAMP can regulate transcription of many genes, principally through PKA and its downstream effectors, such as the transcription factor, cAMP-responsive element binding protein (CREB). DARPP-32 is now known to play a central role in regulating both biochemical and electrophysical roles to both physiological and pharmacological stimuli. Dopamine and numerous other neurotransmitters have been shown to regulate DARPP-32 phosphorylation, this can also be modulated by drugs of abuse, including cocaine and nicotine (reviewed in (12)).

The cellular effects of DARPP-32 are now known to be modulated by several phosphorylation events, with the principal DARPP-32 phosphorylation sites being Threonine-34 and Threonine-75; DARPP-32 can act as a bifunctional signalling protein acting as a kinase or a phosphatase inhibitor. Phosphorylation of DARPP-32 at Thr-34 by PKA allows DARPP-32 to act as a potent inhibitor of PP-1; whereas phosphorylation of DARPP-32 at Thr-75 by cyclin-dependent kinase 5 (Cdk5) allows DARPP-32 to inhibit PKA (13) (Figure 3-1). Further complexity is provided through dephosphorylation at Thr-34 by calcineurin (PP2B) and dephosphorylation of Thr-75 by protein phosphatase-2A (14).

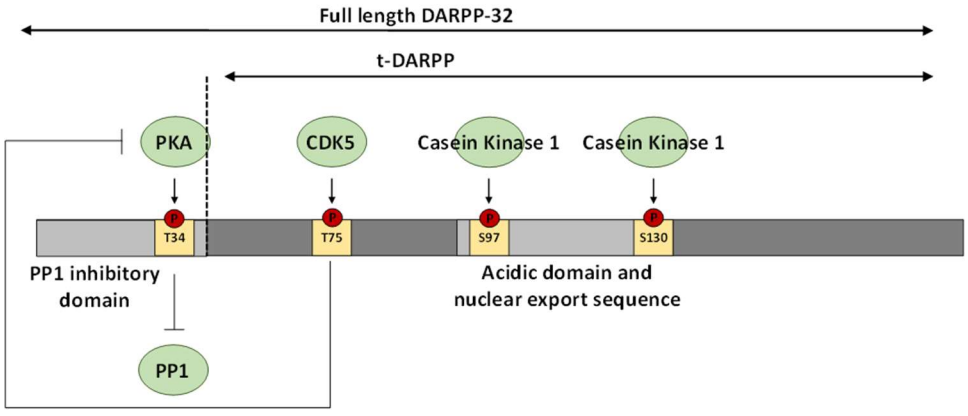


Figure 3-1: DARPP-32 and t-DARPP; phosphorylation sites are shown with kinases responsible. Protein domains are indicated, including the PP1 inhibitory domain and the acidic domain that contains the nuclear export sequence.

DARPP-32 is an established molecular switch within the brain; a role for DARPP-32 in cancer is now being explored. A novel, cancer specific, splice variant, truncated-DARPP (t-DARPP), was first described in gastric cancer in 2002; importantly, t-DARPP lacks the Thr-34 phosphorylation site (15) (Figure 3-1). The expression of both DARPP-32 and t-DARPP were found to be overexpressed in gastric cancers in comparison to normal gastric epithelium (15). This was closely followed by research that demonstrated DARPP-32 was expressed at a higher levels breast, prostate, colon, and stomach cancer tissue when compared with normal tissue, with these tumours also expressing t-DARPP (16, 17). In 2004, DARPP-32 expression was shown to arise after a phase of dysplasia in oesophageal squamous cell carcinomas, and that tumours with DARPP-32 expression progressed less rapidly that those that did not express DARPP-32 (18). Small scale studies emerged over subsequent years, investigating the expression of DARPP-32 and t-DARPP in various tumour types and exploring potential relationship with clinicopathological criteria of patients; however, these studies were often small in scale and did not assess the relationship between DARPP-32 expression and patient survival. Most research on DARPP-32 and t-DARPP has focussed on gastric, breast, and more recently lung cancer, which will be discussed in depth.

3.2 DARPP-32 and gastric cancer

The truncated DARPP-32 variant, t-DARPP, was first described in gastric cancer, with t-DARPP subsequently described in numerous other tumour types (15). DARPP-32 expression has been investigated in normal, gastritis to metaplasia, dysplasia and adenocarcinoma specimens to demonstrate increasing DARPP-32 expression through the transition from intestinal metaplasia to neoplasia; unfortunately, clinical outcome was not available to determine how DARPP-32 expression would affect patient survival (19).

In gastric cancer cell lines, expression of t-DARPP leads to increase in Bcl-2 protein through increase in expression and phosphorylation of CREB and ATF-1, blocking caspase-3 and caspase-9 activation (20). Increased t-DARPP expression also resulted in increased in Akt kinase activity (20); further studies have also shown that t-DARPP expression resulted in increased accumulation and nuclear translocation of β-catenin (21). When DARPP-32 is overexpressed in gastric cancer cells an increase in cellular invasion is observed *in vitro*, mediated through an increase in membrane type 1 matrix metalloproteinase (MT1-MMP) and CXCR4 protein levels (22).

DARPP-32, and in particular t-DARPP, has been implicated in treatment response in gastric cancer. In vincristine-resistant gastric adenocarcinoma cells, DARPP-32 expression could enhance the sensitivity of the cells towards vincristine, adriamycin, 5-fluorouracil and cisplatin, also decreasing adriamycin efflux from the cells (23). The role of DARPP-32 in the multi drug resistance of gastric cells may be due to down-regulation of ZNRD1 (zinc ribbon domain containing 1) and p-glycoprotein

(24). Gastric cancers can also become resistant to gefitinib, an epidermal growth factor receptor (EGFR) inhibitor; overexpression of DARPP-32 in gastric cells that do not normally express DARPP-32 can stop gefitinib-induced apoptosis, whereas knockdown if DARPP-32 can increase sensitivity (25). DARPP-32 was shown to activate phosphatidylinositol-3-kinase (PI3K)-Akt signalling and to increase stability of EGFR (25). Expression of DARPP-32 can also suppress TRAIL induced cytochrome c release in gastric cancer, or knockdown of DARPP-32 in resistant cell lines can mediate TRAIL induced apoptosis; this was shown to be mediated through BCL-xL expression through activation of Src/STAT3 signalling (26).

Amplifications at 17q21 are associated with breast, gastric and pancreatic cancers. The concomitant amplification of DARPP-32 with ERBB2 and TOP2A has been observed in gastric cancers with intestinal-type morphology (27), prior to a 168-kb amplicon in 17q12-q21 being described (expression of 11 genes in genomic order: *NEUROD, PPP1R1B, STARD3, TACP. PNMT, PERLD1, ERBB2, C17orf37, GRB7, ZNFN1A3* and *TOP2A*), in 30% of gastrointestinal adenocarcinomas (28). Later, a PPP1R1B-STARD3 fusion transcript was described in 21.3% of primary gastric cancers, but not matched adjacent normal tissue; overexpression of PPP1R1B-STARD3 in gastric cancer cells has been shown to increase cell proliferation (29).

In both breast and gastric cancers, t-DARPP expression has been linked with Bcl-2; further research has demonstrated that Bcl-2 docks DARPP-32 and calcineurin in a complex on the inositol 1,4,5-triphosphate receptor (InsP3R) to prevent exaggerated Ca(2+) release through reduction of PKA mediated InsP3R phosphorylation (30).

3.3 DARPP-32 and breast cancer

Although limited in scope, increasing evidence is demonstrating that DARPP-32 plays a role in breast cancer. One of the initial studies to investigate DARPP-32 in breast cancer transfected DARPP-32 into MCF-7 cells to show reduced cellular migration, whereas reduced migration was not observed when DARPP-32 was transfected into MDA-MD-231 cells that were deficient in the adhesion receptor DDR1 (discoidin domain receptor 1) expression (31). Reduced migration was observed in MDA-MB-231 cells when both DARPP-32 and DDR1 were co-expressed and the effect of DARPP-32 on cellular migration was dependent upon Threonine-34 phosphorylation (31). Subsequently, Threonine-34 phosphorylation was a result of Wnt-5A triggering cAMP elevation at the plasma membrane, and Wnt-5A was able to induce DARPP-32 dependent inhibition of breast cancer cell migration (32).

HER2 plays an important role in the pathogenesis of breast cancer, and amplification of the HER2 gene locus is linked with tumourigenesis via complex cellular mechanisms (reviewed in (33)). HER2 positive breast cancer has a number of targeted therapeutic options, including trastuzumab and lapatinib (reviewed in (34)). HER2

positive breast cancer cell lines engineered to stably express t-DARPP develop resistance to trastuzumab through increased Bcl-2 expression; similarly, knockdown of t-DARPP in trastuzumab resistant breast cancer cells results in decreased cell viability (35). Further work has shown that, *in vitro*, trastuzumab resistant breast cancer cells express t-DARPP which is phosphorylated at Threonine-75 either in the presence or absence of trastuzumab, and Threonine-75 phosphorylation is required for Akt phosphorylation (36). In addition, t-DARPP over expression is sufficient to confer resistance to trastuzumab (36); interestingly, co-expression of DARPP-32 can reverse the effect of t-DARPP on trastuzumab resistance and Akt phosphorylation (37). Induction of Akt phosphorylation following t-DARPP over-expression has also been shown to increase cellular proliferation and anchorage dependent and independent growth (38). The finding that t-DARPP can confer resistance to trastuzumab has also been translated into oesophageal adenocarcinomas (39), and the role of t-DARPP has been expanded to other HER-2 therapeutic agents, such as lapatinib (40). Expanding on the findings in HER2 positive disease, in the presence of trastuzumab but not absence, trastuzumab resistant breast cancer cells expressing t-DARPP are sensitised to EGFR inhibition (41). More recently, *PPP1R1B* was one of the most upregulated genes in trastuzumab resistant breast cancer cell lines, identified using RNA-Sequencing (RNA-Seq) (42).

Hamel *et al.* (2010) was first to investigate DARPP-32 and t-DARPP expression is a cohort of breast cancer patients and (n=230) and indicated that high expression of a combination of t-DARPP and DARPP-32 was associated with poor survival of patients, but information on the patient cohort was absent (36). Expression of t-DARPP has also been determined to show increased expression in breast tumours in comparison to normal breast tissue (38). Interestingly, a shift in expression from DARPP-32 to t-DARPP has been observed during mammary tumourigenesis (43). Studies from our research group have demonstrated investigated large numbers of breast cancer patients to investigate DARPP-32, Cdk-5, PKA and PP-1 expression (6, 44-46). DARPP-32 protein expression was determined in over 3000 tumours from breast cancer patients to demonstrate that low levels of DARPP-32 expression is associated with shortened patient survival which is independent of other prognostic variables; furthermore, stronger associations with survival of patients with ER positive tumours was observed (6). Additional analysis of *PPP1R1B* mRNA expression also demonstrated that low expression was associated with shortened survival of patients with ER positive tumours (6). Artificial neural network analysis using the METABRIC dataset, identified genes associated with *PPP1R1B* expression, that included *CDC42* and *GRB7* (6). There have been some direct indications that DARPP-32 can be modulated by oestrogen, including that oestrogen increases DARPP-32 Threonine-34 phosphorylation (47); this has been further supported through work investigating the oestrous cycle in rats when investigating the response to cocaine (48).

Although research linking DARPP-32 and oestrogen is limited, there is substantial research linking PKA and oestrogen signalling. PKA can phosphorylate ERα at Ser-305 to redirect the receptor to new transcriptional start sites and is associated

with patients with tamoxifen resistance in breast cancer; typically, through MYC (49). PKA activation with forskolin has been shown to supress E2 dependent growth of both the ER positive MCF-7 and T47D breast cancer cell lines (50). In addition to links between PKA and oestrogen signalling, indirect links between dopamine and oestrogen in the brains of women have been described (reviewed in (51)), including dopaminergic activation of ER (52).

3.4 DARPP-32 and lung cancer

In addition to gastric and breast cancer, a role for DARPP-32 in lung cancer has been described. Initially, DARPP-32 and t-DARPP expression were found to promote lung tumour growth *in vivo*, and loss of DARPP-32 in non-small cell lung cancer (NSCLC reduces tumour growth (53). Further studies have demonstrated that both DARPP-32 and t-DARPP promote small cell lung cancer (SCLC) growth through Akt/Erk (54). Interestingly, DARPP-32 has also been shown to physically interact with inhibitory kappa B kinase-α (IKKα) to promote migration through nuclear factor kappa-light-chain-enhancer of activated B cells-2 (NF-κB) in NSCLC (53). In SCLC, achaete-scute homologue 1 (ASCL1) has been shown to transcriptionally activate DARPP-32 isoform expression (54). In EGFR tyrosine kinase inhibitor refractory lung cancer, DARPP-32 has been shown to recruit ERBB3 to EGFR to bypass EGFR tyrosine kinase inhibitor inhibited EGFR signalling (55).

Assessment of patient derived tumours has demonstrated an association between t-DARPP and tumour stage in NSCLC (53), and that DARPP-32 isoforms are present in SCLC but not normal lung (54).

3.5 DARPP-32 in other tumour types

There is small scale evidence that DARPP-32 may play a role in a wider range of tumour types; however, evidence is often limited to single studies. In pancreatic cancer, hypoxia inducible factor 1 alpha (*HIF1A*) knockout cells have increased expression of DARPP-32, which has been shown to promote degradation of p53 by stabilising phosphorylation of MDM2 (56). High expression of DARPP-32 in human pancreatic ductal carcinomas is associated with shorter survival of patients; and knockdown of DARPP-32 reduced the pancreatic cancer lung metastasis *in vivo (56)*. In ovarian cancer, low DARPP-32 expression is strongly associated with shorter patient survival (44). In glioblastomas, high ratios of DARPP-32/STAT3 and DARPP-32/STAT5B has been shown to be associated with longer patient survival (57).

3.6 Summary

There is accumulating evidence that DARPP-32 and its truncated splice variant, t-DARPP, may play an important role in cancer, particularly gastric, breast and lung cancer. There is conflicting data available for the role of full length DARPP-32, which appears to be context and tumour type dependent; however, t-DARPP expression appears to be exclusively linked to tumourigenesis. It is unclear how DARPP-32 mediates its effects in breast cancer; however, it appears to function as a regulator and/or activator of various important cancer-associated signalling pathways.

4 Hypothesis

We have previously demonstrated that breast cancer patients with low DARPP-32 expression and ER positive disease have a significantly worse survival when compared to those patients with high DARPP-32 expression, or low DARPP-32 expression in ER negative disease. We hypothesise that loss of DARPP-32 expression in ER positive cell lines results in changes in the transcriptome that promotes aggressive cancer cell behaviour by altering pathways associated with phenotype changes that promote tumour progression or metastasis.

5 Objectives

The overarching objective of this research is to determine transcriptomic changes that occur in the absence and presence of DARPP-32 expression using a bioinformatics pipeline including pathway analysis. For clarity, the overarching research objective has been separated into three components.

5.1 Objective 1

Use RNA-Seq to reveal variations in the transcriptome that occur following loss of DARPP-32 expression in an ER positive breast cancer cell *in vitro*. Identify up and downregulated genes and perform pathway analysis to identify alterations in key cancer pathways.

5.2 Objective 2

Identify how oestrogen signalling can have a differential effect on cells with wild type expression of DARPP-32 compared to cells with reduced DARPP-32 expression using RNA-Seq. Identify up and downregulated genes and perform gene enrichment analysis to identify alterations in key cancer pathways.

5.3 Objective 3

Identify how inhibition of PKA effects the transcriptome of an ER positive breast cancer cell line with wild type and reduced expression of DARPP-32 using RNA-Seq. Identify gene expression of known and putative DARPP-32 signalling partners and perform pathway analysis to identify alterations to key cancer pathways.

6 Methods

6.1 DARPP-32 knockdown and treatments

DARPP-32 knockdown cells and cell treatments were performed by Behnaz Saidy (PhD candidate supervised by S. Storr). T47D cells were used for all experiments and are an ER positive breast cancer cell line purchased from the American Type Tissue Collection (ATTC). To knockdown DARPP-32 expression, T47D cells were transfected for 48 hours with 8nM human DARPP-32 (SR313371C) siRNA oligo duplex or 8nM negative control (SR30004) siRNA (OriGene), using Lipofectamine RNAiMAX in Opti-MEM reduced serum medium (both from Thermo Fisher Scientific). Reduction of DARPP-32 expression was confirmed by Western blotting and real-time PCR. Knockdown or control cells were treated with 10nM estradiol17β (E2) (Sigma) dissolved in absolute ethanol for 24 hours in the E2 treatment group. E2 treatment was performed in in phenol red free media containing 10% charcoal stripped FBS (Gibco, UK) to remove endogenous serum steroids and eliminate the known weak oestrogen agonistic activity of phenol red. Knockdown or control cells were also treated with 3μM PKA inhibitor (PKA inhibitor fragment (6-22) amide) (Tocris) dissolved in water, for 24 hours in the PKA inhibition treatment group. PKA inhibition was performed in Dulbecco's modified Eagle's medium with high glucose (Sigma, UK) and 10% iron supplemented Donor Calf Serum (Gibco, UK) without the presence of antibiotics. PKA activity was determined using ELISA (Thermo Fisher Scientific). Following siRNA transfection and treatment, cells were washed, and $3x10^6$ cells were frozen as cell pellets in 500μl Trizol for RNA-Seq. Three biological repeats were included for each condition and treatment group. A summary of the cells utilised for experiments is detailed in Table 6-1.

Cell line	Subtype	Additional treatment	Replicates
T47D	Negative control siRNA (SR30004)	None	3
T47D	Negative control siRNA (SR30004)	10nM estradiol17β (24 hours)	3
T47D	Negative control siRNA (SR30004)	3μM PKA inhibitor fragment (6-22) amide (24 hours)	3
T47D	DARPP-32 siRNA (SR313371C)	None	3
T47D	DARPP-32 siRNA (SR313371C)	10nM estradiol17β (24 hours)	3
T47D	DARPP-32 siRNA (SR313371C)	3μM PKA inhibitor fragment (6-22) amide (24 hours)	3

Table 6-1: Cell lines, siRNA knockdown and additional treatment conditions utilised for RNA-Seq experiments.

6.2 RNA-Seq

RNA extraction, sample quality control, mRNA library preparation and RNA-Seq was performed by Novogene. Briefly, mRNA was purified from total RNA via poly-T oligo attached magnetic beads prior to fragmentation which was followed by first strand cDNA synthesis using random hexamer primers then second strand cDNA

synthesis. The library was complete following end-repair, A-tailing, adapter ligation, size selection, amplification, and purification. The library was checked with Qubit and real-time PCR for quantification and bioanalyser for size detection before being sequenced on Illumina NovaSeq platforms which utilise a paired-end 150 base pair sequencing strategy. Data output was greater than 20 million read pairs per sample. The data have been deposited in NCBI's Gene Expression Omnibus (GEO), and are accessible through GEO Series accession number GSE204836 (https://www.ncbi.nlm.nih.gov/geo/query/acc.cgi?acc=GSE204836), with secure token access code: yxuvuicehxuhtin (58).

6.3 Quality control

Initial quality control was performed using FastQC to interrogate the initial quality of sequencing data, prior to using Trim Galore. FastQC was developed by Simon Andrews at the Babraham Institute and allowed quality control checks to be performed on raw sequence data (https://www.bioinformatics.babraham.ac.uk/projects/fastqc/). Trim Galore is a wrapper script for Cut Adapt and FastQC for FastQ files, developed by Felix Krueger, (https://www.bioinformatics.babraham.ac.uk/projects/trim_galore/)) and was used to automate quality and adapter trimming and quality control. Trim Galore version 0.6.7 was used to remove the first 13 base pairs of Illumina standard adaptors (AGATCGGAAGAGC), perform quality trimming (Phred score cutoff 20), and allowed subsequent FastQC analysis. Terminal command code for these assessments has been deposited online (https://github.com/sarahstorr/MRes/blob/fca50b0bbaf4ab6c387afdbd621045606af1ff16/Terminal_code). There are many data quality control and pre-processing packages that can be utilised instead of Cut Adapt, including widely used Trimmomatic; each with their own specific advantages and limitations (59). Cut Adapt, included in the Trim Galore wrapper was favoured in this instance, including adaptor removal and quality trimming.

6.4 Pseudoalignment and quantification

Kallisto was used to quantify the abundance of transcripts from RNA-Seq data using pseudoalignent to rapidly determine the compatibility of reads with targets without alignment of individual bases, and was developed by Bray et al. (2016) (60). Pseudoalignement was transformational for RNA-Seq analysis, as it removed a major time constraint (alignment of individual bases) whilst maintaining similar accuracy. Kallisto was run with 100 bootstraps, which allowed repeating analyses after resampling with replacement of the data to quantify the uncertainty of abundance estimates and terminal command code for these assessments has been deposited

online (https://github.com/sarahstorr/MRes/blob/fca50b0bbaf4ab6c387afdbd621045606af1ff16/Terminal_code). The human reference genome was GENCODE GRCh38 version 36 for transcript identification and quantification, containing the nucleotide sequences of all transcripts on the reference genome (https://www.gencodegenes.org/human/).

Kallisto was utilised for pseudoalignment; however, other alignment free quantification tools can also be utilised, including Salmon and Sailfish. It was outside the scope of the project objectives to compare the advantages and limitations of Salmon compared with Kallisto (61). In addition to pseudoalignment, traditional alignment programmes are available such as HISAT2, STAR and TopHat2.

6.5 Differential transcript expression

The differential expression of transcripts was determined using DESeq2 (1.36.0) in the statistical environment RStudio, relying on input from Kallisto using Tximport. RStudio version 2022.07.1+554 running R version 4.2.0, with Bioconductor version 3.15 were used for assessments. DESeq2 is an evolution of DESeq, an R/Bioconductor package developed by Anders and Huber in 2010 (62). DESeq2 fits negative binomial generalised linear models for each transcript or gene and uses the Wald test for significance testing; this method normalised count data to account for the differences in library sizes and composition. The list of transcripts was subject to a multiple test adjustment ranked by a P <0.05 and a greater than two-fold change. DESeq2 uses shrinkage estimation for dispersions to avoid false positives by shrinking log2 foldchanges (LFC) estimates towards zero to improve stability and reproducibility of analysis results. In addition, log transformation transforms skewed data to normality, improving the clustering/distances for visualisation methods. Normalised count data was plotted for the visualisation of differences between experimental data and control data including principal component analysis (PCA) and heatmaps.

The open-source visualisation package ggplot2 was also used within the RStudio environment to create volcano plots and clustered heatmaps were generated using Pheatmap. RStudio script for use of Tximport, DESeq2, ggplot2 and pheatmap have been deposited online (https://github.com/sarahstorr/MRes/blob/fca50b0bbaf4ab6c387afdbd621045606af1ff16/RStudio_DESeq2).

6.6 Gene overrepresentation analysis

Gene enrichment analysis was performed using Qiagen Ingenuity Pathway Analysis (IPA), version 76765844; a pathway analysis application that can be used to

predict downstream effects and identify new targets or candidate biomarkers (https://digitalinsights.qiagen.com/). QIAGEN IPA analyses the effect of differentially expressed gene sets on a signalling pathway or a biological process using a literature-based database to uncover alterations in gene networks, canonical pathways and diseases. Qiagen IPA takes a similar approach to Gene Set Enrichment Analysis (GSEA) in identifying significantly enriched groups of genes. IPA applied a pre-defined cut off for the gene set by using the right-tailed Fisher's exact test P <0.05 and a greater than two-fold log-ratio change. Z-scores were used to represent the directional effect of two molecules or more in the dataset, to provide a prediction of activation or inhibition of a pathway/gene, where a negative Z-score indicated inhibition of an overall pathway, and a positive Z-score indicated activation of an overall pathway (63).

In addition to Qiagen IPA, other programmes are available to explore enriched or overrepresented pathways in differentially expressed transcript/gene lists. To understand the limitations and advantages of these programmes, in comparison to Qiagen IPA, a selection were explored using the differentially expressed gene lists for the DARPP-32 knockdown cell versus control cell analysis. Gene Ontology (GO) was used within the RStudio environment, (code deposited online https://github.com/sarahstorr/MRes/blob/fca50b0bbaf4ab6c387afdbd621045606af1ff16/RStudio_DESeq2), which connects to the analysis tool from the panther classification system; and free online tools, Reactome (https://reactome.org/PathwayBrowser/#TOOL=AT) and WEB-based Gene SeT AnaLysis Toolkit (WebGestalt www.webgestalt.org) to explore Reactome, KEGG and Panther, were utilised. Panther, Reactome and KEGG are some of the large-scale classification systems that map gene function, ontology and pathways; although the databases are similar, there are differences in the methods in their curation, updates and specificity. Comparisons of human cell signalling pathway databases have been made; however, no industry standard platform exists, with each database having its own advantages and limitations (reviewed in (64).

6.7 METABRIC data

Details of the Molecular Taxonomy of Breast Cancer International Consortium (METABRIC) data set (n=1980) data set have been published elsewhere (65). This study is reported according to reporting recommendations for tumour marker prognostic studies (REMARK) criteria (66); METABRIC samples were collected by five centres in the UK and Canada between 1977–2005 and were acquired with appropriate consent from the respective institutional review boards. Breast cancer specific survival was calculated as the time interval between primary surgery and death resultant from breast cancer. Almost all ER negative and lymph node positive patients received adjuvant chemotherapy, whereas ER negative and/or lymph node positive patient did not. No patients with HER2 overexpression received trastuzumab. Median follow-up was 141 months determined using the reverse Kaplan-Meier method. DNA and RNA

were isolated from samples and hybridised to the Affymetrix SNP 6.0 and Illumina HT-12 v3 platforms for genomic and transcriptional profiling as described by Curtis *et al* (2012) (65). Information on gene expression in breast cancer is also openly available in The Cancer Genome Atlas (TCGA) (67); however, METABRIC was favoured for use in this study as the University of Nottingham was a tissue contributing site, and tissue samples are available to assess protein expression as part of future studies.

Genes identified from RNA-Seq bioinformatics were reviewed for subsequent downstream assessment within the METABRIC cohort. Probe level information for genes of interest were recovered and compared with probe level information available for DARPP-32; with subsequent assessment of the impact of gene of interest expression and patient survival. Statistical analysis was performed using IBM SPSS Statistics (Version 28). All differences were deemed statistically significant at the level of $P \leq 0.05$. The Pearson χ^2 test of association was used to determine the relationship between gene expression categorised around the median value and clinicopathological variables. Survival curves were plotted according to the Kaplan-Meier method with significance determined using the log-rank test. In addition, Cox (proportional hazards) regression was used to determine the relationship between continuous data on gene expression and patient survival, including as a multivariate approach where a set of covariates were included. SPSS data files have been deposited online (https://github.com/sarahstorr/MRes/blob/fca50b0bbaf4ab6c387afdbd621045606af1ff16/METABRIC.sav).

7 Results

7.1 DARPP-32 knockdown

ER positive (luminal B subtype) T47D breast cancer cell lines were treated with either human DARPP-32 siRNA oligo duplex or negative control siRNA to knockdown DARPP-32 expression prior to transcriptomic comparison. DARPP-32 expression was effectively reduced using siRNA knockdown; protein expression of DARPP-32 was reduced by over 95% determined using Western blotting, and over 60% at the mRNA level, using real-time PCR (Figure 7-1); negative control siRNA did not cause a reduction in DARPP-32 expression when compared to wild-type T47D cells. In addition to DARPP-32 knockdown, T47D cells were subject to stimulation with E2 or inhibition of PKA using PKA inhibitor fragment (6-22) amide. PKA inhibitor fragment (6-22) amide, PKAi, caused a dose dependent decrease in PKA activity determined by ELISA in T47D breast cancer cells (Figure 7-1). For RNA-Seq, DARPP-32 knockdown and control T47D breast cancer cells were treated with 3µM PKA inhibitor for 24 hours, which resulted in a 60% reduction in PKA activity, and a 60% reduction in DARPP-32 Thr-34 phosphorylation, which was also determined by ELISA (Figure 7-1).

RNA-Seq was performed on T47D breast cancer cells that were treated either human DARPP-32 siRNA oligo duplex or negative control siRNA; referred to as DARPP-32 knockdown or control cells respectively. Both DARPP-32 knockdown and control cells were stimulated with E2 or subjected to PKA inhibition with PKA inhibitor fragment (6-22) amide prior to RNA-Seq.

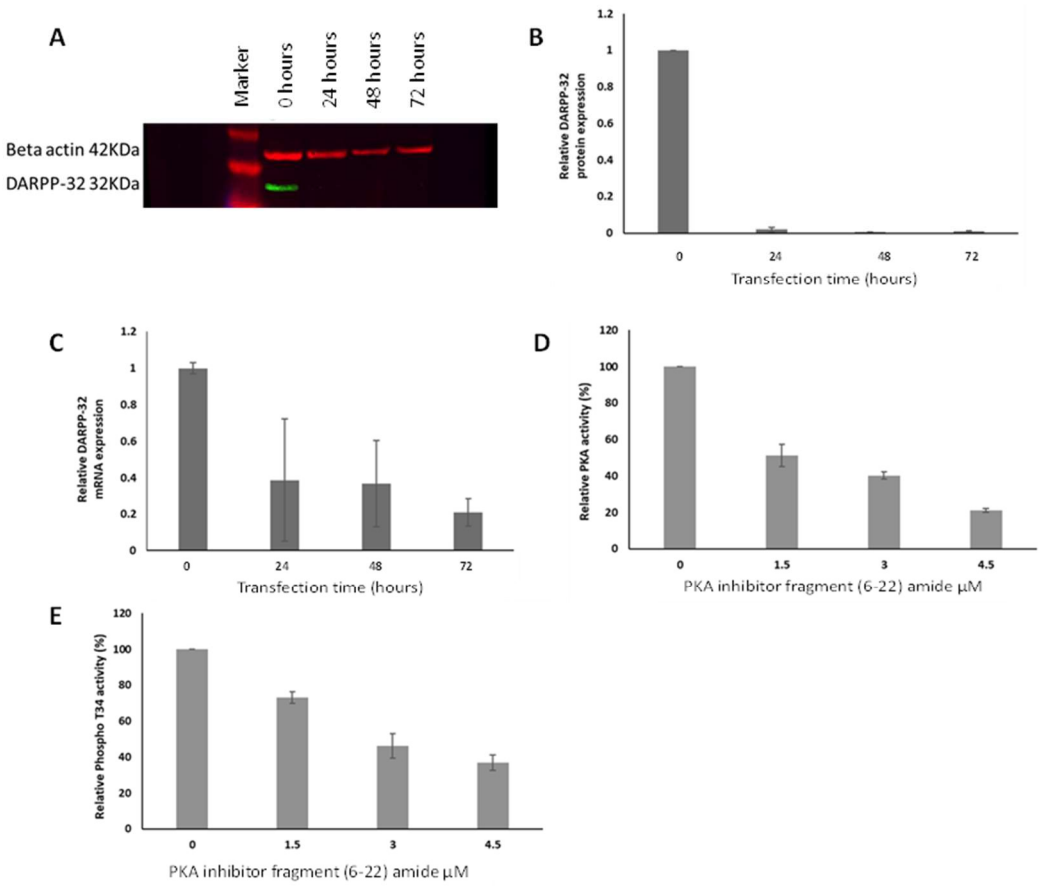


Figure 7-1: A: Expression of DARPP-32 and beta actin (control) in T47D cell lines treated with DARPP-32 siRNA oligo duplex with expression determined 24, 48 and 72 hours after treatment, B: Expression of DARPP-32 determined by Western blot quantified using Li-Cor, C: DARPP-32 mRNA expression determined 24, 48 and 72 hours after treatment with DARPP-32 siRNA oligo duplex, D: PKA activity determined after treatment with increasing concentrations of PKA inhibitor fragment (6-22) amide, E: DARPP-32 Thr-34 phosphorylation determined by ELISA after treatment with increasing concentration of PKA inhibitor fragment (6-22) amide.

7.2 Quality control

Trim Galore was used to remove adaptors and perform quality trimming on FASTQ files prior to quantifying the abundance of transcripts using Kallisto. Kallisto was used for transcript quantification prior to DESeq2 because it is a lightweight algorithm tool that exploits pseudoalignment, which does not require the alignment of a read to a specific location of the genome, ultimately reducing the computing resources required.

7.3 DESeq2

DESeq2 was used to identify differentially expressed transcripts by taking the raw counts from Kallisto; which allowed an internal normalisation against the geometric mean for each transcript across each sample to account for library size and RNA composition. Analyses of various treatment groups was performed to address the specific research objectives outlined previously within the Objectives. DARPP-32 knockdown cells, created following treatment with human DARPP-32 siRNA oligo duplex, were compared against control cells, treated with negative control siRNA, to determine the effect of reduced DARPP-32 expression in ER positive breast cancer cells. To determine the effect of E2 stimulation, a number of analyses were performed; these analyses comprised of DARPP-32 knockdown cells versus DARPP-32 knockdown cells treated with E2, control cells versus control cells treated with E2 and DARPP-32 knockdown cells treated with E2 versus control cells treated with E2. Pairwise differential transcript comparisons of all condition combinations were performed to ensure subtle changes were not lost. To determine the effect of PKA inhibition, three analyses were performed; DARPP-32 knockdown cells versus DARPP-32 knockdown cells treated with PKAi, control cells versus control cells treated with PKAi and DARPP-32 knockdown cells treated with PKAi versus control cells treated with PKAi.

Results from DESeq2 assessment were visualised between different RNA-Seq analyses groups using a number of different methods, including visualising count data directly (Figure 7-2). This was also demonstrated by dispersion estimate plots and principal component analysis shown in the appendix (Appendix 1). The largest number of changes in transcript expression were observed when either DARPP-32 knockdown or control cells were stimulated with E2. Differentially expressed transcripts for further analysis were defined as transcripts with a greater than 2-fold change in expression and a *P*-adjusted value of <0.05. The *P*-adjusted value was a Benjamini-Hochberg adjusted Wald test *P*-value and accounted for multiple testing. Only transcripts that had a *P* value less than <0.05 and a greater than two-fold change were included in any downstream assessments.

202 differentially expressed transcripts were identified in the DARPP-32 knockdown cell versus control cell analysis. When E2 was used to stimulate DARPP-32 knockdown cells and/or control cells, 42641 differentially expressed transcripts were identified in the DARPP-32 knockdown cell versus DARPP-32 knockdown cell treated with E2 analysis; 40065 differentially expressed transcripts were identified in the control cell versus control cell treated with E2 analysis and 193 differentially expressed transcripts were identified in the DARPP-32 knockdown cell treated with E2 versus control cell treated with E2 analysis. When a PKA inhibitor was used to treat DARPP-32 knockdown cells and/or control cells, 1155 differentially expressed transcripts were identified in the DARPP-32 knockdown cell versus DARPP-32 knockdown cell treated with PKAi analysis, 1704 differentially expressed transcripts were identified within the control cell versus control cell treated with PKAi analysis, and 181 differentially

identified transcripts were identified in the DARPP-32 knockdown treated with PKAi cell versus the control cell treated with PKAi analysis. Volcano plots from DESeq2 assessments were generated using ggplot2 from the different RNA-seq analysis condition groups are shown in Figure 7-3, with significant differentially expressed transcripts highlighted in red. Lists of differentially expressed transcripts for each analysis have been deposited online, and links to their location are shown in Table 7-1.

Analysis group	DET	Permalink to deposited to differentially expressed transcript list
DARPP-32 knockdown cell versus control cell	202	https://github.com/sarahstorr/MRes/blob/fca50b0bbaf4ab6c387afdbd621045606af1ff16/DARPPvControlDET.xlsx
DARPP-32 knockdown cell versus DARPP-32 knockdown cell treated with E2	42641	https://github.com/sarahstorr/MRes/blob/fca50b0bbaf4ab6c387afdbd621045606af1ff16/DARPPvDARPPE2DET.xlsx
Control cell versus control cell treated with E2	40065	https://github.com/sarahstorr/MRes/blob/fca50b0bbaf4ab6c387afdbd621045606af1ff16/ControlvControlE2DET.xlsx
DARPP-32 knockdown cell treated with E2 versus control cell treated with E2	193	https://github.com/sarahstorr/MRes/blob/fca50b0bbaf4ab6c387afdbd621045606af1ff16/DARPPE2vControlE2DET.xlsx
DARPP-32 knockdown cell versus DARPP-32 knockdown cell treated with PKAi	1155	https://github.com/sarahstorr/MRes/blob/fca50b0bbaf4ab6c387afdbd621045606af1ff16/DARPPvDARPPPKiDET.xlsx
Control cell versus control cell treated with PKAi	1704	https://github.com/sarahstorr/MRes/blob/fca50b0bbaf4ab6c387afdbd621045606af1ff16/ControlvControlPKAiDET.xlsx
DARPP-32 knockdown cell treated with PKAi versus control cell treated with PKAi	181	https://github.com/sarahstorr/MRes/blob/fca50b0bbaf4ab6c387afdbd621045606af1ff16/DARPPPKAivControlPKAiDET.xlsx

Table 7-1: Number of differentially expressed transcripts identified in each analysis and link to online data deposit.

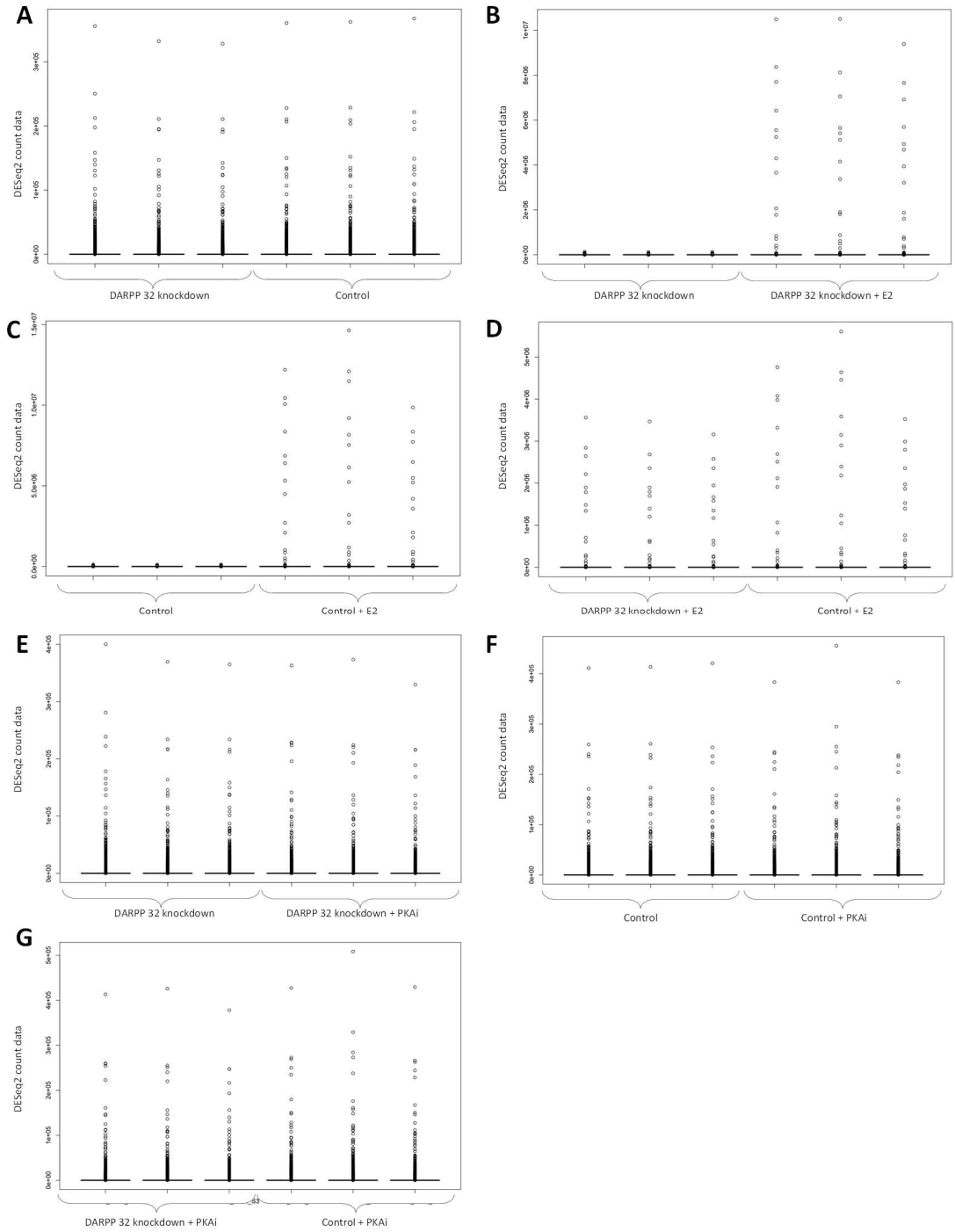


Figure 7-2: DESeq2 count data between analyses. A: DARPP-32 knockdown cells versus control cells, B: DARPP-32 knockdown cells versus DARPP-32 knockdown cells treated with E2, C: control cells versus control cells treated with E2, D: DARPP-32 knockdown cells treated with E2 versus control cells treated with E2, E: DARPP-32 knockdown cells versus DARPP-32 knockdown cells treated with PKAi, F: control cells versus control cells treated with PKAi, G: DARPP-32 knockdown cells treated with PKAi versus control cells treated with PKAi.

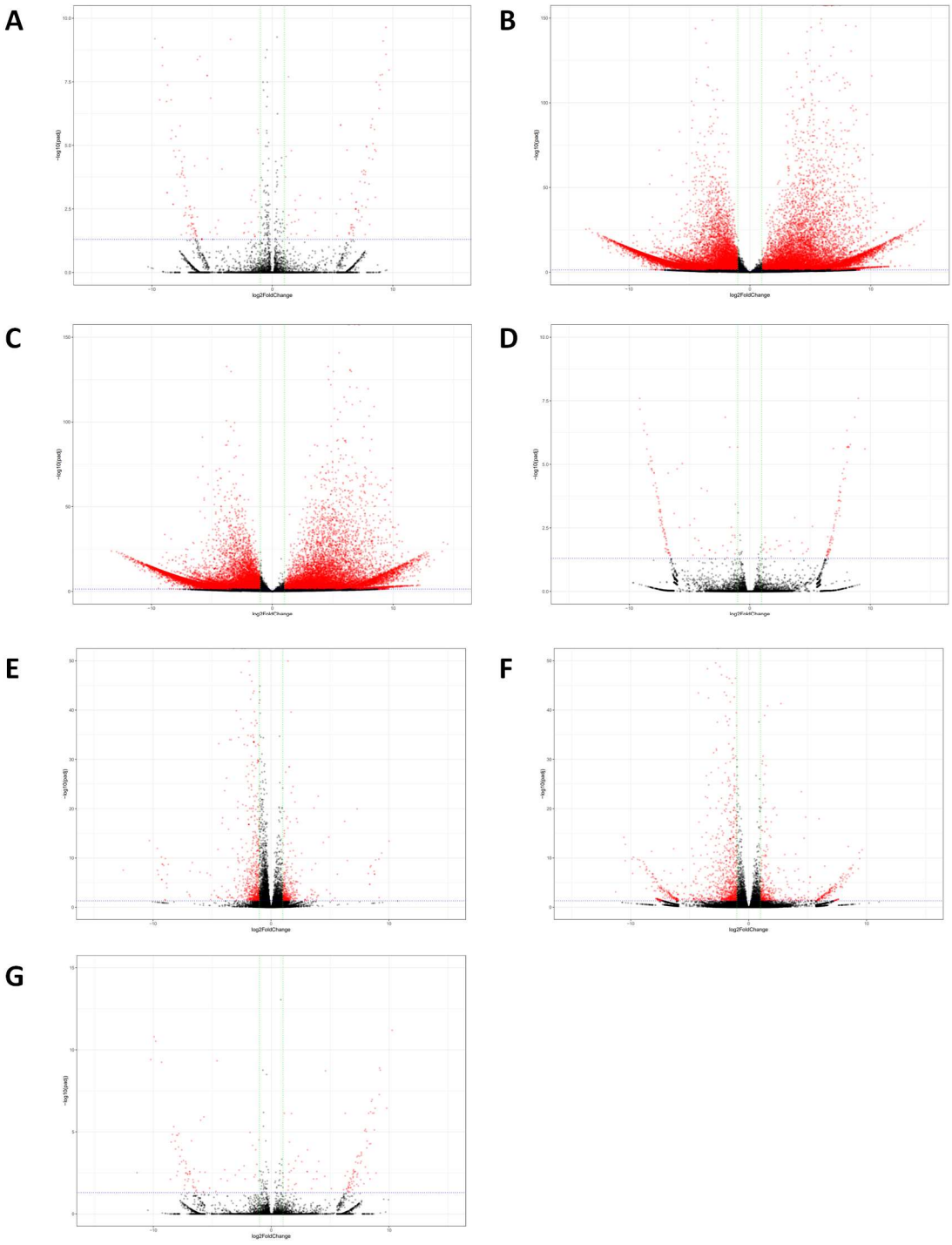


Figure 7-3: Volcano plots of DESeq2 analyses. Volcano plots of log10 P-adjusted was plotted against the log2 fold change of transcripts generated from DESeq2 analysis; red dots those show those with P<0.05. A: DARPP-32 knockdown cells versus control cells, B: DARPP-32 knockdown cells versus DARPP-32 knockdown treated cells with E2, C: control cells versus control cells treated with E2, D: DARPP-32 knockdown cells treated with E2 versus control cells treated with E2, E: DARPP-32 knockdown cells versus DARPP-32 knockdown cells treated with PKAi, F: control cells versus control cells treated with PKAi, G: DARPP-32 knockdown cells treated with PKAi versus control cells treated with PKAi.

Heatmaps of differentially expressed transcripts were used to visualise the top 50 most significant (*P*- adjusted) transcripts with a greater than 2-fold change in expression for DARPP-32 knockdown cell versus control cell analysis (Figure 7-4), DARPP-32 knockdown cell versus DARPP-32 knockdown cell treated with E2 analysis (Figure 7-5), control cell versus control cell treated with E2 analysis (Figure 7-6), DARPP-32 knockdown cell treated with E2 versus control cell treated with E2 analysis (Figure 7-7), DARPP-32 knockdown cell versus DARPP-32 knockdown cell treated with PKAi analysis (Figure 7-8), control cell versus control cell treated with PKAi (Figure 7-9) and DARPP-32 knockdown cell treated with PKAi versus control cell treated with PKAi (Figure 7-10). The heatmaps for each analysis show that within the differentially expressed transcripts there is a range of both up and down regulated genes which are largely reproducible throughout the biological replicates (Figure 7-5 and Figure 7-6).

The top three significant differentially expressed transcripts identified in the DARPP-32 knockdown cell versus control cell analysis were ENST00000443236.6 (*CPAMD8*), ENST00000521309.5 (*YWHAZ*), and another transcript of *CPAM8*, ENST00000651564.1 (Figure 7-4). Interestingly, one *CPAM8* transcript was reduced, and one was increased in the DARPP-32 knockdown cells, whereas *YWHAZ* expression was reduced in DARPP-32 knockdown cells. CPAMD8, or C3 and PZP like alpha-2 macroglobulin domain containing 8 is a protease inhibitor and YWHAZ, or tyrosine 3-monooxygenase/tryptophan 5-monooxygenase activation protein zeta, belongs to the 14-3-3 family of proteins that mediate signal transduction by binding phosphoserine containing proteins and interacts with the insulin receptor substrate (IRS1). There are 20 listed transcripts of CPAM8, with 5 listed as protein coding. ENST00000443236.6 is the transcript identifier that corresponds to a 1885 amino acid protein, whereas ENST00000651564.1 corresponds to a 1815 amino acid protein. The top 10 up and down regulated transcripts in terms of log2 fold change in expression in the DARPP-32 knockdown cell versus control cell analysis are shown in (Table 7-2). In the DARPP-32 knockdown cells, the top 10 downregulated genes by change in expression were *CLN8*, *GRAMD2B*, *HNRNPC*, *ZCCHC7*, *CMIP*, *OSBPL2*, *TSEN34*, *MAN2C1*, *NDUFS1*, and *MAP2*. The top 10 upregulated genes by change in expression following DARPP-32 knockdown were *KBTBD11*, *ZNF230*, *BCL2L11*, *ZNF227*, *VKORC1L1*, *C19orf25*, *TSEN35*, *SART3*, *AAGAB* and *CHEK2*.

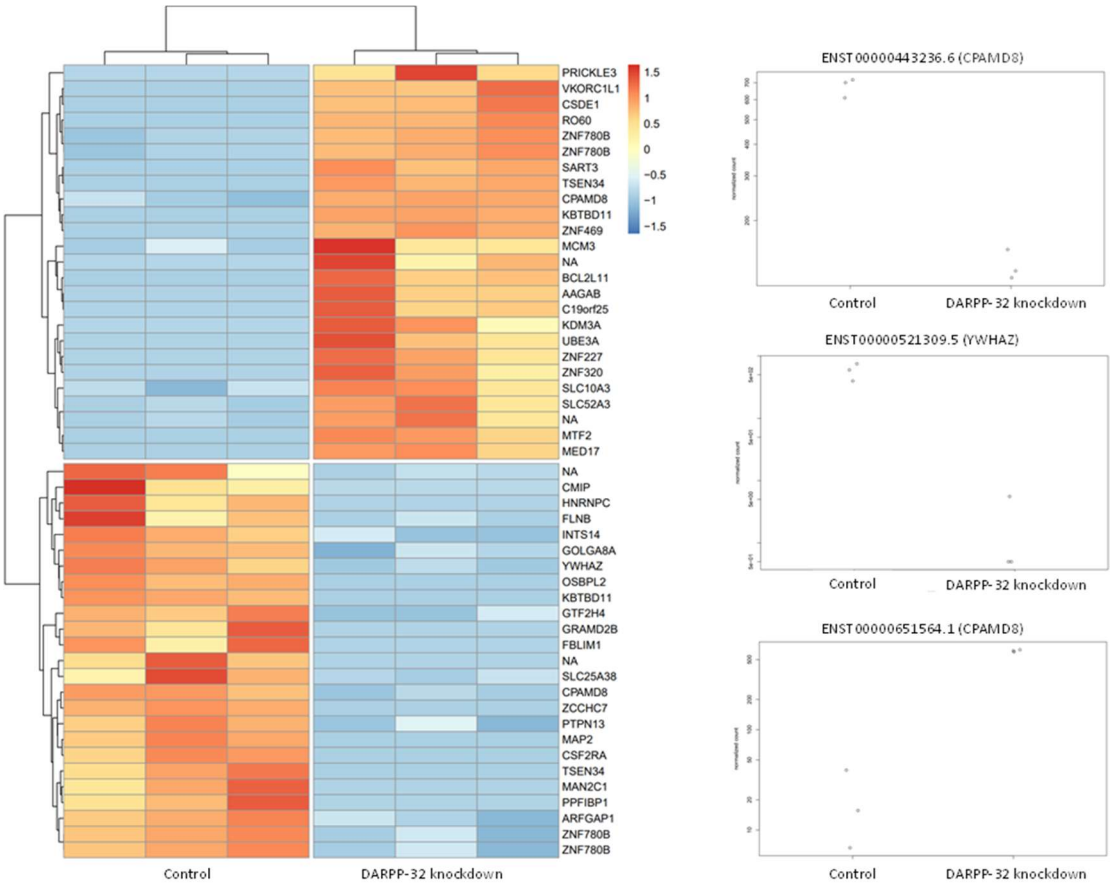


Figure 7-4: Differential transcript expression is summarised for the DARPP-32 knockdown versus the control cells analysis. The top 50 most significant (P- adjusted) transcripts with a greater than 2-fold change in expression labelled with the corresponding gene identifier are displayed in a heatmap, with the three most significant (P- adjusted) transcripts from the analyses displayed. NA are transcripts without annotation.

Downregulated genes				
Transcript ID	**Gene ID**	**Protein Name**	**Log 2 fold change**	***P*-adj**
ENST00000331222.5	CLN8	CLN8 transmembrane ER and ERGIC protein	-11.06	2.32E-14
ENST00000542322.5	GRAMD2B	GRAM domain containing 2B	-10.07	4.82E-11
ENST00000553753.5	HNRNPC	Heterogeneous nuclear ribonucleoprotein C	-9.75	6.40E-10
ENST00000534928.5	ZCCHC7	Zinc finger CCHC-type containing 7	-9.70	1.94E-11
ENST00000566513.5	CMIP	C-maf inducing protein	-9.35	1.63E-07
ENST00000643981.1	OSBPL2	Oxysterol binding protein like 2	-9.13	1.40E-09
ENST00000302937.8	TSEN34	TRNA splicing endonuclease subunit 34	-9.12	7.32E-09
ENST00000565683.5	MAN2C1	Mannosidase alpha class 2C member 1	-8.78	1.88E-07
ENST00000457011.5	NDUFS1	NADH:Ubiquinone oxidoreductase core subunit S1	-8.73	7.28E-04
ENST00000360351.8	MAP2	Microtubule associated protein 2	-8.69	4.24E-08

Upregulated genes				
Transcript ID	**Gene ID**	**Protein Name**	**Log 2 fold change**	***P*-adj**
ENST00000617214.2	KBTBD11	Kelch repeat and BTB domain containing 11	8.64	3.25E-08
ENST00000595635.5	ZNF230	Zinc finger protein 230	8.86	3.52E-07
ENST00000615946.4	BCL2L11	BCL2 like 11	8.87	4.20E-08
ENST00000589005.5	ZNF227	Zinc finger protein 227	8.95	6.37E-08
ENST00000360768.5	VKORC1L1	Vitamin K epoxide reductase complex subunit 1 like 1	8.96	1.71E-08
ENST00000588871.5	C19orf25	Chromosome 19 open reading frame 25	9.13	1.63E-08
ENST00000396388.3	TSEN34	TRNA splicing endonuclease subunit 34	9.2	7.81E-10
ENST00000651280.1	SART3	Splicosome associated factor 3, U4/U6 recycling protein	9.43	2.28E-10
ENST00000538028.1	AAGAB	Alpha and gamma adaptin binding protein	9.44	2.61E-09
ENST00000328354.10	CHEK2	Checkpoint kinase 2	9.69	1.08E-08

Table 7-2: Top 10 up and down regulated differentially expressed transcripts following DARPP-32 knockdown with log fold change and P-adjusted value shown for each transcript.

In the DARPP-32 knockdown cell versus the DARPP-32 knockdown cell treated with E2 analysis the top three identified transcripts were ENST00000361390.2 (*MT-ND1*), ENST00000361453.3 (*MT-ND2*), and ENST00000361624.2 (*MT-CO1)* (Figure 7-5). In all three cases, E2 stimulation caused an increase in transcript expression and all three resultant proteins function to enable NADH dehydrogenase activity within the mitochondrial respiratory chain. MT-ND1 is mitochondrially encoded NADH:ubiquinone oxidoreductase core subunit-1; MT-ND2 is mitochondrially encoded NADH:ubiquinone oxidoreductase core subunit-2 and MT-ND1, is mitochondrial encoded NADH:ubiquinone oxidoreductase core subunit-1.

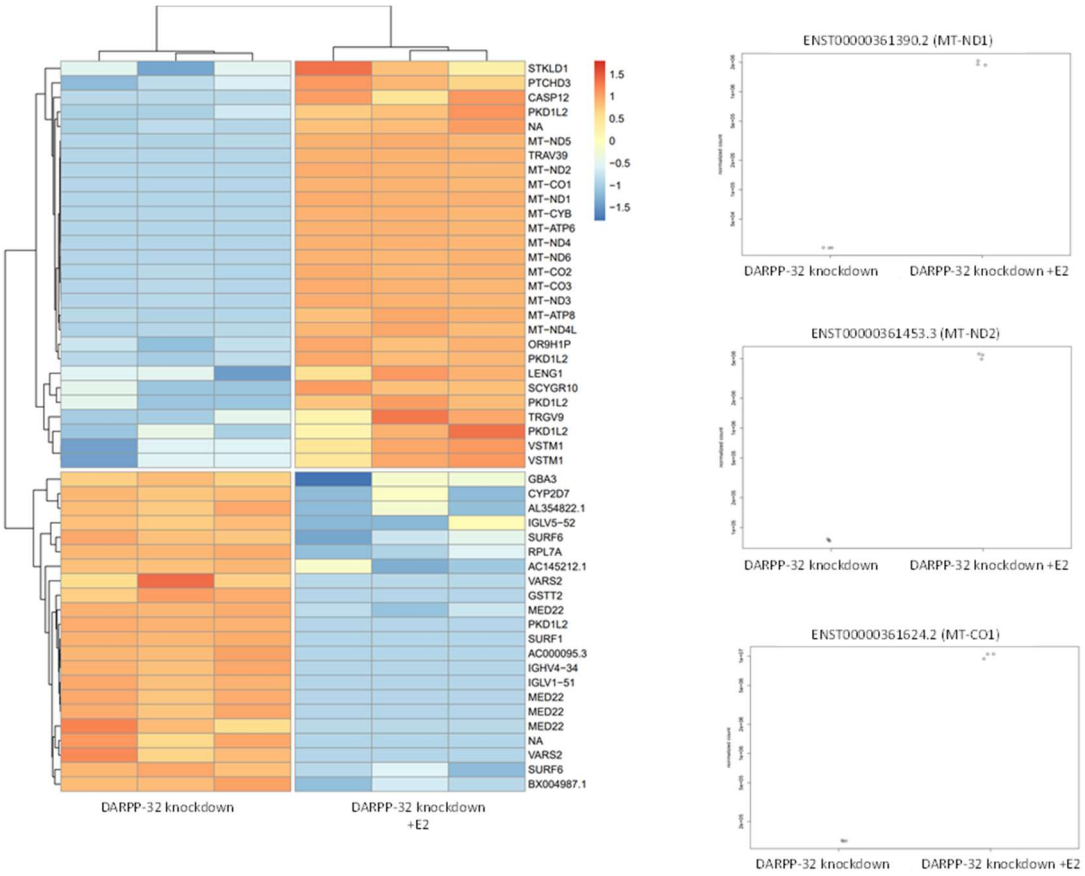


Figure 7-5: Differential transcript expression is summarised for the DARPP-32 knockdown cells versus DARPP-32 knockdown cells treated with E2 cells analysis. The top 50 most significant (P- adjusted) transcripts with a greater than 2-fold change in expression labelled with the corresponding gene identifier are displayed in a heatmap, with the three most significant (P- adjusted) transcripts from the analyses displayed. NA are transcripts without annotation.

In the control cell versus the control cell treated with E2 analysis the three most significant transcripts were ENST00000361681.2 (*MT-ND6*), and two transcripts of *MTRNR2L11,* ENST00000604646.1 and ENST00000540040.2; all three transcripts were observed at a higher level following E2 stimulation (Figure 7-6). MT-ND6 is mitochondrially encoded NADH:ubiquinone oxidoreductase core subunit-6, and functions to enable NADH dehydrogenase activity within the mitochondrial respiratory chain. MT-RNR2 Like 11 (pseudogene) is predicted to enable receptor antagonist activity functioning in the negative regulation of the execution phase of apoptosis.

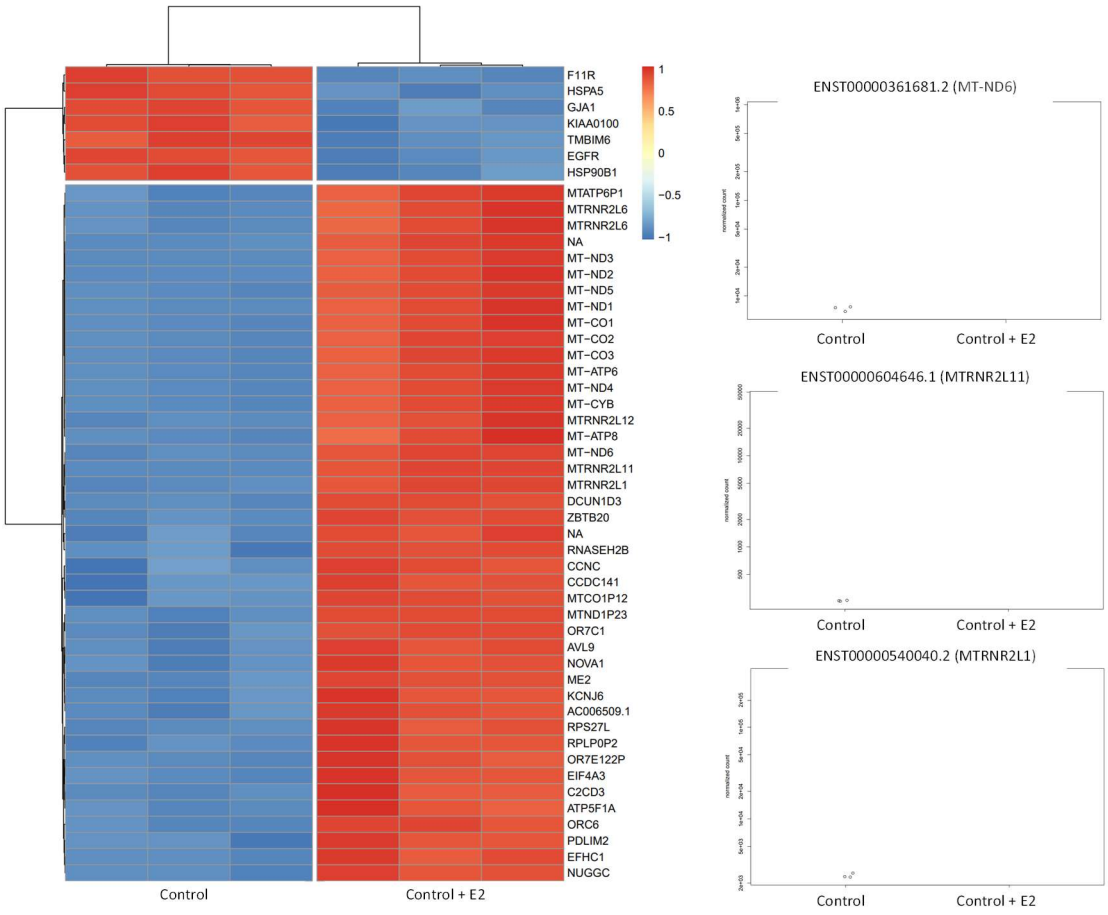


Figure 7-6: Differential transcript expression is summarised for the control cells versus control cells treated with E2 analysis. The top 50 most significant (P- adjusted) transcripts with a greater than 2-fold change in expression labelled with the corresponding gene identifier are displayed in a heatmap, with the three most significant (P- adjusted) transcripts from the analyses displayed. NA are transcripts without annotation.

In the DARPP-32 knockdown cell treated with E2 versus control cell treated with E2 the three most significant differentially expressed transcripts were ENST00000375258.8 (*METTL8*), ENST00000593035.5 (*TPGS2*), and ENST00000515059.5 (*BMPR1B*) (Figure 7-7). *METTL8*, or methyltransferase 8, methylcytidine enables mRNA methyltransferase activity and is involved in mRNA methylation was decreased when DARPP-32 knockdown cells were stimulated with E2 compared with control. *TGPS2*, or tubulin polyglutamylase complex subunit-2 was downregulated in DARPP-32 knockdown cells versus control, when both stimulated with E2, and encodes a component of the neuronal polyglutamase complex that plays a role in the post-translational addition of glutamate to tubulin tales. *BMPR1B*, or bone morphogenetic protein (BMP) receptor type 1B was upregulated in DARPP-32

knockdown cells were treated with E2 when compared with control cells treated with E2. *BMPR1B* is a member of the BMP receptor family; BMPs, the ligands of the receptor are involved in bone formation and embryogenesis.

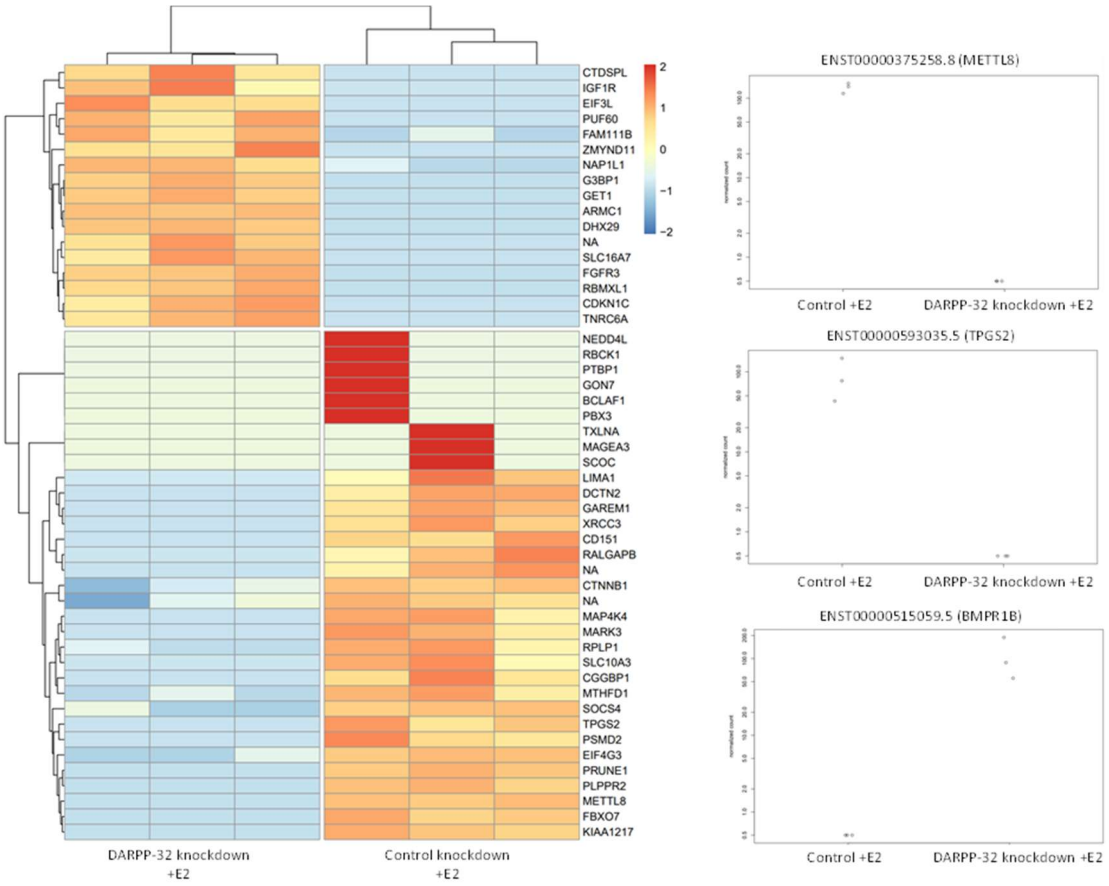


Figure 7-7: Differential transcript expression is summarised for the DARPP-32 knockdown cells treated with E2 versus the control cells treated with E2 analysis. The top 50 most significant (P- adjusted) transcripts with a greater than 2-fold change in expression labelled with the corresponding gene identifier are displayed in a heatmap, with the three most significant (P- adjusted) transcripts from the analyses displayed. NA are transcripts without annotation.

The top three significant differentially expressed transcripts identified in the DARPP-32 knockdown cell treated versus DARPP-32 knockdown cell treated with PKAi analysis were ENST00000260356.5 (*THBS1*), ENST00000295524.4 (*CLDN1*), and ENST00000224784.10 (*ACTA2*) (Figure 7-8). In all cases, a down regulation of transcripts were observed in DARPP-32 cells treated with PKAi cells when compared to DARPP-32 cells alone. THSBP1, or thrombospondin-1, is an adhesive glycoprotein that mediates cell to cell and cell to matrix interactions. CLDN1, or claudin-1, also plays a role in cell adhesion in tight junctions. ACTA2, or actin alpha-2, smooth muscle is one of six actin proteins involved in a variety of cellular functions including cell motility and structure. There are 9 genes identified in one control replicate and no others; future studies should include a minimum of 5 biological replicates.

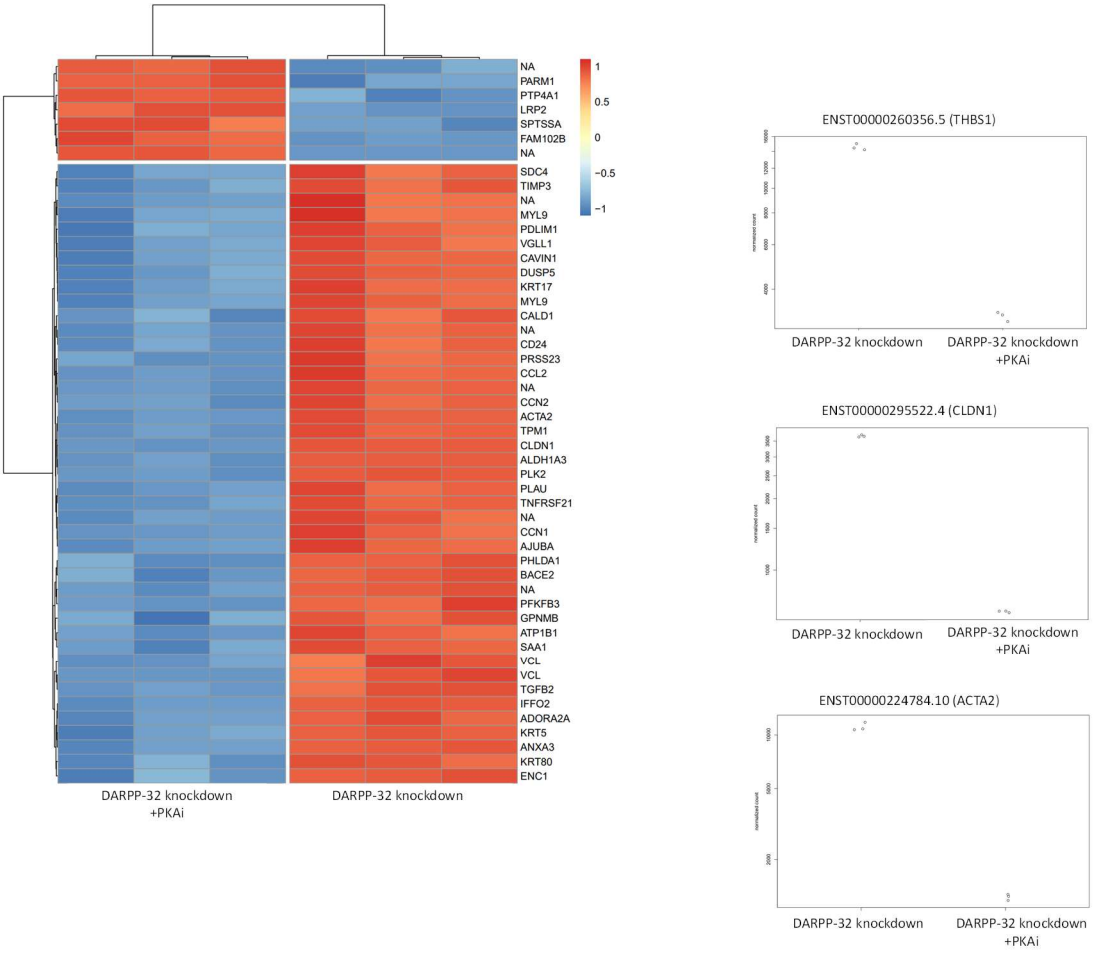


Figure 7-8: Differential transcript expression is summarised for the DARPP-32 knockdown cells versus DARPP-32 knockdown cells treated with PKAi analysis. The top 50 most significant (P- adjusted) transcripts with a greater than 2-fold change in expression labelled with the corresponding gene identifier are displayed in a heatmap, with the three most significant (P- adjusted) transcripts from the analyses displayed. NA are transcripts without annotation.

The top three significant differentially expressed transcripts identified in the control cell versus control cell treated with PKAi analysis were ENST00000372764.4 (*PLAU*), ENST00000451137.7 *(CCN1*) and ENST00000223095.4 (*SERPINE1*); in all three cases, transcripts were downregulated following the addition of PKAi (Figure 7-9). *PLAU*, or plasminogen activator urokinase, is a serine protease that converts plasminogen to plasmin, *CCN1*, or cellular communication network factor-1 functions to promote endothelial cell adhesion, and *SERPIN1*, or serpin family E member-1, is a member of the serine protease inhibitor superfamily and acts to inhibit tissue plasminogen activator and urokinase.

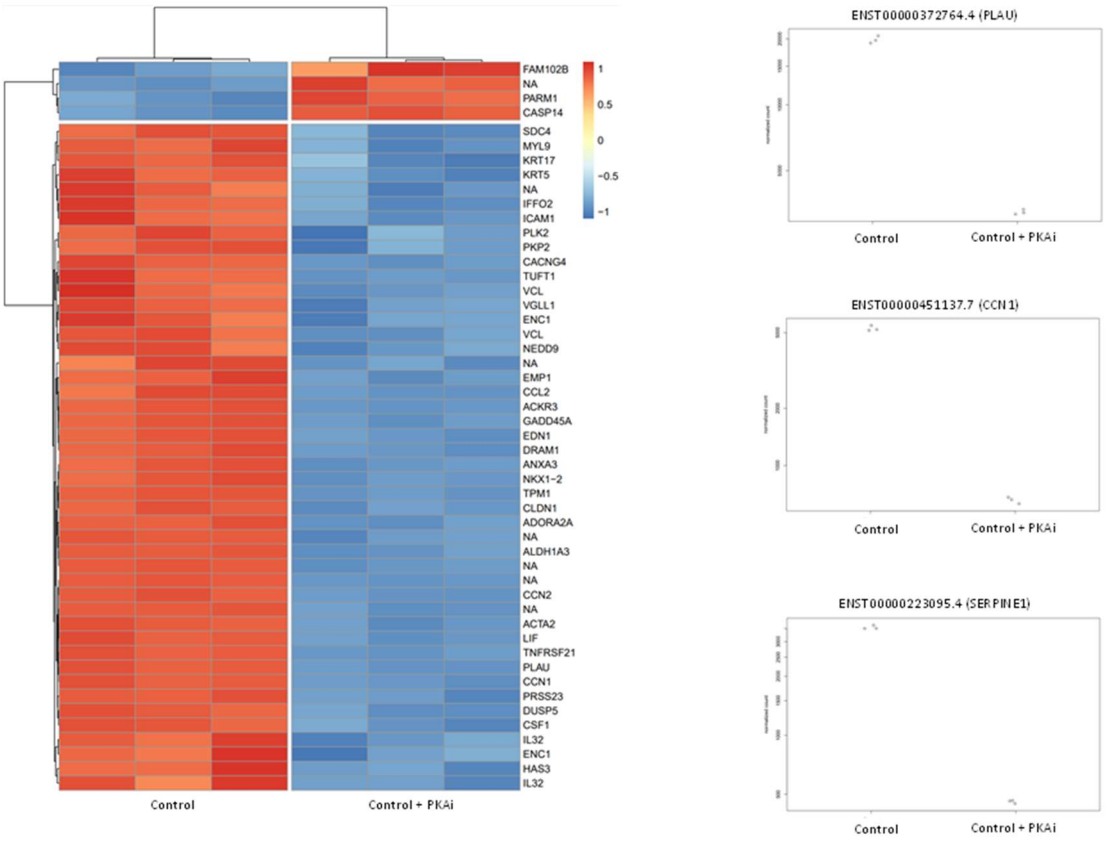


Figure 7-9: Differential transcript expression is summarised for the control cells versus control cells treated with PKAi analysis. The top 50 most significant (P- adjusted) transcripts with a greater than 2-fold change in expression labelled with the corresponding gene identifier are displayed in a heatmap, with the three most significant (P- adjusted) transcripts from the analyses displayed. NA are transcripts without annotation.

The top three significant transcripts identified when DARPP-32 knockdown cells treated with PKAi were compared with control cells treated with PKAi were ENST00000652269.1 (*ELMO3*), ENST00000643625.1 (*TSC1*) and ENST00000637526.1 (*ATP6AP2*) (Figure 7-10). Downregulation of *ELMO3*, or engulfment and cell motility-3, was observed in DARPP-32 cells treated with a PKAi, and functions in cell migration. Upregulation of *TSC1*, or hamartin, was observed in DARPP-32 knockdown cells treated with PKAi is a tumour suppressor that interacts and stabilises GTPase activating protein tuberin to negatively regulate mammalian target of rapamycin complex 1 (mTORC1).

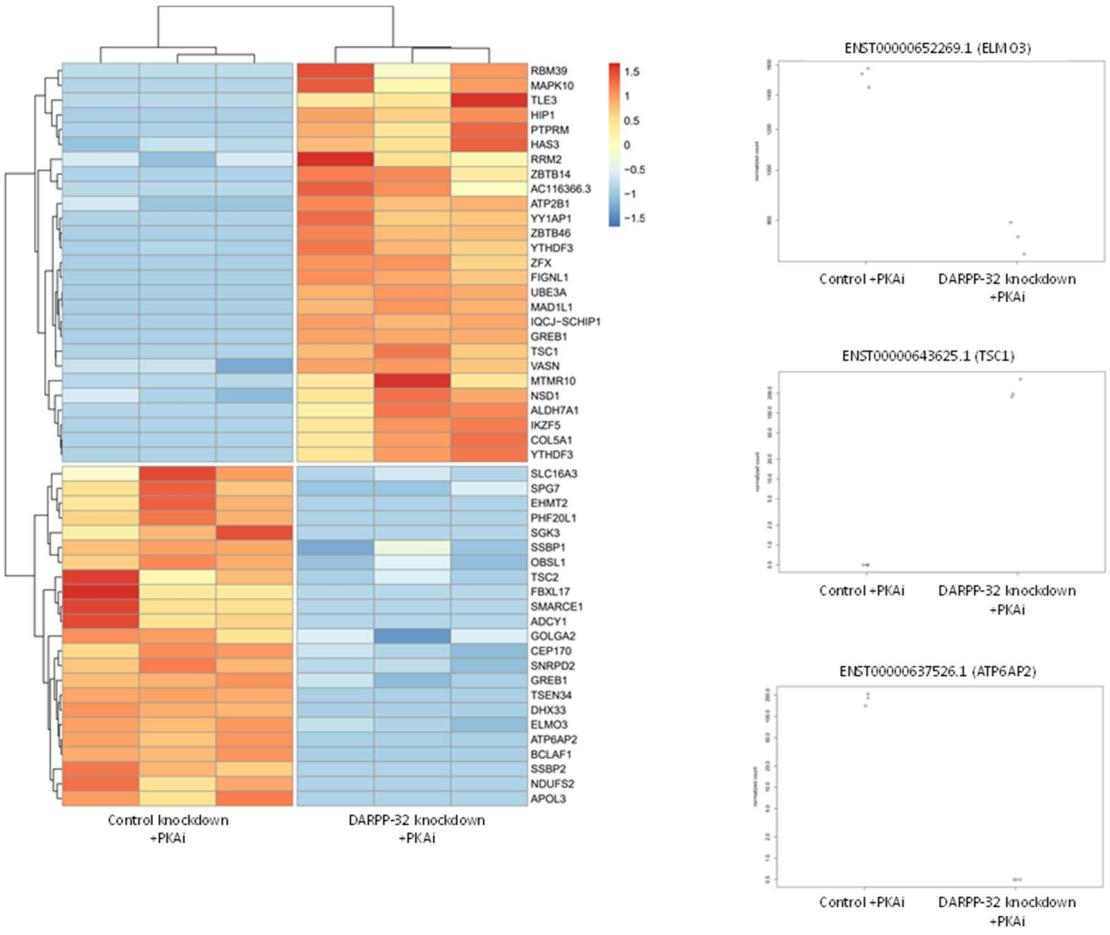


Figure 7-10: Differential transcript expression is summarised for the DARPP-32 knockdown cell treated with PKAi versus control cell treated with PKAi analysis. The top 50 most significant (P- adjusted) transcripts with a greater than 2-fold change in expression labelled with the corresponding gene identifier are displayed in a heatmap, with the three most significant (P- adjusted) transcripts from the analyses displayed. NA are transcripts without annotation.

A Venn diagram was created as a graphical solution to indicate overlap between the differentially expressed transcripts in the analysis groups defined by E2 stimulation (Figure 7-11), or PKA inhibition (Figure 7-12). There were two transcripts common to the DARPP-32 knockdown cells versus control cells and the DARPP-32 knockdown cells treated with E2 versus control cells treated with E2 analysis groups; ENST00000625998.2 and ENST00000651280.1, which correspond to transcripts of gene identifier *PROSER1* (proline and serine rich 1) and *SART3* (spliceosome associated factor 3 U4/U6 recycling protein) respectively; all other genes were unique to each of the two analyses (Figure 7-11).

When four analyses were compared to determine the effect of E2 on cells with differing expression levels of DARPP-32 (Figure 7-11), there were 51 transcripts unique to DARPP-32 knockdown cells versus control cells, and only 9 unique transcripts to the DARPP-32 knockdown cells treated with E2 versus control cells treated with E2. There

were a large proportion of overlapping transcripts (29775) between cells treated with E2, irrespective of DARPP-32 expression levels; however, this meant that there were 12866 unique transcripts were identified when DARPP-32 knockdown cells were compared with DARPP-32 knockdown cells treated with E2, and 10290 transcripts when control cells were compared with control cells treated with E2.

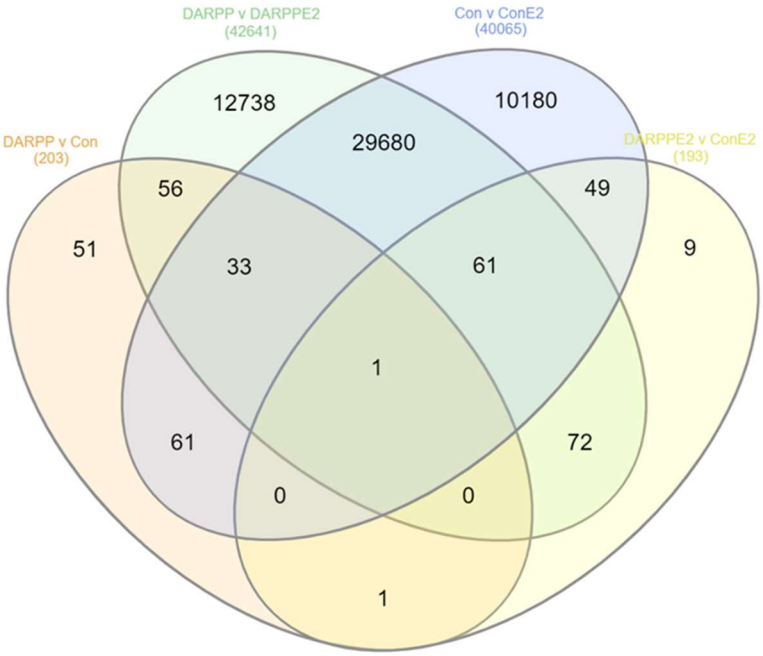


Figure 7-11: Venn diagram to show overlap in differentially expressed transcripts between the four different analysis group, created using InteractiVenn, created by Heberle et al (2015) (68). Group names are reduced: DARPP v Con: DARPP-32 knockdown versus control cells, DARPP v DARPPE2: DARPP-32 knockdown versus DARPP-32 knockdown treated with E2, Con v ConE2: control cells versus control cells treated with E2, DARPPE2 v ConE2: DARPP-32 knockdown cells treated with E2 versus control cells treated with E2.

When four analyses were compared to determine the effect of PKA inhibition on cells with differing expression levels of DARPP-32 (Figure 7-12), there were a number of overlapping transcripts identified. Between DARPP-32 knockdown cells treated with PKAi, and the control cells treated with PKAi, there was 519 overlapping transcripts. When DARPP-32 knockdown cells treated with a PKAi were directly compared with control cells treated with PKAi 130 unique transcripts were identified.

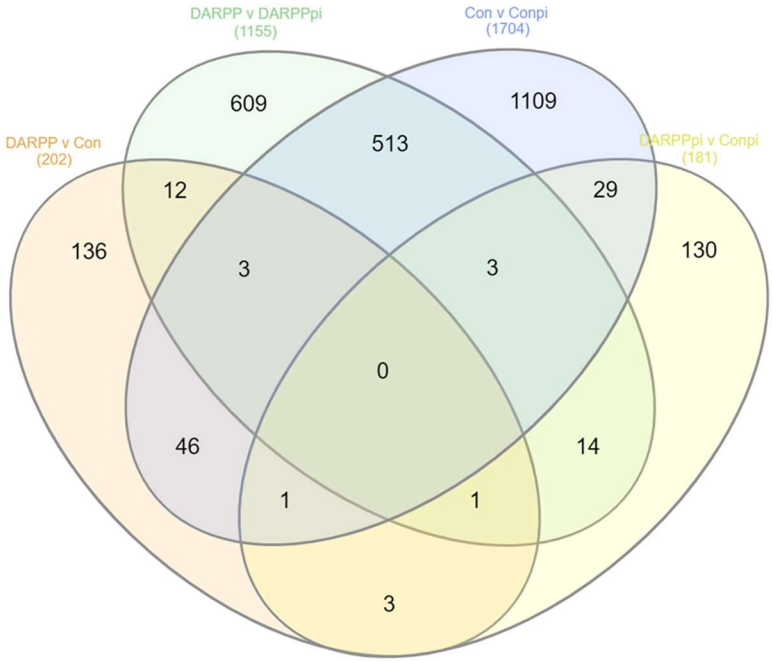


Figure 7-12: Venn diagram to show overlap in differentially expressed transcripts between the four different analysis group, created using InteractiVenn, created by Heberle et al (2015) (68). Group names are reduced: DARPP v Con: DARPP-32 knockdown versus control cells, DARPP v DARPPpi: DARPP-32 knockdown versus DARPP-32 knockdown treated with PKAi, Con v Conpi: control cells versus control cells treated with PKAi, DARPPpi v Conpi: DARPP-32 knockdown cells treated with PKAi versus control cells treated with PKAi.

7.4 DARPP-32 signalling partners in DARPP-32 knockdown cells

Qiagen IPA was used to explore the list of differentially expressed genes in each analyses for a known or putative relationship with DARPP-32 (*PPP1R1B*). Only one direct node, *MAPK3*, was identified in the DARPP-32 knockdown cell versus control cell analysis; however, this fed into others, including *YWHAZ*, *TRAP1* and *TRAF5* (Figure 7-13). *YWHAZ* was one of the top three most significant differentially expressed transcripts identified in this analysis.

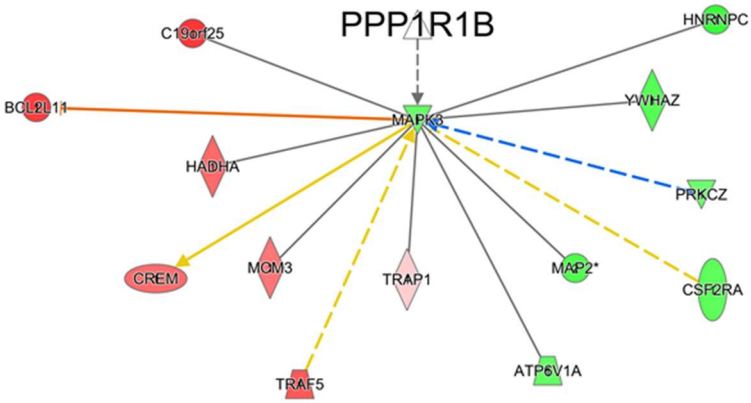


*Figure 7-13: Differentially expressed genes in the DARPP-32 knockdown cell versus control cell analysis were searched to determine if a known relationship with DARPP-32 (PPP1R1B) had previously been reported. Differentially expressed genes were then searched to determine if a relationship had been reported with these direct nodes. Genes in red showed increased expression and genes in green showed decreased expression. Connecting lines are coloured orange when the relationship leads to activation, blue when it leads to inhibition, yellow if the finding is inconsistent with the state of the downstream molecule and grey when the effect is not predicted. Solid lines denote a direct interaction and a dotted line denotes an indirect interaction, * denotes that there are multiple identifiers within the dataset for the gene.*

7.5 DARPP-32 signalling partners and E2 stimulation

DARPP-32 knockdown cells or control cells treated with E2 were examined using Qiagen IPA to identify known or putative relationships with DARPP-32; this was then expanded to determine if there were any further differentially expressed genes directly associated with this related partner if there were less than 5 known genes with an interaction with DARPP-32. There were many genes identified with a known effect up or downstream of DARPP-32 in both the DARPP-32 knockdown cell versus the DARPP-32 knockdown cell treated with E2 and the control cell versus control cell treated with E2 analysis; however, many of these were common to both data sets and were therefore most likely an effect of E2 stimulation (Figure 7-14 and Figure 7-15). Analysis of genes unique in the DARPP-32 knockdown cell versus DARPP-32 knockdown cell treated with E2 compared with the control cell versus control cell treated with E2 were identified for further analysis.

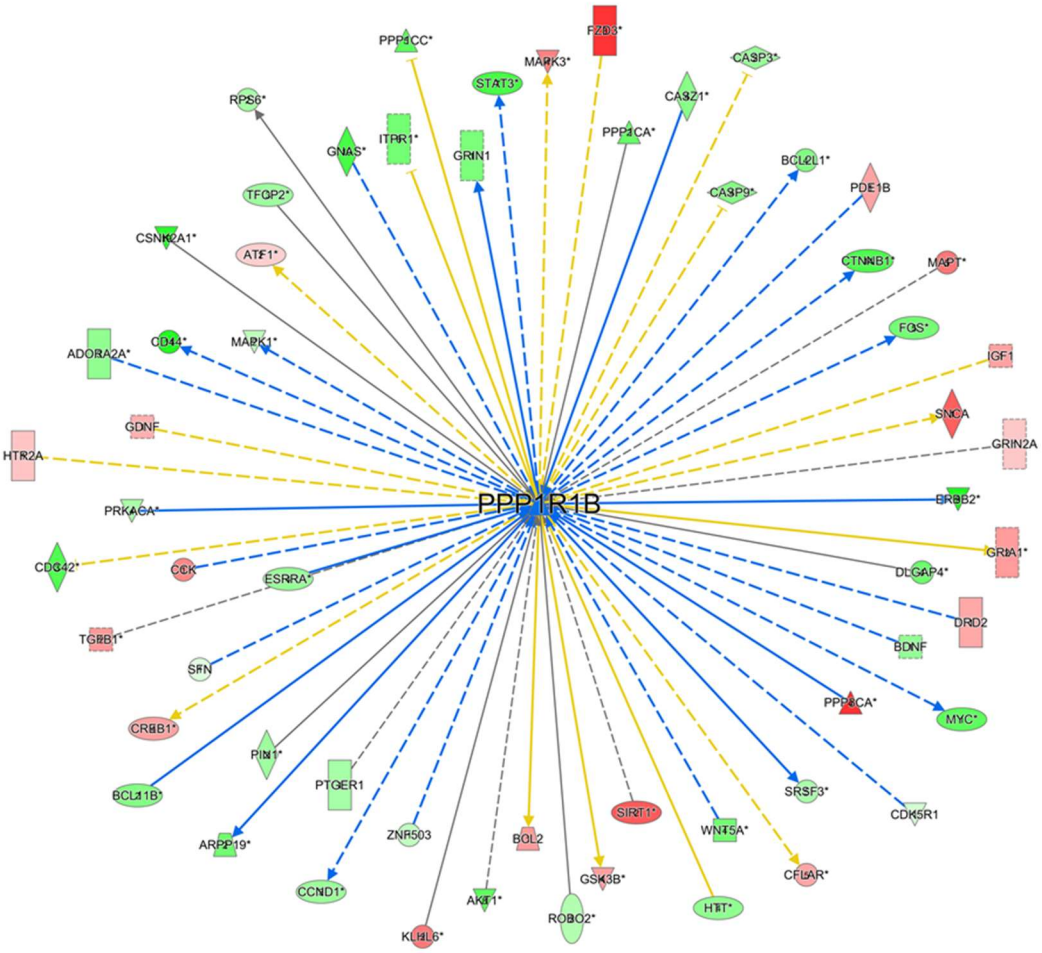


*Figure 7-14: Differentially expressed genes in the DARPP-32 knockdown cell versus DARPP-32 knockdown cell treated with E2 analysis were searched to determine if a known relationship with DARPP-32 (PPP1R1B) had previously been reported. Genes in red showed increased expression and genes in green showed decreased expression. Connecting lines are coloured orange when the relationship leads to activation, blue when it leads to inhibition, yellow if the finding is inconsistent with the state of the downstream molecule and grey when the effect is not predicted. Solid lines denote a direct interaction and a dotted line denotes an indirect interaction, * denotes that there are multiple identifiers within the dataset for the gene.*

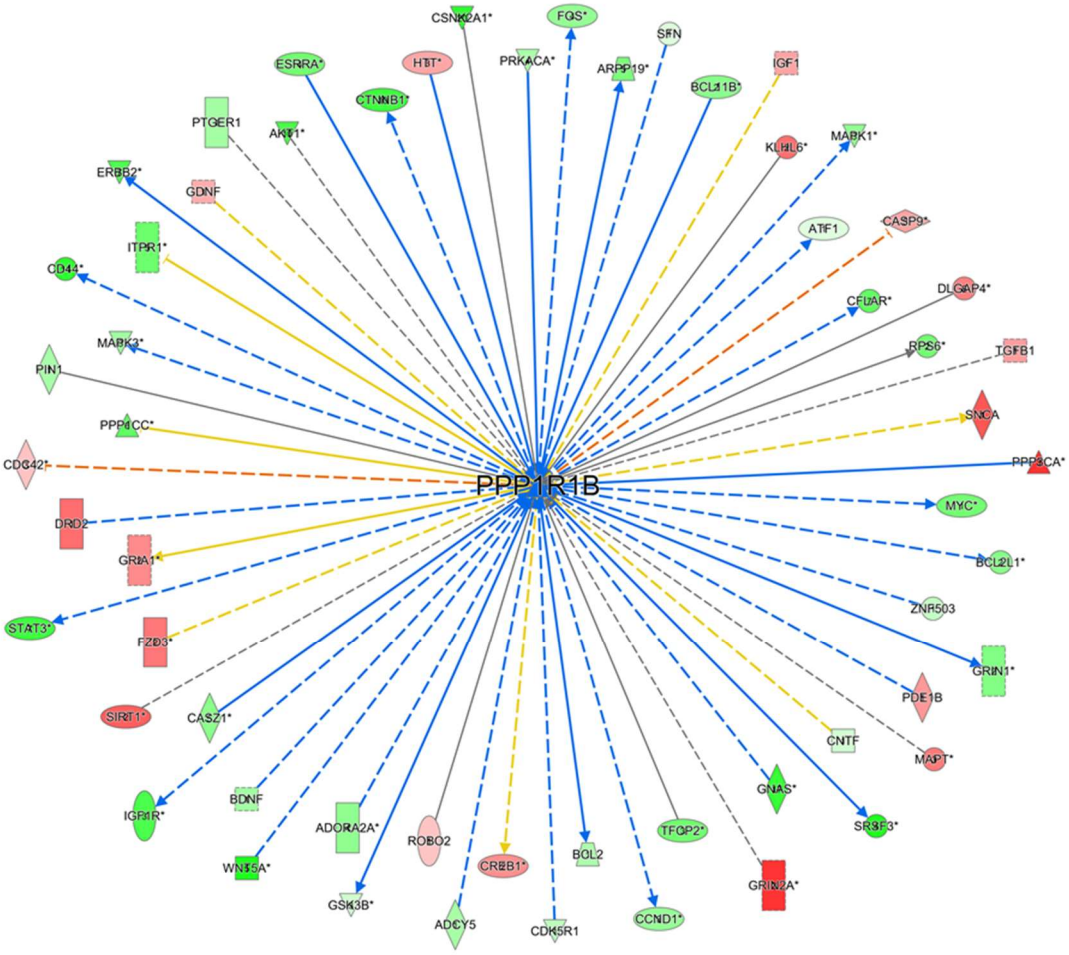


*Figure 7-15: Differentially expressed genes in the control cell versus control cell treated with E2 analysis were searched to determine if a known relationship with DARPP-32 (PPP1R1B) had previously been reported. Genes in red showed increased expression and genes in green showed decreased expression. Connecting lines are coloured orange when the relationship leads to activation, blue when it leads to inhibition, yellow if the finding is inconsistent with the state of the downstream molecule and grey when the effect is not predicted. Solid lines denote a direct interaction and a dotted line denotes an indirect interaction, * denotes that there are multiple identifiers within the dataset for the gene.*

There were three genes with a known or putative interaction with DARPP-32 identified in the DARPP-32 knockdown cell treated with E2 versus control cell treated with E2 analysis; these were *SIRT1*, *CTNNB1* and *IGF1R* (Figure 7-16). Only *SIRT1* was identified in both DARPP-32 and control cell treated with E2 analyses; the other two genes were unique to this analysis.

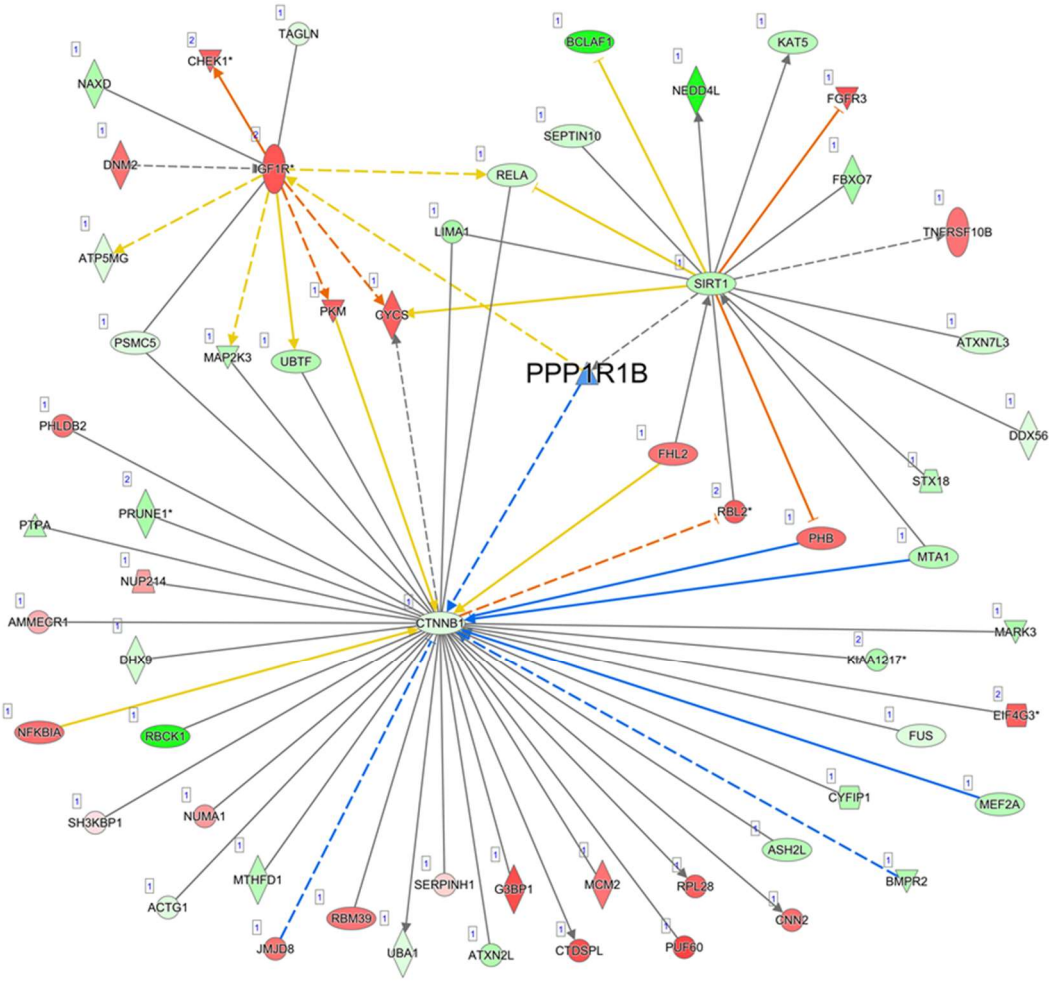


*Figure 7-16: Differentially expressed genes in the DARPP-32 knockdown cell treated with E2 versus control cell treated with E2 analysis were searched to determine if a known relationship with DARPP-32 (PPP1R1B) had previously been reported. Differentially expressed genes were then searched to determine if a relationship had been reported with these direct nodes. Genes in red showed increased expression and genes in green showed decreased expression. Connecting lines are coloured orange when the relationship leads to activation, blue when it leads to inhibition, yellow if the finding is inconsistent with the state of the downstream molecule and grey when the effect is not predicted. Solid lines denote a direct interaction and a dotted line denotes an indirect interaction, * denotes that there are multiple identifiers within the dataset for the gene.*

The top 10 up and down regulated genes in terms of log2 fold change in expression in the DARPP-32 knockdown cell treated with E2 versus control cell treated with E2 analysis are shown in Table 7-3. The top 10 downregulated genes were *BCLAF1*, *NEDD4L*, *MAGEA3*, *RBCK1*, *PTBP1*, *GON7*, *PBX3*, *TXLNA*, and *METTL8*. The top 10 upregulated genes were *CTDSPL*, *ARMC1*, *FGFR3*, *G3BP1*, *TNRC6A*, *EIF3L*, *CDKN1C*, *PUF60*, *BMPR1B*, and *SLC16A7*.

Downregulated genes				
Transcript ID	**Gene ID**	**Protein Name**	**Log 2 fold change**	***P*-adj**
ENST00000527613.5	BCLAF1	BCL2 associated transcription factor 1	-21.71	2.22E-05
ENST00000400345.8	NEDD4L	NEDD4 like ubiquitin protein ligase	-21.69	2.22E-05
ENST00000598245.2	MAGEA3	MAGE family member A3	-21.69	2.22E-05
ENST00000415942.5	RBCK1	RANBP2-type and C3HC4-type zinc finger containing 1	-21.67	2.22E-05
ENST00000394601.8	PTBP1	Polypyrimidine tract binding protein 1	-27.67	2.22E-05
ENST00000621279.2	GON7	GON7 subunit of KEOPS complex	-21.65	2.22E-05
ENST00000394201.8		Novel transcript	-21.65	2.22E-05
ENST00000373489.10	PBX3	PBX homeobox 3	-21.63	2.23E-05
ENST00000373609.1	TXLNA	Taxilin alpha	-21.14	4.13E-05
ENST00000375258.8	METTL8	Methyltransferase 8, methylcytidine	-9.74	8.97E-11

Upregulated genes				
Transcript ID	**Gene ID**	**Protein Name**	**Log 2 fold change**	***P*-adj**
ENST00000273179.10	CTDSPL	CTD small phosphatase like	8.07	8.24E-06
ENST00000458464.3	ARMC1	Armadillo repeat containing 1	8.09	2.11E-06
ENST00000340107.8	FGFR3	Fibroblast growth receptor 3	8.10	2.11E-06
ENST00000394123.7	GSBP1	G3BP stress granule assembly factor 1	8.16	1.95E-06
ENST00000395799.8	TNRC6A	Trinucleotide repeat containing adaptor 6A	8.20	2.11E-06
ENST00000477256.5	EIF3L	Eukaryotic translation initiation factor 3 subunit L	8.23	2.11E-06
ENST00000631604.1	CDKN1C	Cyclin dependent kinase inhibitor 1C	8.35	1.66E-06
ENST00000453551.6	PUF60	Polu(U) binding splicing factor 60	8.71	1.41E-07
ENST00000515059.5	BMPR1B	Bone morphogenic protein receptor type 1B	9.01	2.53E-07
ENST00000547379.6	SLC16A7	Solute carrier family 16 member 7	9.56	2.49E-06

Table 7-3: Top 10 up and down regulated differentially expressed transcripts in the DARPP-32 knockdown cell treated with E2 versus control cell treated with E2 analysis with log fold change and P-adjusted value shown for each transcript.

A further analysis was then run that compared unique transcripts in the DARPP-32 knockdown cell versus DARPP-32 knockdown cell treated with E2 analysis when compared with control cell versus control cell treated with E2 analysis (n=12866) (Figure 7-17). The top 10 upregulated and downregulated genes that were unique to E2 stimulation in DARPP-32 knockdown cells are shown in Table 7-4. The top 10 downregulated genes when DARPP-32 knockdown cells were treated with E2 were *TMTC1*, *AMOTL1*, *ANO6*, *NACC2*, *MYO1C*, *ECT2*, *RACGAP1*, *PRRC2A*, *TLE3* and *PIK3C2B*. The top 10 upregulated genes were *RACK1*, *PSMA3*, *SPART*, *NCAM1*, *CLPTM1L*, *KIF20A*, *SERINEC2*, *SPATS2L*, *NSMF*, and *RING1*.

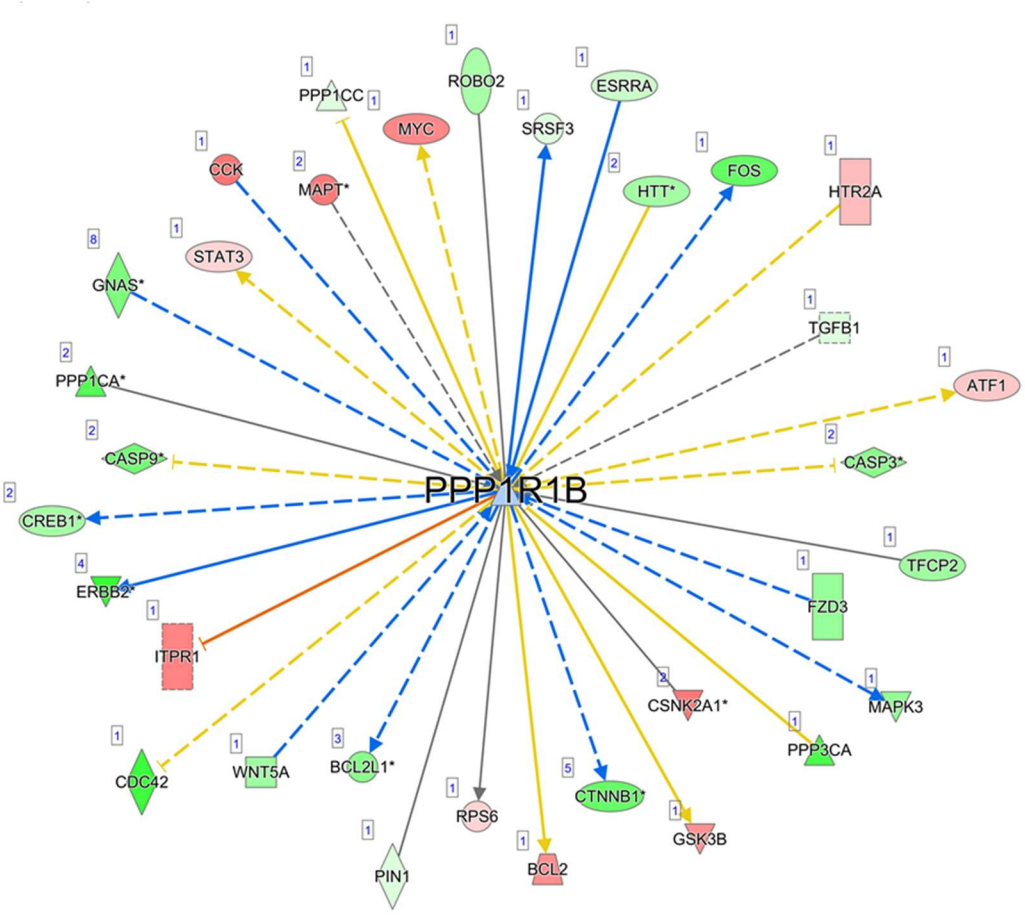


*Figure 7-17: Unique differentially expressed genes the DARPP-32 knockdown cell versus DARPP-32 knockdown cell treated with E2 analysis when compared with control cell versus control cell treated with E2 analysis were searched to determine if a known relationship with DARPP-32 (PPP1R1B) had previously been reported. Differentially expressed genes were then searched to determine if a relationship had been reported with these direct nodes. Genes in red showed increased expression and genes in green showed decreased expression. Connecting lines are coloured orange when the relationship leads to activation, blue when it leads to inhibition, yellow if the finding is inconsistent with the state of the downstream molecule and grey when the effect is not predicted. Solid lines denote a direct interaction and a dotted line denotes an indirect interaction, * denotes that there are multiple identifiers within the dataset for the gene.*

Downregulated Genes				
Transcript ID	**Gene ID**	**Protein Name**	**Log 2 fold change**	***P*-adj**
ENST00000256062.9	TMTC1	Transmembrane O-mannosyltransferase targeting cadherins 1	-11.66	1.75E-19
ENST00000433060.3	AMOTL1	Angiomotin like 1	-11.62	1.03E-19
ENST00000320560.13	ANO6	Anoctamin 6	-11.51	1.03E-19
ENST00000277554.4	NACC2	NACC family member 2	-11.21	7.44E-19
ENST00000361007.7	MYO1C	Myosin IC	-11.07	7.81E-18
ENST00000232458.9	ECT2	Epithelial cell transforming 2	-10.90	5.68E-18
ENST00000312377.10	RACGAP1	Rac GTPase activating protein 1	-10.89	1.8E-17
ENST00000458561.6	PRRC2A	Proline rich coiled-coil 2A	-10.64	1.62E-15
ENST00000558939.5	TLE3	TLE family member 3, transcriptional corepressor	-10.64	8.09E-17
ENST00000367187.7	PIK3C2B	Phosphatidylinositol-4-phosphate 3-kinase catalytic subunit type 2 bet	-10.51	9.67E-17
Upregulated Genes				
Transcript ID	**Gene ID**	**Protein Name**	**Log 2 fold change**	***P*-adj**
ENST00000376817.8	RACK1	Receptor for activated C kinase 1	22.92	4.04E-08
ENST00000557508.5	PSMA3	Proteasome 20S subunit alpha 3	22.85	4.48E-08
ENST00000355182.8	SPART	Spartin	22.76	5.1E-08
ENST00000618266.4	NCAM1	Neural cell adhesion molecule 1	22.74	5.27E-08
ENST00000507807.3	CLPTM1L	CLPTM1 like	22.67	5.83E-08
ENST00000508792.5	KIF20A	Kinesin family member 20A	22.54	7.03E-08
ENST00000373710.5	SERINC2	Serine incorporator 2	22.51	7.33E-08
ENST00000358677.9	SPATS2L	Spermatogenesis associated serine rich 2 like	22.49	7.52E-08
ENST00000371472.6	NSMF	NMDA receptor synaptonuclear signaling and neuronal migration facto	22.47	7.72E-08
ENST00000415941.2	RING1	Ring finger protein 1	22.41	8.44E-08

Table 7-4: Top 10 up and down unique regulated differentially expressed transcripts in the DARPP-32 knockdown cell versus DARPP-32 knockdown cell treated with E2 analysis when compared with control cell versus control cell treated with E2 analysis with log fold change and P-adjusted value shown for each transcript.

7.6 DARPP-32 signalling partners and PKA inhibition

DARPP-32 knockdown cells or control cells treated with a PKA inhibitor were examined using Qiagen IPA to identify known or putative relationships with DARPP-32; this was then expanded to determine if there were any further differentially expressed genes directly associated with this related partner if there were less than 5 known genes with an interaction with DARPP-32. Direct DARPP-32 interacting partners in the DARPP-32 knockdown cell versus DARPP-32 knockdown cell treated with PKAi analysis are shown in Figure 7-18, the control cell versus control cell treated with PKAi analysis in Figure 7-19 and DARPP-32 knockdown cell treated with PKAi versus control cell treated with PKAi analysis in Figure 7-20.

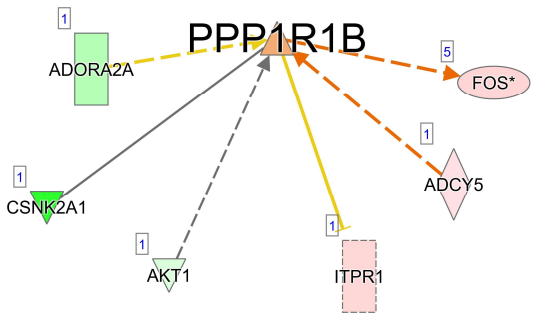


*Figure 7-18: Differentially expressed genes the DARPP-32 knockdown cell versus DARPP-32 knockdown cell treated with PKAi analysis were searched to determine if a known relationship with DARPP-32 (PPP1R1B) had previously been reported. Differentially expressed genes were then searched to determine if a relationship had been reported with these direct nodes. Genes in red showed increased expression and genes in green showed decreased expression following treatment with PKAi. Connecting lines are coloured orange when the relationship leads to activation, blue when it leads to inhibition, yellow if the finding is inconsistent with the state of the downstream molecule and grey when the effect is not predicted. Solid lines denote a direct interaction and a dotted line denotes an indirect interaction, * denotes that there are multiple identifiers within the dataset for the gene.*

When the PKA inhibitor is given to cells that have reduced DARPP-32 expression, a decrease in *ADORA2*, *CSNK2A1*, and *AKT* is observed compared to an increased expression of *FOS*, *ADCY5*, and *ITPR1* (Figure 7-18). When control cells, with wild-type DARPP-32 expression, are treated with a PKAi some of the same genes are identified, indicating a change that is induced by the PKA inhibitor that is independent of DARPP-32 expression and includes *ADORA2*, *CSNK2A1, FOS*, *ADCY5* (Figure 7-19). Some of these genes were identified when cells were also treated with E2, including *ADORA2* and *FOS* (Figure 7-14 and Figure 7-15). Interestingly, following the addition of a PKAi, Qiagen IPA predicts an increase in DARPP-32 activity in both settings; this is due to the assumption DARPP-32 is having increased PKA inhibitory action, rather than the addition of PKA inhibitor fragment (6-22) amide.

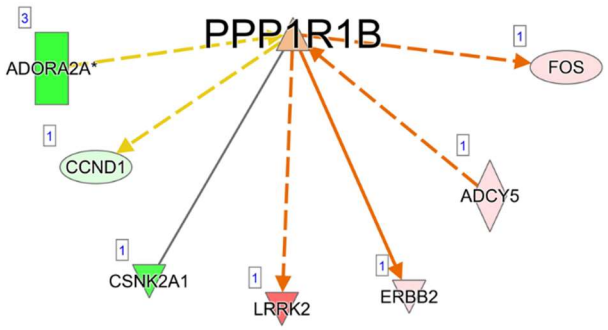


*Figure 7-19: Differentially expressed genes the control cell versus control cell treated with PKAi analysis were searched to determine if a known relationship with DARPP-32 (PPP1R1B) had previously been reported. Differentially expressed genes were then searched to determine if a relationship had been reported with these direct nodes. Genes in red showed increased expression and genes in green showed decreased expression following treatment with a PKAi. Connecting lines are coloured orange when the relationship leads to activation, blue when it leads to inhibition, yellow if the finding is inconsistent with the state of the downstream molecule and grey when the effect is not predicted. Solid lines denote a direct interaction and a dotted line denotes an indirect interaction, * denotes that there are multiple identifiers within the dataset for the gene.*

PKA inhibition in DARPP-32 knockdown cells induced a reduction in gene expression *CTNNB1* in direct comparison to control cells treated with the same inhibitor (Figure 7-20). *CTNNB1* was also identified in the DARPP-32 knockdown cell treated with E2 versus control cell treated with E2 analysis and the Unique differentially expressed genes the DARPP-32 knockdown cell versus DARPP-32 knockdown cell treated with E2 analysis when compared with control cell versus control cell treated with E2 (Figure 7-16 and Figure 7-17).

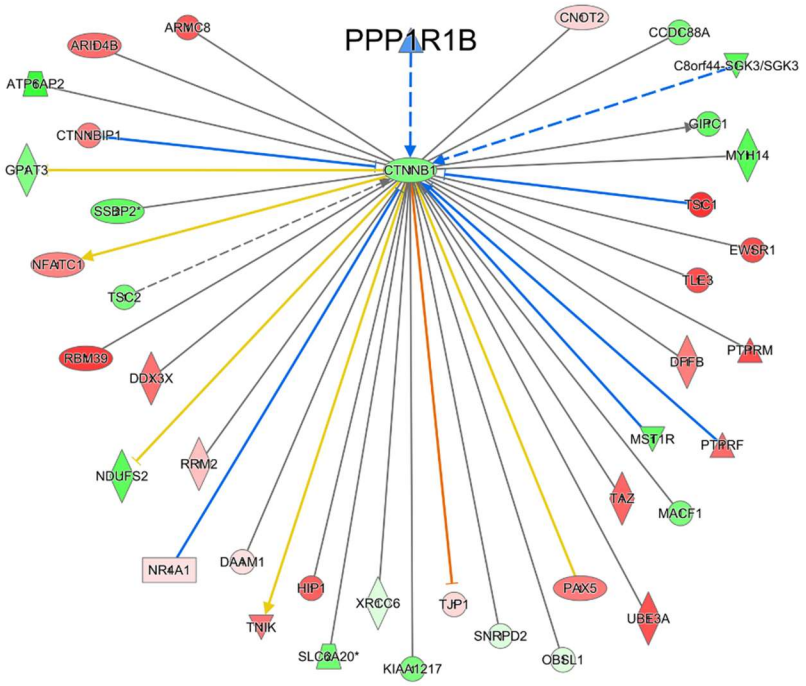


*Figure 7-20: Differentially expressed genes the DARPP-32 knockdown cell treated with PKAi versus control cell treated with PKAi analysis were searched to determine if a known relationship with DARPP-32 (PPP1R1B) had previously been reported. Differentially expressed genes were then searched to determine if a relationship had been reported with these direct nodes. Genes in red showed increased expression and genes in green showed decreased expression. Connecting lines are coloured orange when the relationship leads to activation, blue when it leads to inhibition, yellow if the finding is inconsistent with the state of the downstream molecule and grey when the effect is not predicted. Solid lines denote a direct interaction and a dotted line denotes an indirect interaction, * denotes that there are multiple identifiers within the dataset for the gene.*

7.7 Pathway analyses

Qiagen IPA was then used to perform pathway analysis. Pathway analysis in Qiagen IPA is limited to a maximum of 8000 analysis ready genes, but is preferably limited to between 100 and 2000 genes. For pathway analysis, both the DARPP-32 knockdown cell versus DARPP-32 knockdown cell treated with E2 and the control cell versus the control cell treated with E2 analyses had to be reduced applying a cut off on *P*-adjusted value included to $P<1x10^{-22}$. This cut off reduced the DARPP-32 knockdown cell versus DARPP-32 knockdown cell treated with E2 analysis to 1956 analysis ready molecules and control cell versus the control cell treated with E2 analysis to 1380.

The top 10 most significant pathways identified for each analysis are shown in Figure 7-21. There were 14 canonical signalling pathways that were significantly altered

when DARPP-32 knockdown cells were compared with control cells, 105 pathways significantly altered when DARPP-32 knockdown cells were compared with DARPP-32 cells treated with E2, 94 pathways significantly altered when control cells were compared with control cells treated with E2, and 84 pathways identified when DARPP-32 knockdown cells treated with E2 were compared with control cells treated with E2. For PKA inhibition, the DARPP-32 knockdown cell versus DARPP-32 knockdown cell treated with PKAi analysis identified 241 significantly altered pathways, 296 significantly altered pathways for control cell versus control cell treated with PKAi and 38 significantly altered pathways for the DARPP-32 knockdown cell treated with PKAi versus control cell treated with PKAi analysis.

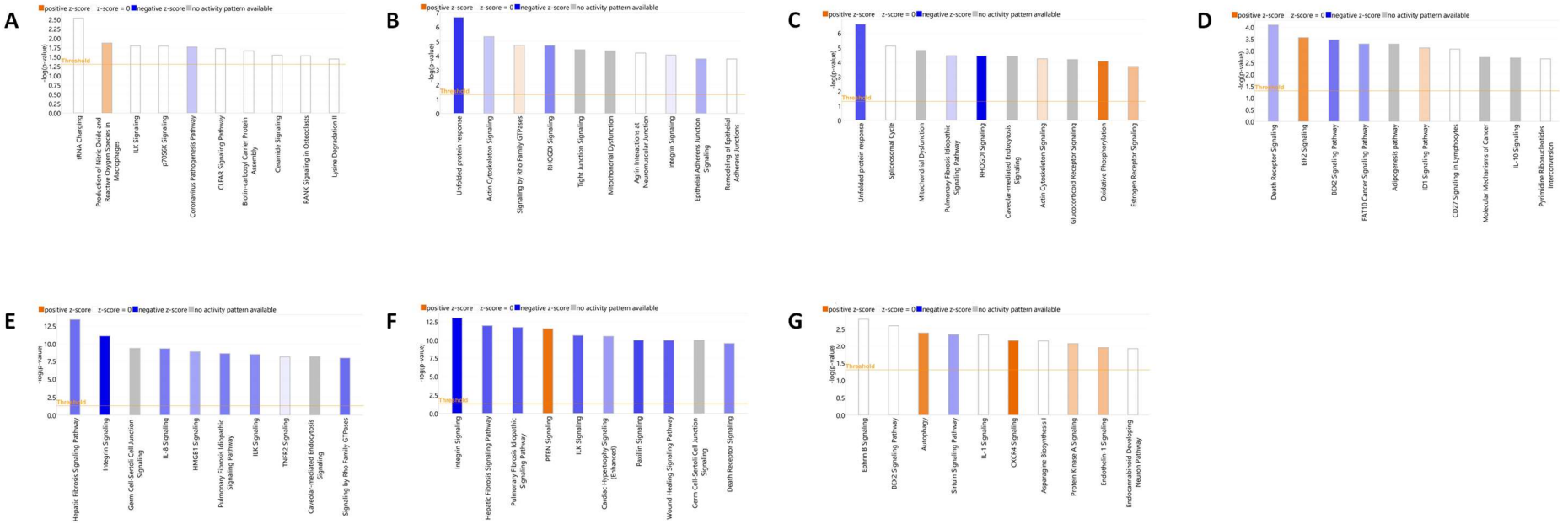


Figure 7-21: Top 10 significant pathways by P value (equivalent P<0.05 threshold indicated) identified using Qiagen IPA, where a positive z-score (orange bar fill) indicates pathway activation, and a negative Z score (blue bar fill) indicates pathway inhibition. A: DARPP-32 knockdown cell versus control cell analysis, B: DARPP-32 knockdown cell versus DARPP-32 knockdown cell treated with E2 analysis, C: control cell versus control cell treated with E2 analysis, D: DARPP-32 knockdown cell treated with E2 versus control cell treated with E2 analysis, E: DARPP-32 knockdown cell versus DARPP-32 knockdown cell treated with PKAi analysis, F: control cell versus control cell treated with PKAi analysis, and G: DARPP-32 knockdown cells treated with PKAi versus control cell treated with PKAi analysis.

Significantly altered pathways identified using Qiagen IPA for DARPP-32 knockdown and E2 treatment are shown in Table 7-5. There were unique and common pathways to the four analysis groups. One pathway was common to all four analyses (ILK signalling), two pathways were common to all DARPP-32 knockdown groups irrespective of E2 treatment (CLEAR signalling pathway and tight junction signalling). One pathway was common to the DARPP-32 knockdown cells versus control cells analysis and the DARPP-32 knockdown cells treated with E2 versus control cells treated with E2 analysis (ceramide signalling). There were three pathways that were common to the DARPP-32 knockdown cells versus control cells analysis and the DARPP-32 knockdown cells versus DARPP-32 knockdown cells treated with E2 (tRNA charging, coronavirus pathogenesis pathway and IGF-1 signalling), with no common pathways with the control cells versus control cells treated with E2 analysis. Pathways common to multiple assessments were assigned higher importance as they were enriched in all analyses were DARPP-32 expression was reduced.

Of the common pathways identified in Qiagen IPA, tight junction signalling and the CLEAR signalling pathway were identified in every situation where DARPP-32 was knocked down when compared with control, irrespective of E2 treatment. The tight junction signalling pathway and CLEAR signalling pathway were explored further in Qiagen IPA, adding DARPP-32 to the pathway as a node (Figure 7-22 and Figure 7-23). In the tight junction pathway, an observed change in expression of PP2A was observed, mapped known and putative changes in activation state based on *PPP1R1B* expression are included in Figure 7-22. The effect on PP2A is mediated by different subunit components in both analyses, with an effect on *PPP2R5C* (protein phosphatase 2 regulatory subunit B gamma) in the DARPP-32 knockdown cell versus control cell analysis and *PTPA* (protein phosphatase 2 phosphatase activator) in the DARPP-32 knockdown cell treated with E2 versus control cell treated with E2 analyses. In the CLEAR signalling pathway, relationships with various known and putative partners fed into change of expression or activity of 14-3-3 and *TFEB*, often through changes in PP2A (Figure 7-23).

Table 7-5: Pathways identified as significantly altered using Qiagen IPA in each analysis. Orange highlighted pathways are common to the DARPP-32 knockdown cells compared with DARPP-32 knockdown cells treated with E2 analysis and the control cells compared with control cells treated with E2 analysis. Yellow highlighted pathways are those pathways common with the DARPP-32 knockdown cells versus control cells analysis and blue highlighted pathways are common with the DARPP-32 knockdown cells treated with E2 versus control cells treated with E2 analysis. The pathway highlighted in green is common to all four pathways. The pathway highlighted in red is common between the DARPP-32 knockdown cells versus control cells analysis and the DARPP-32 knockdown cells treated with E2 versus control cells treated with E2 analysis. The pathways highlighted in grey are common to all pathways except the control cells versus control cells treated with E2 analysis.

DARPP knockdown cells v control cells	DARPP-32 knockdown cells v DARPP-32 knockdown + E2 treated cells	Control cells v control + E2 treated cells	DARPP-32 knockdown + E2 treated cells v control + E2 treated cells
tRNA Charging	Unfolded protein response	Unfolded protein response	Death Receptor Signaling
Production of Nitric Oxide and Reactive Oxygen Species in Macrophages	Actin Cytoskeleton Signaling	Spliceosomal Cycle	EIF2 Signaling
ILK Signaling	Signaling by Rho Family GTPases	Mitochondrial Dysfunction	BEX2 Signaling Pathway
p70S6K Signaling	RHOGDI Signaling	Pulmonary Fibrosis Idiopathic Signaling Pathway	FAT10 Cancer Signaling Pathway
Coronavirus Pathogenesis Pathway	Tight Junction Signaling	RHOGDI Signaling	Adipogenesis pathway
CLEAR Signaling Pathway	Mitochondrial Dysfunction	Caveolar-mediated Endocytosis Signaling	ID1 Signaling Pathway
Biotin-carboxyl Carrier Protein Assembly	Agrin Interactions at Neuromuscular Junction	Actin Cytoskeleton Signaling	CD27 Signaling in Lymphocytes
Ceramide Signaling	Integrin Signaling	Glucocorticoid Receptor Signaling	Molecular Mechanisms of Cancer
RANK Signaling in Osteoclasts	Epithelial Adherens Junction Signaling	Oxidative Phosphorylation	IL-10 Signaling
Lysine Degradation II	Remodeling of Epithelial Adherens Junctions	Estrogen Receptor Signaling	Pyrimidine Ribonucleotides Interconversion
IGF-1 Signaling	Phagosome Maturation	Actin Nucleation by ARP-WASP Complex	TWEAK Signaling
Tight Junction Signaling	Semaphorin Signaling in Neurons	Integrin Signaling	Toll-like Receptor Signaling
Telomerase Signaling	Estrogen Receptor Signaling	Signaling by Rho Family GTPases	Pyrimidine Ribonucleotides De Novo Biosynthesis
Dopamine-DARPP32 Feedback in cAMP Signaling	Spliceosomal Cycle	Role of OCT4 in Mammalian Embryonic Stem Cell Pluripotency	STAT3 Pathway
	Sirtuin Signaling Pathway	Ferroptosis Signaling Pathway	ILK Signaling
	CLEAR Signaling Pathway	Axonal Guidance Signaling	MSP-RON Signaling in Cancer Cells Pathway
	Antigen Presentation Pathway	Regulation of Cellular Mechanics by Calpain Protease	Role of OCT4 in Mammalian Embryonic Stem Cell Pluripotency
	TR/RXR Activation	PTEN Signaling	PTEN Signaling
	Germ Cell-Sertoli Cell Junction Signaling	Agrin Interactions at Neuromuscular Junction	CLEAR Signaling Pathway
	Clathrin-mediated Endocytosis Signaling	Hepatic Fibrosis Signaling Pathway	Small Cell Lung Cancer Signaling
	Coronavirus Pathogenesis Pathway	Neuregulin Signaling	Granzyme B Signaling
	Iron homeostasis signaling pathway	Semaphorin Signaling in Neurons	p53 Signaling
	Insulin Secretion Signaling Pathway	Leukocyte Extravasation Signaling	ATM Signaling
	Aryl Hydrocarbon Receptor Signaling	Clathrin-mediated Endocytosis Signaling	Role of Osteoblasts, Osteoclasts and Chondrocytes in Rheumatoid Arthritis
	Protein Ubiquitination Pathway	Paxillin Signaling	TNFR1 Signaling
	HER-2 Signaling in Breast Cancer	Sirtuin Signaling Pathway	Senescence Pathway
	Synaptogenesis Signaling Pathway	PI3K/AKT Signaling	HER-2 Signaling in Breast Cancer
	ILK Signaling	Remodeling of Epithelial Adherens Junctions	Apoptosis Signaling
	Caveolar-mediated Endocytosis Signaling	Sumoylation Pathway	Lymphotoxin β Receptor Signaling
	Axonal Guidance Signaling	Sertoli Cell-Sertoli Cell Junction Signaling	CSDE1 Signaling Pathway
	Leukocyte Extravasation Signaling	Synaptogenesis Signaling Pathway	FAT10 Signaling Pathway
	Oxidative Phosphorylation	NRF2-mediated Oxidative Stress Response	Osteoarthritis Pathway
	Regulation of the Epithelial-Mesenchymal Transition Pathway	Epithelial Adherens Junction Signaling	Role of IL-17A in Arthritis
	Role of OCT4 in Mammalian Embryonic Stem Cell Pluripotency	Germ Cell-Sertoli Cell Junction Signaling	Polyamine Regulation in Colon Cancer
	tRNA Charging	HER-2 Signaling in Breast Cancer	Prostate Cancer Signaling
	IGF-1 Signaling	Ephrin Receptor Signaling	Induction of Apoptosis by HIV1
	NRF2-mediated Oxidative Stress Response	MSP-RON Signaling in Cancer Cells Pathway	Cardiomyocyte Differentiation via BMP Receptors
	Tumor Microenvironment Pathway	Regulation of Actin-based Motility by Rho	IL-15 Production
	Regulation Of The Epithelial Mesenchymal Transition By Growth Factors Pathway	Bladder Cancer Signaling	CD40 Signaling
	mTOR Signaling	G Beta Gamma Signaling	RHOA Signaling
	Glucocorticoid Receptor Signaling	Bupropion Degradation	Remodeling of Epithelial Adherens Junctions
	Superpathway of Serine and Glycine Biosynthesis I	ID1 Signaling Pathway	Clathrin-mediated Endocytosis Signaling
	Pulmonary Fibrosis Idiopathic Signaling Pathway	Aryl Hydrocarbon Receptor Signaling	PPARα/RXRα Activation
	Endoplasmic Reticulum Stress Pathway	PPAR Signaling	IL-6 Signaling
	Hepatic Fibrosis Signaling Pathway	Dilated Cardiomyopathy Signaling Pathway	Pulmonary Healing Signaling Pathway
	Dilated Cardiomyopathy Signaling Pathway	Phagosome Formation	Gα12/13 Signaling
	Reelin Signaling in Neurons	STAT3 Pathway	Role of PKR in Interferon Induction and Antiviral Response
	Virus Entry via Endocytic Pathways	TGF-β Signaling	Huntington's Disease Signaling
	Xenobiotic Metabolism AHR Signaling Pathway	TR/RXR Activation	Role of p14/p19ARF in Tumor Suppression
	Aldosterone Signaling in Epithelial Cells	2-ketoglutarate Dehydrogenase Complex	mTOR Signaling
	Renal Cell Carcinoma Signaling	Semaphorin Neuronal Repulsive Signaling Pathway	Role of BRCA1 in DNA Damage Response
	Molecular Mechanisms of Cancer	KAC Signaling	NAD+ Repair
	Regulation of Cellular Mechanics by Calpain Protease	FAT10 Cancer Signaling Pathway	Glutathione Biosynthesis
	Paxillin Signaling	Molecular Mechanisms of Cancer	Autophagy
	Sertoli Cell-Sertoli Cell Junction Signaling	PPARα/RXRα Activation	TNFR2 Signaling
	Huntington's Disease Signaling	Hypoxia Signaling in the Cardiovascular System	BAG2 Signaling Pathway
	BAG2 Signaling Pathway	PXR/RXR Activation	UPS-stimulated MAPK Signaling
	Glioblastoma Multiforme Signaling	ILK Signaling	4-1BB Signaling in T Lymphocytes
	Sumoylation Pathway	Endoplasmic Reticulum Stress Pathway	BMP signaling pathway
	Ferroptosis Signaling Pathway	Virus Entry via Endocytic Pathways	Type II Diabetes Mellitus Signaling
	Hereditary Breast Cancer Signaling	ERK/MAPK Signaling	MIF-mediated Glucocorticoid Regulation
	Senescence Pathway	Protein Ubiquitination Pathway	Ceramide Signaling
	RHOA Signaling	PAK Signaling	Epithelial Adherens Junction Signaling
	IL-9 Signaling	Cardiac Hypertrophy Signaling	IL-17A Signaling in Fibroblasts
	Regulation of Actin-based Motility by Rho	HGF Signaling	IL-1 Signaling
	Bladder Cancer Signaling	Maturity Onset Diabetes of Young (MODY) Signaling	TGF-β Signaling
	Pancreatic Adenocarcinoma Signaling	CREB Signaling in Neurons	Pulmonary Fibrosis Idiopathic Signaling Pathway
	Serine Biosynthesis	Opioid Signaling Pathway	Human Embryonic Stem Cell Pluripotency
	Palmitate Biosynthesis I (Animals)	NAD biosynthesis II (from tryptophan)	Creatine-phosphate Biosynthesis
	p53 Signaling	Cholesterol Biosynthesis I	Tetrahydrofolate Salvage from 5,10-methenyltetrahydrofolate
	Glycogen Degradation III	Cholesterol Biosynthesis II (via 24,25-dihydrolanosterol)	Folate Polyglutamylation
	Natural Killer Cell Signaling	Cholesterol Biosynthesis III (via Desmosterol)	VEGF Signaling
	IL-8 Signaling	Adipogenesis pathway	Mitochondrial Dysfunction
	Sonic Hedgehog Signaling	Endocannabinoid Neuronal Synapse Pathway	April Mediated Signaling
	MSP-RON Signaling in Cancer Cells Pathway	Role of JAK1 and JAK3 in γc Cytokine Signaling	B Cell Activating Factor Signaling
	AMPK Signaling	Wound Healing Signaling Pathway	MIF Regulation of Innate Immunity
	Glioma Invasiveness Signaling	Tumor Microenvironment Pathway	Virus Entry via Endocytic Pathways
	Actin Nucleation by ARP-WASP Complex	Huntington's Disease Signaling	Tight Junction Signaling
	Ephrin A Signaling	Death Receptor Signaling	Regulation of eIF4 and p70S6K Signaling
	PXR/RXR Activation	DNA Double-Strand Break Repair by Non-Homologous End Joining	PPAR Signaling
	Folate Transformations I	TCA Cycle II (Eukaryotic)	Role of RIG1-like Receptors in Antiviral Innate Immunity
	Colorectal Cancer Metastasis Signaling	Serotonin and Melatonin Biosynthesis	IL-23 Signaling Pathway
	Mitotic Roles of Polo-Like Kinase	Tryptophan Degradation to 2-amino-3-carboxymuconate Semialdehyde	iNOS Signaling
	Cardiac Hypertrophy Signaling	UVA-Induced MAPK Signaling	Acute Phase Response Signaling
	Mismatch Repair in Eukaryotes	Gαi Signaling	
	D-myo-inositol (1,4,5)-trisphosphate Degradation	Dermatan Sulfate Biosynthesis (Late Stages)	
	Adipogenesis pathway	Pulmonary Healing Signaling Pathway	
	Polyamine Regulation in Colon Cancer	Natural Killer Cell Signaling	
	PI3K/AKT Signaling	GP6 Signaling Pathway	
	Neuregulin Signaling	Dermatan Sulfate Biosynthesis	
	Xenobiotic Metabolism CAR Signaling Pathway	CDK5 Signaling	
	Cell Cycle: G2/M DNA Damage Checkpoint Regulation	Telomere Extension by Telomerase	
	VDR/RXR Activation	Role of Tissue Factor in Cancer	
	IL-7 Signaling Pathway	Melatonin Degradation I	
	RAC Signaling		
	PCP (Planar Cell Polarity) Pathway		
	Maturity Onset Diabetes of Young (MODY) Signaling		
	Ephrin Receptor Signaling		
	Inhibition of ARE-Mediated mRNA Degradation Pathway		
	Xenobiotic Metabolism PXR Signaling Pathway		
	Hepatic Fibrosis / Hepatic Stellate Cell Activation		
	Oncostatin M Signaling		
	PPARα/RXRα Activation		
	JAK/STAT Signaling		
	BER (Base Excision Repair) Pathway		

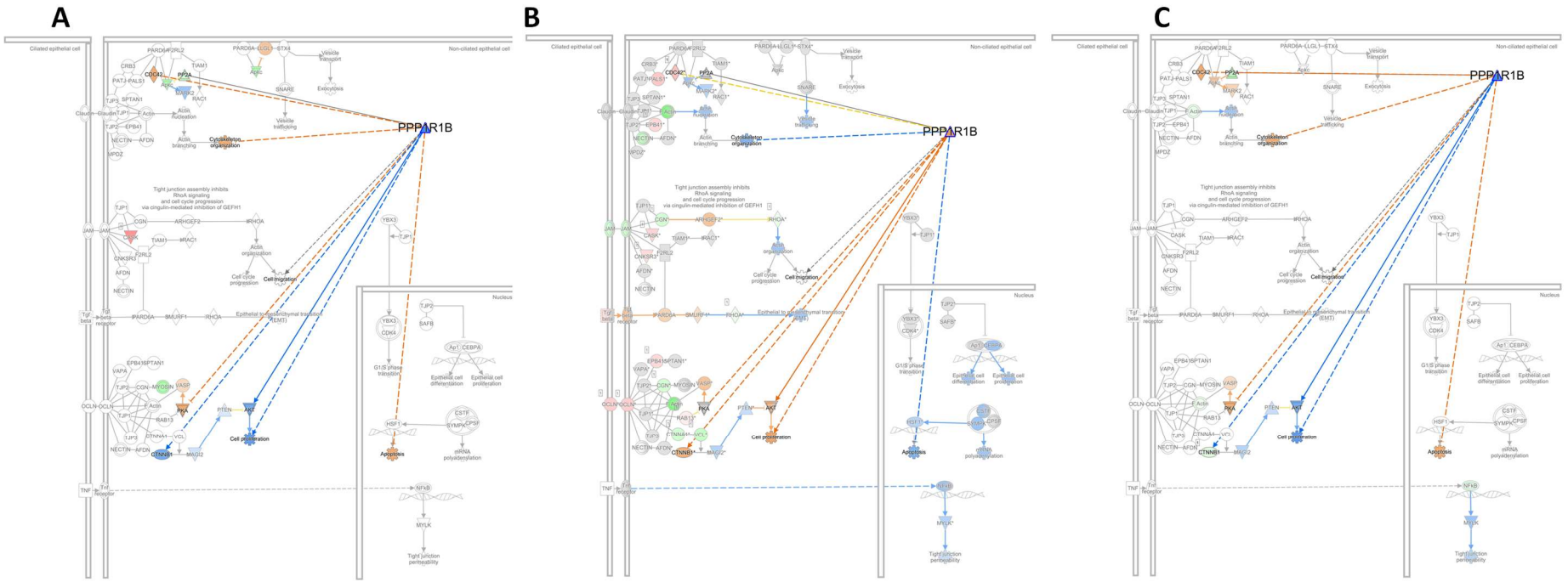


Figure 7-22: Tight junction canonical pathway with PPP1R1B (DARPP-32) added to the pathway. A: DARPP-32 knockdown cell versus control cell analysis, B: DARPP-32 knockdown cell versus DARPP-32 knockdown cell treated with E2 analysis, C: DARPP-32 knockdown cell treated with E2 versus control cell treated with E2 analysis. Genes in red showed increased expression and genes in green showed decreased expression. Genes in blue have a predicted inhibition and genes in orange have a predicted activation. Connecting lines are coloured orange when the relationship leads to activation, blue when it leads to inhibition, yellow if the finding is inconsistent with the state of the downstream molecule and grey when the effect is not predicted.

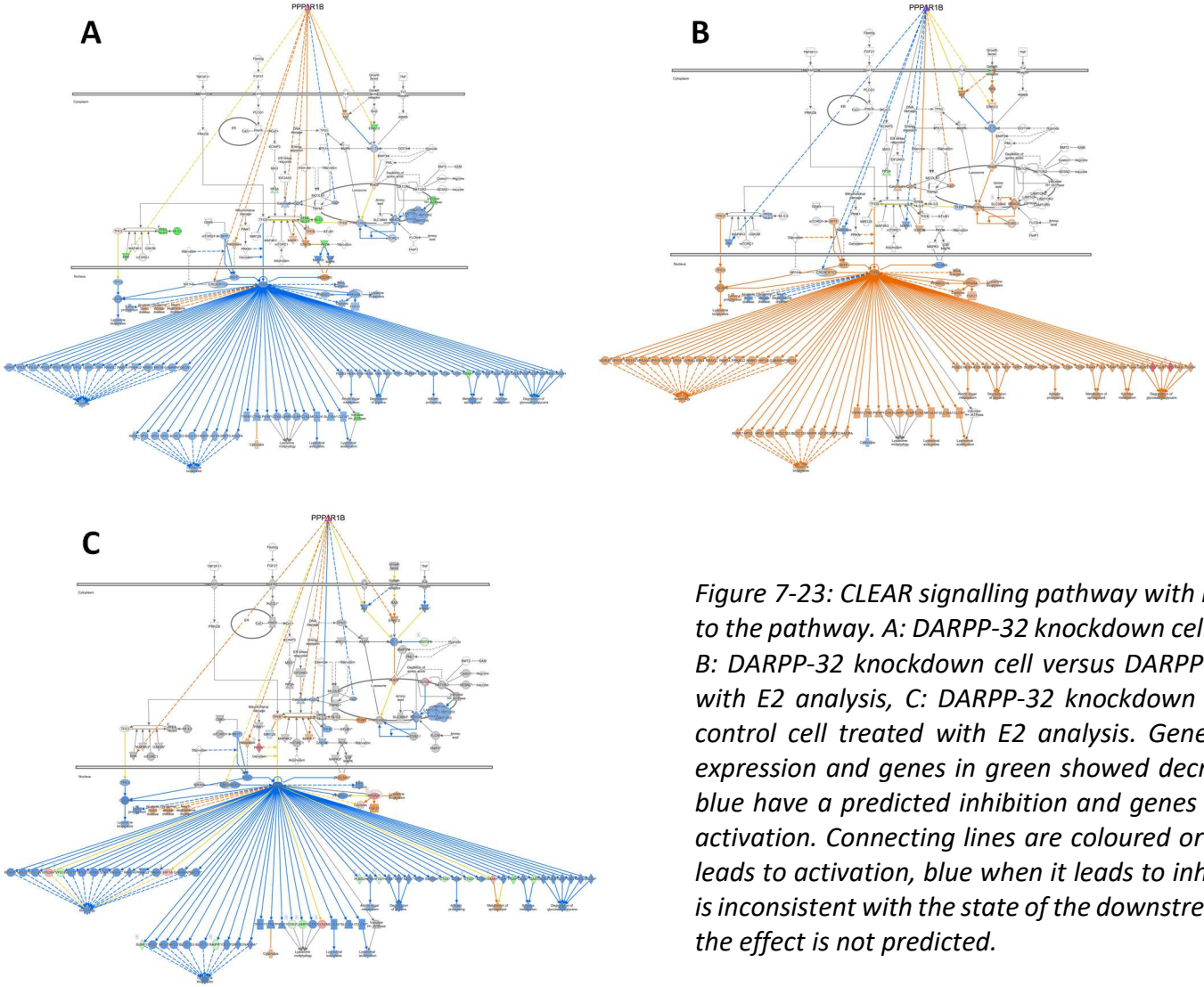


Figure 7-23: CLEAR signalling pathway with PPP1R1B (DARPP-32) added to the pathway. A: DARPP-32 knockdown cell versus control cell analysis, B: DARPP-32 knockdown cell versus DARPP-32 knockdown cell treated with E2 analysis, C: DARPP-32 knockdown cell treated with E2 versus control cell treated with E2 analysis. Genes in red showed increased expression and genes in green showed decreased expression. Genes in blue have a predicted inhibition and genes in orange have a predicted activation. Connecting lines are coloured orange when the relationship leads to activation, blue when it leads to inhibition, yellow if the finding is inconsistent with the state of the downstream molecule and grey when the effect is not predicted.

An addition analysis was run on the transcripts identified as unique in the DARPP-32 knockdown cell versus DARPP-32 knockdown cell treated with E2 analysis when compared with control cell versus control cell treated with E2 analysis (Figure 7-24). Qiagen IPA pathway analysis was reduced by applying a cut off on *P*-adjusted value included to $P<1x10^{-5}$.

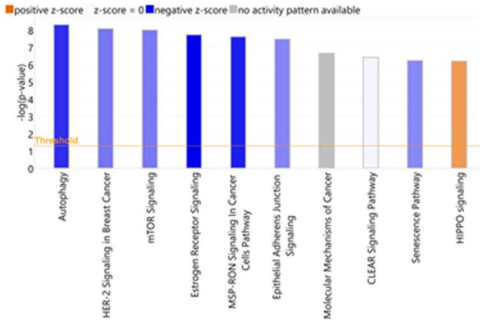


Figure 7-24: Top 10 significant pathways by P value (equivalent P<0.05 threshold indicated) identified using Qiagen IPA, where a positive z-score (orange bar fill) indicates pathway activation and a negative Z score (blue bar fill) indicates pathway inhibition. Analysis performed transcripts identified as unique in the DARPP-32 knockdown cell versus DARPP-32 knockdown cell treated with E2 analysis when compared with control cell versus control cell treated with E2 analysis.

The same pathway assessments were performed following PKA inhibition. Significantly altered pathways identified using Qiagen IPA for DARPP-32 knockdown and PKAi treatment are shown in Table 7-6. Many more pathways were enriched when PKA was inhibited than following E2 stimulation, despite the increased number of differentially expressed transcripts observed following E2 stimulation. There were unique and common pathways in the four analysis groups. One pathway was common to all four analyses: the tight junction pathway. This pathway was also common to all DARPP-32 knockdown groups irrespective of E2 treatment observed in Table 7-5. Pathways common to multiple assessments were assigned higher importance as they were enriched in all analyses were DARPP-32 expression was reduced.

Table 7-6: Pathways identified as significantly altered using Qiagen IPA in each analysis. Orange highlighted pathways are common to the DARPP-32 knockdown cell compared with DARPP-32 knockdown cell treated with PKAi analysis and the control cell compared with control cell treated with PKAi analysis. Yellow highlighted pathways are those pathways common with the DARPP-32 knockdown cell versus control cell analysis and blue highlighted pathways are common with the DARPP-32 knockdown cell treated with PKAi versus control cell treated with PKAi analysis. The pathway highlighted in red is common between the DARPP-32 knockdown cell versus control cell analysis and the DARPP-32 knockdown cell treated with PKAi versus control cell treated with PKAi analysis. Table is continued on following pages.

DARPP-32 knockdown cells v control cells	DARPP-32 knockdown cells v DARPP-32 knockdown cells + PKAi	Control cells v control cells + PKAi	DARPP-32 knockdown + PKAi v control cells + PKAi
tRNA Charging	Hepatic Fibrosis Signaling Pathway	Integrin Signaling	Ephrin B Signaling
Production of Nitric Oxide and Reactive Oxygen Species in Macrophages	Integrin Signaling	Hepatic Fibrosis Signaling Pathway	BEX2 Signaling Pathway
ILK Signaling	Germ Cell-Sertoli Cell Junction Signaling	Pulmonary Fibrosis Idiopathic Signaling Pathway	Autophagy
p70S6K Signaling	IL-8 Signaling	PTEN Signaling	Sirtuin Signaling Pathway
Coronavirus Pathogenesis Pathway	HMGB1 Signaling	ILK Signaling	IL-1 Signaling
CLEAR Signaling Pathway	Pulmonary Fibrosis Idiopathic Signaling Pathway	Cardiac Hypertrophy Signaling (Enhanced)	CXCR4 Signaling
Biotin-carboxyl Carrier Protein Assembly	ILK Signaling	Paxillin Signaling	Asparagine Biosynthesis I
Ceramide Signaling	TNFR2 Signaling	Wound Healing Signaling Pathway	Protein Kinase A Signaling
RANK Signaling in Osteoclasts	Caveolar-mediated Endocytosis Signaling	Germ Cell-Sertoli Cell Junction Signaling	Endothelin-1 Signaling
Lysine Degradation II	Signaling by Rho Family GTPases	Death Receptor Signaling	Endocannabinoid Developing Neuron Pathway
IGF-1 Signaling	Actin Cytoskeleton Signaling	Caveolar-mediated Endocytosis Signaling	CDP-diacylglycerol Biosynthesis I
Tight Junction Signaling	CXCR4 Signaling	Molecular Mechanisms of Cancer	Choline Degradation I
Telomerase Signaling	Death Receptor Signaling	Sertoli Cell-Sertoli Cell Junction Signaling	GABA Receptor Signaling
Dopamine-DARPP32 Feedback in cAMP Signaling	Cardiac Hypertrophy Signaling (Enhanced)	HGF Signaling	Oxytocin Signaling Pathway
	IL-6 Signaling	Regulation Of The Epithelial Mesenchymal Transition By Growth Factors Pathway	Phosphatidylglycerol Biosynthesis II (Non-plastidic)
	Actin Nucleation by ARP-WASP Complex	Actin Cytoskeleton Signaling	Apelin Endothelial Signaling Pathway
	Molecular Mechanisms of Cancer	Virus Entry via Endocytic Pathways	Endocannabinoid Cancer Inhibition Pathway
	Regulation of Actin-based Motility by Rho	Glucocorticoid Receptor Signaling	Glycerol-3-phosphate Shuttle
	PI3K/AKT Signaling	Hepatic Fibrosis / Hepatic Stellate Cell Activation	4-aminobutyrate Degradation I
	Virus Entry via Endocytic Pathways	Regulation of Actin-based Motility by Rho	Endocannabinoid Neuronal Synapse Pathway
	RHOGDI Signaling	HMGB1 Signaling	Apelin Adipocyte Signaling Pathway
	Paxillin Signaling	PAK Signaling	AMPK Signaling
	Sertoli Cell-Sertoli Cell Junction Signaling	PI3K/AKT Signaling	Death Receptor Signaling
	Thrombin Signaling	IL-8 Signaling	Gaq Signaling
	MSP-RON Signaling In Cancer Cells Pathway	TNFR2 Signaling	Germ Cell-Sertoli Cell Junction Signaling
	Regulation of Cellular Mechanics by Calpain Protease	MSP-RON Signaling In Cancer Cells Pathway	Glioblastoma Multiforme Signaling
	Acute Phase Response Signaling	Osteoarthritis Pathway	DNA Methylation and Transcriptional Repression Signaling
	Glioblastoma Multiforme Signaling	Senescence Pathway	Lysine Degradation II
	Cholecystokinin/Gastrin-mediated Signaling	Regulation of Cellular Mechanics by Calpain Protease	Lysine Degradation V
	Gα12/13 Signaling	TNFR1 Signaling	Glutamate Degradation III (via 4-aminobutyrate)
	Protein Kinase A Signaling	Axonal Guidance Signaling	April Mediated Signaling
	PPAR Signaling	Signaling by Rho Family GTPases	B Cell Activating Factor Signaling
	Leukocyte Extravasation Signaling	Erythropoietin Signaling Pathway	Tight Junction Signaling
	Hepatic Fibrosis / Hepatic Stellate Cell Activation	Agrin Interactions at Neuromuscular Junction	G Protein Signaling Mediated by Tubby
	Cardiac Hypertrophy Signaling	Tumor Microenvironment Pathway	α-Adrenergic Signaling
	FAT10 Cancer Signaling Pathway	p53 Signaling	Glycerol Degradation I
	Glioma Invasiveness Signaling	Ephrin Receptor Signaling	Colorectal Cancer Metastasis Signaling
	ERK/MAPK Signaling	IL-6 Signaling	Apelin Muscle Signaling Pathway
	TNFR1 Signaling	Actin Nucleation by ARP-WASP Complex	
	Ephrin Receptor Signaling	Apoptosis Signaling	
	Wound Healing Signaling Pathway	STAT3 Pathway	
	Role of Tissue Factor in Cancer	CLEAR Signaling Pathway	
	Dermatan Sulfate Degradation (Metazoa)	Role of Tissue Factor in Cancer	
	Production of Nitric Oxide and Reactive Oxygen Species in Macrophages	RHOGDI Signaling	
	VDR/RXR Activation	HER-2 Signaling in Breast Cancer	
	NF-κB Activation by Viruses	Role of Macrophages, Fibroblasts and Endothelial Cells in Rheumatoid Arthritis	
	Apoptosis Signaling	IL-17A Signaling in Gastric Cells	
	Role of Macrophages, Fibroblasts and Endothelial Cells in Rheumatoid Arthritis	ID1 Signaling Pathway	
	PTEN Signaling	Agranulocyte Adhesion and Diapedesis	
	Agranulocyte Adhesion and Diapedesis	Neuroinflammation Signaling Pathway	
	IL-1 Signaling	MSP-RON Signaling Pathway	
	TWEAK Signaling	Aryl Hydrocarbon Receptor Signaling	
	Gαq Signaling	CD40 Signaling	
	PEDF Signaling	April Mediated Signaling	
	Axonal Guidance Signaling	Neuregulin Signaling	
	Colorectal Cancer Metastasis Signaling	Chronic Myeloid Leukemia Signaling	
	IL-17A Signaling in Fibroblasts	PPAR Signaling	
	PI3K Signaling in B Lymphocytes	B Cell Activating Factor Signaling	
	ERK5 Signaling	NF-κB Activation by Viruses	
	Semaphorin Signaling in Neurons	Semaphorin Neuronal Repulsive Signaling Pathway	
	Sumoylation Pathway	Role of NFAT in Cardiac Hypertrophy	
	Senescence Pathway	Pulmonary Healing Signaling Pathway	
	Tumor Microenvironment Pathway	Cardiac Hypertrophy Signaling	
	mTOR Signaling	PI3K Signaling in B Lymphocytes	
	PAK Signaling	Protein Kinase A Signaling	
	CLEAR Signaling Pathway	TWEAK Signaling	
	CD40 Signaling	Crosstalk between Dendritic Cells and Natural Killer Cells	
	Osteoarthritis Pathway	Coronavirus Pathogenesis Pathway	
	RAC Signaling	IL-17A Signaling in Fibroblasts	
	Estrogen-Dependent Breast Cancer Signaling	Clathrin-mediated Endocytosis Signaling	
	RHOA Signaling	Oxytocin Signaling Pathway	
	Protein Ubiquitination Pathway	PEDF Signaling	
	Apelin Endothelial Signaling Pathway	Pancreatic Adenocarcinoma Signaling	
	Epithelial Adherens Junction Signaling	Activation of IRF by Cytosolic Pattern Recognition Receptors	
	Endothelin-1 Signaling	Induction of Apoptosis by HIV1	
	VEGF Signaling	HIF1α Signaling	
	Erythropoietin Signaling Pathway	RAC Signaling	
	CDK5 Signaling	Acute Phase Response Signaling	
	IL-10 Signaling	CD27 Signaling in Lymphocytes	
	iNOS Signaling	Role of IL-17A in Arthritis	
	HGF Signaling	Macropinocytosis Signaling	
	Dilated Cardiomyopathy Signaling Pathway	IL-17 Signaling	
	Gap Junction Signaling	Cholecystokinin/Gastrin-mediated Signaling	
	IGF-1 Signaling	Hereditary Breast Cancer Signaling	
	Ceramide Signaling	MYC Mediated Apoptosis Signaling	
	Sphingosine-1-phosphate Signaling	FAT10 Cancer Signaling Pathway	
	NGF Signaling	Ferroptosis Signaling Pathway	
	Crosstalk between Dendritic Cells and Natural Killer Cells	GADD45 Signaling	
	Angiopoietin Signaling	GNRH Signaling	
	Chronic Myeloid Leukemia Signaling	Renal Cell Carcinoma Signaling	
	Toll-like Receptor Signaling	Epithelial Adherens Junction Signaling	
	Granulocyte Adhesion and Diapedesis	Colorectal Cancer Metastasis Signaling	
	Opioid Signaling Pathway	Acute Myeloid Leukemia Signaling	
	Fcγ Receptor-mediated Phagocytosis in Macrophages and Monocytes	G-Protein Coupled Receptor Signaling	
	GNRH Signaling	BEX2 Signaling Pathway	
	Regulation Of The Epithelial Mesenchymal Transition By Growth Factors Pathway	Role of PKR in Interferon Induction and Antiviral Response	
	Oxytocin Signaling Pathway	Role of MAPK Signaling in the Pathogenesis of Influenza	
	BEX2 Signaling Pathway	IL-10 Signaling	
	Small Cell Lung Cancer Signaling	CDK5 Signaling	

Table 7.6 continued

DARPP-32 knockdown cells v control cells	DARPP-32 knockdown cells v DARPP-32 knockdown cells + PKAi	Control cells v control cells + PKAi	DARPP-32 knockdown + PKAi v control cells + PKAi
	Role of Osteoblasts, Osteoclasts and Chondrocytes in Rheumatoid Arthritis	Cellular Effects of Sildenafil (Viagra)	
	Human Embryonic Stem Cell Pluripotency	FGF Signaling	
	Oncostatin M Signaling	Corticotropin Releasing Hormone Signaling	
	HIF1α Signaling	Opioid Signaling Pathway	
	Non-Small Cell Lung Cancer Signaling	Regulation of eIF4 and p70S6K Signaling	
	fMLP Signaling in Neutrophils	BMP signaling pathway	
	Endometrial Cancer Signaling	PPARα/RXRα Activation	
	GADD45 Signaling	GDNF Family Ligand-Receptor Interactions	
	Insulin Secretion Signaling Pathway	Hypoxia Signaling in the Cardiovascular System	
	Role of MAPK Signaling in Promoting the Pathogenesis of Influenza	14-3-3-mediated Signaling	
	Ferroptosis Signaling Pathway	mTOR Signaling	
	Coronavirus Replication Pathway	Role of Pattern Recognition Receptors in Recognition of Bacteria and Viruses	
	TGF-β Signaling	Gαq Signaling	
	Synaptic Long Term Depression	G Beta Gamma Signaling	
	p53 Signaling	Airway Inflammation in Asthma	
	Melanocyte Development and Pigmentation Signaling	Superpathway of Citrulline Metabolism	
	UVA-Induced MAPK Signaling	Role of PI3K/AKT Signaling in the Pathogenesis of Influenza	
	Differential Regulation of Cytokine Production in Macrophages and T Helper Cells by IL-17A and IL-17F	Xenobiotic Metabolism General Signaling Pathway	
	Role of PKR in Interferon Induction and Antiviral Response	Ovarian Cancer Signaling	
	FLT3 Signaling in Hematopoietic Progenitor Cells	Thyroid Cancer Signaling	
	Natural Killer Cell Signaling	Inhibition of Angiogenesis by TSP1	
	Activation of IRF by Cytosolic Pattern Recognition Receptors	CSDE1 Signaling Pathway	
	ERB2-ERBB3 Signaling	Cell Cycle: G1/S Checkpoint Regulation	
	Stearate Biosynthesis I (Animals)	Pyroptosis Signaling Pathway	
	Gαi Signaling	Sphingosine-1-phosphate Signaling	
	Cyclins and Cell Cycle Regulation	Pathogenesis of Multiple Sclerosis	
	BAG2 Signaling Pathway	MIF-mediated Glucocorticoid Regulation	
	FcγRIIB Signaling in B Lymphocytes	NRF2-mediated Oxidative Stress Response	
	HIPPO signaling	Role of JAK1, JAK2 and TYK2 in Interferon Signaling	
	IL-15 Production	White Adipose Tissue Browning Pathway	
	RAR Activation	Ephrin B Signaling	
	Circadian Rhythm Signaling	Endometrial Cancer Signaling	
	PDGF Signaling	UVA-Induced MAPK Signaling	
	Cell Cycle: G1/S Checkpoint Regulation	Gαs Signaling	
	Acetyl-CoA Biosynthesis III (from Citrate)	PDGF Signaling	
	UVC-Induced MAPK Signaling	AMPK Signaling	
	BMP signaling pathway	Melanoma Signaling	
	Role of JAK1 and JAK3 in γc Cytokine Signaling	Protein Ubiquitination Pathway	
	α-Adrenergic Signaling	Antigen Presentation Pathway	
	Complement System	UVC-Induced MAPK Signaling	
	Endocannabinoid Neuronal Synapse Pathway	WNT/β-catenin Signaling	
	Ephrin B Signaling	Ceramide Signaling	
	NAD Signaling Pathway	Mouse Embryonic Stem Cell Pluripotency	
	Ketolysis	GDP-glucose Biosynthesis	
		Fc Epsilon RI Signaling	
		ERB2-ERBB3 Signaling	
		Mechanisms of Viral Exit from Host Cells	
		P2Y Purigenic Receptor Signaling Pathway	
		IL-3 Signaling	
		HOTAIR Regulatory Pathway	
		p38 MAPK Signaling	
		Sperm Motility	
		Telomerase Signaling	
		Fcγ Receptor-mediated Phagocytosis in Macrophages and Monocytes	
		Glucose and Glucose-1-phosphate Degradation	
		NAD Signaling Pathway	
		FLT3 Signaling in Hematopoietic Progenitor Cells	
		Factors Promoting Cardiogenesis in Vertebrates	
		Putrescine Degradation III	
		Sirtuin Signaling Pathway	
		Creatine-phosphate Biosynthesis	
		Citrulline-Nitric Oxide Cycle	
		Iron homeostasis signaling pathway	
		Insulin Receptor Signaling	
		Relaxin Signaling	
		UDP-N-acetyl-D-galactosamine Biosynthesis II	
		Cyclins and Cell Cycle Regulation	
		BAG2 Signaling Pathway	
		Cancer Drug Resistance By Drug Efflux	
		FcγRIIB Signaling in B Lymphocytes	
		IL-23 Signaling Pathway	
		ATM Signaling	
		Necroptosis Signaling Pathway	
		Prolactin Signaling	
		Huntington's Disease Signaling	
		Fatty Acid β-oxidation I	
		Phagosome Maturation	
		IL-22 Signaling	
		SPINK1 Pancreatic Cancer Pathway	
		Glycogen Degradation III	
		nNOS Signaling in Skeletal Muscle Cells	
		Apelin Muscle Signaling Pathway	
		Urea Cycle	
		UDP-N-acetyl-D-glucosamine Biosynthesis II	
		EIF2 Signaling	
		Telomere Extension by Telomerase	
		Breast Cancer Regulation by Stathmin1	
		Cell Cycle: G2/M DNA Damage Checkpoint Regulation	
		Role of NANOG in Mammalian Embryonic Stem Cell Pluripotency	
		Apelin Liver Signaling Pathway	
		CCR3 Signaling in Eosinophils	
		FAK Signaling	
		Amyloid Processing	
		Neurotrophin/TRK Signaling	
		D-myo-inositol (1,4,5)-trisphosphate Degradation	
		tRNA Charging	
		WNT/Ca+ pathway	
		Role of BRCA1 in DNA Damage Response	
		Reelin Signaling in Neurons	

Table 7.6 continued

DARPP-32 knockdown cells v control cells	DARPP-32 knockdown cells v DARPP-32 knockdown cells + PKAI	Control cells v control cells + PKAI	DARPP-32 knockdown + PKAI v control cells + PKAI
	Apil Mediated Signaling	Thrombin Signaling	
	JAK/STAT Signaling	ERK/5 Signaling	
	Remodeling of Epithelial Adherens Junctions	LPS-stimulated MAPK Signaling	
	B Cell Activating Factor Signaling	Apelin Endothelial Signaling Pathway	
	Prostate Cancer Signaling	Autophagy	
	Atherosclerosis Signaling	Small Cell Lung Cancer Signaling	
	MIF Regulation of Innate Immunity	IL-1 Signaling	
	CD27 Signaling in Lymphocytes	ERK/MAPK Signaling	
	Role of IL-17A in Arthritis	Role of Hypercytokinemia/hyperchemokinemia in the Pathogenesis of Influenza	
	LPS-stimulated MAPK Signaling	MSP-RON Signaling in Macrophages Pathway	
	NRF2-mediated Oxidative Stress Response	Hepatic Cholestasis	
	Prolactin Signaling	Apelin Cardiac Fibroblast Signaling Pathway	
	Neuregulin Signaling	Xenobiotic Metabolism AHR Signaling Pathway	
	MSP-RON Signaling Pathway	Calcium Signaling	
	Coronavirus Pathogenesis Pathway	Leukocyte Extravasation Signaling	
	Corticotropin Releasing Hormone Signaling	TREM1 Signaling	
	Semaphorin Neuronal Repulsive Signaling Pathway	Angiopoietin Signaling	
	Glucocorticoid Receptor Signaling	Role of MAPK Signaling in Inhibiting the Pathogenesis of Influenza	
	4-1BB Signaling in T Lymphocytes	VEGF Signaling	
	MSP-RON Signaling in Macrophages Pathway	Toll-like Receptor Signaling	
	Type II Diabetes Mellitus Signaling	IL-15 Production	
	Phagosome Formation	Role of MAPK Signaling in Promoting the Pathogenesis of Influenza	
	Role of IL-17F in Allergic Inflammatory Airway Diseases	Differential Regulation of Cytokine Production in Macrophages and T Helper Cells by IL-17A and IL-17F	
	Coagulation System	Sumoylation Pathway	
	Renin-Angiotensin Signaling	Endocannabinoid Developing Neuron Pathway	
	HER-2 Signaling in Breast Cancer	JAK/STAT Signaling	
	Hepatic Cholestasis	4-1BB Signaling in T Lymphocytes	
	Acute Myeloid Leukemia Signaling	Bladder Cancer Signaling	
	LXR/RXR Activation	RAR Activation	
	MIF-mediated Glucocorticoid Regulation	Glioma Invasiveness Signaling	
	Telomerase Signaling	Guanosine Nucleotides Degradation III	
	Regulation of the Epithelial-Mesenchymal Transition Pathway	CXCR4 Signaling	
	Estrogen Receptor Signaling	Regulation of the Epithelial-Mesenchymal Transition Pathway	
	Tight Junction Signaling	Gi-12/13 Signaling	
	14-3-3-mediated Signaling	Glioblastoma Multiforme Signaling	
	Regulation of eIF4 and p70S6K Signaling	Role of IL-17A in Psoriasis	
	Chondroitin Sulfate Degradation (Metazoa)	Urate Biosynthesis/Inosine 5'-phosphate Degradation	
	Endocannabinoid Developing Neuron Pathway	Natural Killer Cell Signaling	
	Induction of Apoptosis by HIV1	Adrenomedullin signaling pathway	
	Renal Cell Carcinoma Signaling	IL-17A Signaling in Airway Cells	
	Antioxidant Action of Vitamin C	iNOS Signaling	
	G Beta Gamma Signaling	Antioxidant Action of Vitamin C	
	Role of PI3K/AKT Signaling in the Pathogenesis of Influenza	Glioma Signaling	
	ID1 Signaling Pathway	RHOA Signaling	
	Antigen Presentation Pathway	Circadian Rhythm Signaling	
	G-Protein Coupled Receptor Signaling	Remodeling of Epithelial Adherens Junctions	
	EIF2 Signaling	Granulocyte Adhesion and Diapedesis	
	Lymphotoxin β Receptor Signaling	Prostate Cancer Signaling	
	WNT/β-catenin Signaling	RANK Signaling in Osteoclasts	
	Relaxin Signaling	Chemokine Signaling	
	Ovarian Cancer Signaling	Production of Nitric Oxide and Reactive Oxygen Species in Macrophages	
	PPAR/RXR Activation	Endothelin-1 Signaling	
	RANK Signaling in Osteoclasts	GM-CSF Signaling	
	Synaptogenesis Signaling Pathway	Estrogen-Dependent Breast Cancer Signaling	
	Calcium Signaling	IGF-1 Signaling	
	Pulmonary Healing Signaling Pathway	Xenobiotic Metabolism Signaling	
	Adrenomedullin signaling pathway	Differential Regulation of Cytokine Production in Intestinal Epithelial Cells by IL-17A and IL-17F	
	Role of RIG1-like Receptors in Antiviral Innate Immunity	Airway Pathology in Chronic Obstructive Pulmonary Disease	
	Pancreatic Adenocarcinoma Signaling	Adenosine Nucleotides Degradation II	
	GDNF Family Ligand-Receptor Interactions	Netrin Signaling	
	Hypoxia Signaling in the Cardiovascular System	Phagosome Formation	
	Macropinocytosis Signaling	Oxytocin in Brain Signaling Pathway	
	IL-2 Signaling	Oncostatin M Signaling	
	TREM1 Signaling	Role of JAK family kinases in IL-6-type Cytokine Signaling	
	Role of MAPK Signaling in Inhibiting the Pathogenesis of Influenza	Dilated Cardiomyopathy Signaling Pathway	
	Role of NFAT in Cardiac Hypertrophy	LXR/RXR Activation	
	Endocannabinoid Cancer Inhibition Pathway	IL-12 Signaling and Production in Macrophages	
	Thyroid Cancer Signaling	Apelin Cardiomyocyte Signaling Pathway	
	IL-17 Signaling	MIF Regulation of Innate Immunity	
	Chemokine Signaling	Coagulation System	
	Cellular Effects of Sildenafil (Viagra)	Lymphotoxin β Receptor Signaling	
	Differential Regulation of Cytokine Production in Intestinal Epithelial Cells by IL-17A and IL-17F	Tight Junction Signaling	
	Apelin Cardiac Fibroblast Signaling Pathway	VDR/RXR Activation	
	P2Y Purigenic Receptor Signaling Pathway	Human Embryonic Stem Cell Pluripotency	
	Role of MAPK Signaling in the Pathogenesis of Influenza	Type II Diabetes Mellitus Signaling	
	STAT3 Pathway	Interferon Signaling	
	Adipogenesis pathway	Role of RIG1-like Receptors in Antiviral Innate Immunity	
	IL-12 Signaling and Production in Macrophages	Purine Nucleotides Degradation II (Aerobic)	
	IL-17A Signaling in Airway Cells	Role of Osteoclasts, Osteoclasts and Chondrocytes in Rheumatoid Arthritis	
	Notch Signaling	Role of IL-17F in Allergic Inflammatory Airway Diseases	
	Neuroinflammation Signaling Pathway	CREB Signaling in Neurons	
	Autophagy	IL-4 Signaling	
	p38 MAPK Signaling	Gap Junction Signaling	
	Creatine-phosphate Biosynthesis	fMLP Signaling in Neutrophils	
	Oxytocin in Brain Signaling Pathway	Atherosclerosis Signaling	
	Role of IL-17A in Psoriasis	Non-Small Cell Lung Cancer Signaling	
	Insulin Receptor Signaling	ERBB Signaling	
	Aryl Hydrocarbon Receptor Signaling	NGF Signaling	
	Agrin Interactions at Neuromuscular Junction	Synaptogenesis Signaling Pathway	
	GM-CSF Signaling	Estrogen Receptor Signaling	
	Regulation Of The Epithelial Mesenchymal Transition In Development Pathway	Endocannabinoid Cancer Inhibition Pathway	
	IL-17A Signaling in Gastric Cells	TGF-β Signaling	
	Role of JAK1, JAK2 and TYK2 in Interferon Signaling	IL-2 Signaling	
	Hereditary Breast Cancer Signaling	Adipogenesis pathway	
	Glioma Signaling	Renin-Angiotensin Signaling	
	CSDE1 Signaling Pathway	Fatty Acid α-oxidation	
	Gos Signaling	Endocannabinoid Neuronal Synapse Pathway	
	Phosphatidylglycerol Biosynthesis II (Non-plastidic)	Semaphorin Signaling in Neurons	

7.8 Alternate pathway assessments

To explore different pathway analysis methods, GO, Reactome and WebGestalt were utilised to explore the differentially expressed transcripts identified in the DARPP-32 knockdown cell versus control cell analysis, to compare against Qiagen IPA. Qiagen IPA is an excellent tool; however, a licence must be purchased for its use. GO identified zero enriched terms when *P* values were adjusted by Benjamini-Hochberg with a cutoff of 0.05. In Reactome, the overrepresentation analysis identified 629 pathways that were significantly overrepresented and pathway topology is shown in Figure 7-25. Pathway topology analysis considers the connectivity between molecules represented by the pathway steps within the pathway.

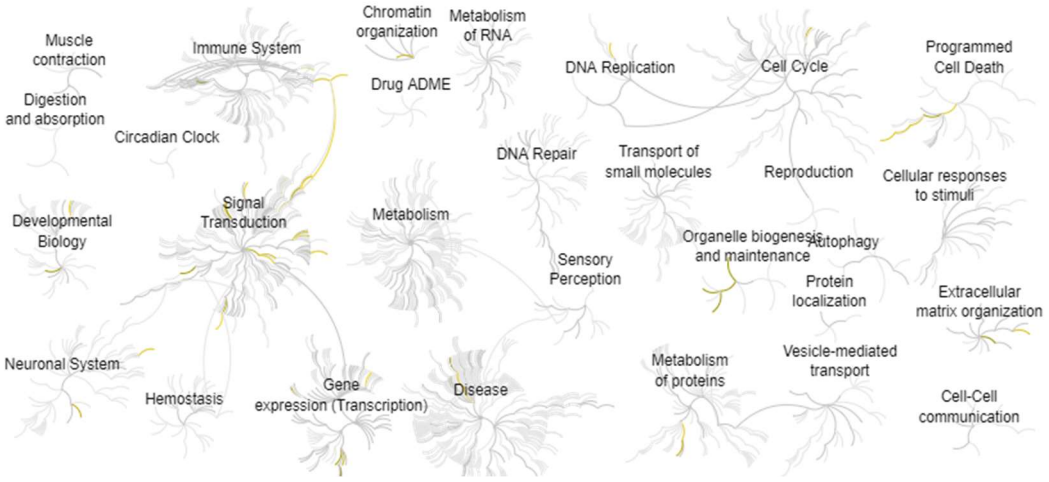


Figure 7-25: Pathway topology of differentially expressed genes mapped using Reactome. Pathways overlayed with colour indicate those overrepresented in the DARPP-32 knockdown cell versus control cell analysis.

WebGestalt was also used to identify pathways in KEGG, Reactome and Panther; but when Benjamini-Hochberg was used as a multiple test of adjustment, no pathways were identified using Panther, KEGG or Reactome; however, assessments could be made less stringent when set to profile the top 10 pathways irrespective of false discovery rate.

7.9 Correlations between signalling partners and DARPP-32 in breast cancer

Known and putative interacting partners of DARPP-32 identified in the DARPP-32 knockdown cell versus control cell analysis, and the DARPP-32 knockdown cell treated with E2 or PKAi versus control cell treated with E2 or PKAi analyses were assessed for associations with patient survival of breast cancer patients using probe level data in the METABRIC cohort. The genes identified in these analyses were *MAPK3*, *SIRT1*,

CTNNB1 and *IGF1R*. As PP2A (subunits *PPP2R5C* and *PTPA*) leading to a *CDC42* change was observed as an overlapping component of the tight junction pathway and *TFEB,* 14-3-3 (isoform *YWHAZ*) in DARPP-32 knockdown cells and E2 stimulation, these genes were also included. This assessment allowed us to determine if a correlation was observed between DARPP-32 expression and differentially expressed transcripts in a large cohort of patient breast tumours, in addition to the links observed in the T47D breast cancer cell line.

Probe level information was retained for assessments, with three probes available for *PPP1R1B*, ILMN_1690096, ILMN_1759012 and ILMN_2304495; for *MAPK3*, two probes were available ILMN_2402341 and ILMN_1667260; for *SIRT1* one probe was available, ILMN_1739083; multiple probes were available for *CTNBB1*, ILMN_1746396, ILMN_1757350, ILMN_1785786, ILMN_1786903, ILMN_1808436, ILMN_1651617, ILMN_1726641; one probe for *IGF1R*, ILMN_1675048, four probes for *CDC42*, ILMN_1675156, ILMN_1696041, ILMN_1738424, ILMN_2408139, one probe for *TFEB*, ILMN_1733616; two probes for YWHAZ, ILMN_1801928 and ILMN_1669286; four probes for *PPP2R5C*, ILMN_1780913, ILMN_1789283, ILMN_1795846 and ILMN_2364971; and finally, four probes for *PPP2R4*, ILMN_2372922, ILMN_1652249, ILMN_1658951 and ILMN_1729123. Each probe aligns a 50-nucleotide sequence within the gene of interest, where multiple probes are available, these often, but not exclusively, map to different gene locations and can correspond to different isoforms.

Spearman rank correlations between *PPP1R1B* probes and the identified partners were determined to identify correlation between probes that exist in patient derived samples and are displayed graphically in Figure 7-26 and in Appendix 2. In breast tumours, consistent observations made between *PPP1R1B* probe expression and *MAPK3, SIRT1* and *IGF1R* expression were observed. *PPP1R1B* was significantly negatively correlated with both *MAPK3* probes (all $P<0.01$, with R^2 values ranging from -0.93 to -0.156), with *SIRT1* expression (all $P<0.05$ with R^2 values ranging from -0.059 to -0.103), and with *IGF1R* probe expression (all $P<0.01$, with R^2 values ranging from -0.125 to -0.221). Less consistent relationships were observed between *PPP1R1B* probes and other signalling partners (Figure 7-26 and Appendix 2).

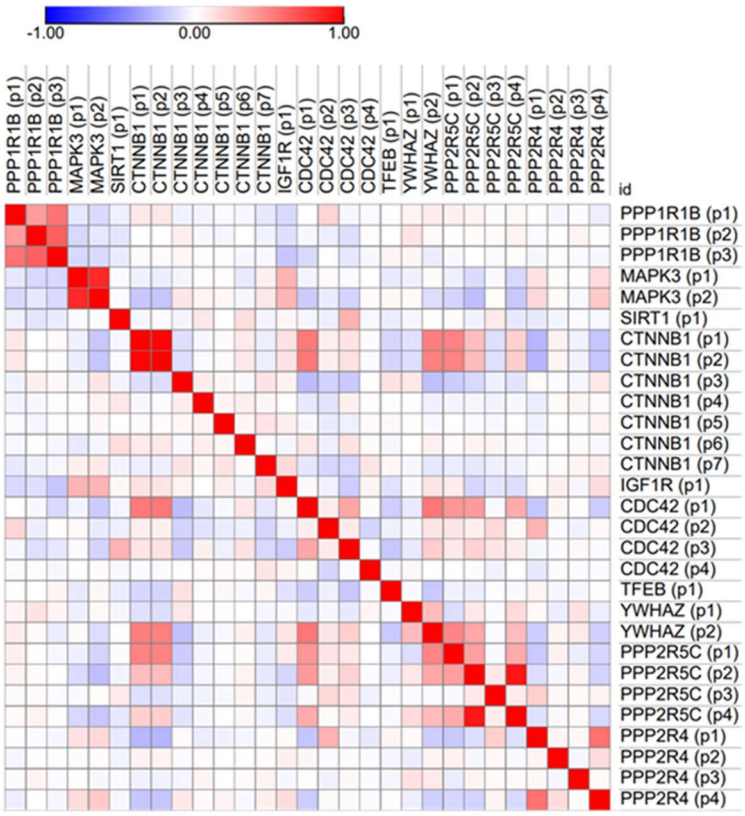


Figure 7-26: Heatmap of Spearman's correlation coefficients for gene expression data for various genes available within the METABRIC cohort.

7.10 Associations between signalling partners and patient survival

Expression of signalling partner probe expression was tested for associations with disease specific survival using the Kaplan-Meier method; this method is typically used when looking at protein expression to determine biomarkers with potential clinically relevant application. Associations between *PPP1R1B* have been described previously (6). Low *SIRT1* expression (P=0.004), low *IGFR1* expression (P<0.001), low *CDC43* (probe 3) expression (P=0.022), high *YWHAZ* (probe 1) expression (P<0.022), low *PPP2R5C* (probe 1) expression (P=0.001), contrasting high expression of *PPP2R5C* probe 2 (P=0.009), and probe 4 (P=0.012), and high expression of *PPP2R4* (probe 3) (P=0.044) were found to be associated with disease specific survival of breast cancer patients Figure 7-27. No associations between *MAPK3*, *CTNNB1*, and *TFEB* expression and survival were observed (data not shown). To expand this research, the continuous data for each gene was explored for association with patient survival using Cox regression (Table 7-7). Similar results were observed to those determined using the Kaplan-Meier method, with *SIRT1*, *IGFR1, CDC42* probe 3, *YWHAZ* probe 1, and *PPP2R5C* probe 1, 2 and 4 all remaining significantly associated with patient survival; in addition, using continuous data, *CTNNB1* probe 3 was now significantly associated with patient survival (Table 7-7).

Gene	Probe	P value	Hazard ratio	95% confidence interval	
				Lower	Upper
MAPK3	probe 1	0.880	0.847	0.699	1.025
	probe 2	0.518	0.942	0.787	1.128
SIRT1	probe 1	**0.008**	0.738	0.590	0.924
CTNNB1	probe 1	0.523	0.959	0.845	1.089
	probe 2	0.402	0.947	0.833	1.076
	probe 3	**0.031**	1.938	1.062	3.535
	probe 4	0.056	1.987	0.982	4.019
	probe 5	0.781	0.904	0.444	1.841
	probe 6	0.176	0.726	0.456	1.155
	probe 7	0.742	0.900	0.481	1.684
IGFR1	probe 1	**>0.001**	0.754	0.649	0.877
CDC42	probe 1	0.281	0.900	0.742	1.091
	probe 2	0.896	1.025	0.713	1.472
	probe 3	**0.014**	0.842	0.734	0.966
	probe 4	0.248	0.698	0.379	1.285
TFEB	probe 1	0.467	1.204	0.730	1.987
YWHAZ	probe 1	**<0.001**	1.547	1.352	1.770
	probe 2	0.790	0.978	0.827	1.156
PPP2R5C	probe 1	**0.002**	0.534	0.358	0.796
	probe 2	**0.001**	1.430	1.147	1.783
	probe 3	0.180	1.300	0.886	1.907
	probe 4	**<0.001**	1.479	1.189	1.839
PPP2R4	probe 1	0.330	1.162	0.859	1.571
	probe 2	0.391	1.311	0.706	2.433
	probe 3	0.439	1.240	0.719	2.139
	probe 4	0.281	1.124	0.909	1.390

Table 7-7: Cox (proportional hazards) regression to determine the relationship between individual continuous gene expression and patient survival with P<0.05 highlighted in bold.

In the METABRIC cohort, tumour size, tumour grade, patient age, ER status, HER2 status, PgR status were all associated with patient survival when assessed using the Kaplan-Meier method (P<0.001). Genes identified as associated with patient survival were included in multivariate assessment including variables associated with patient prognosis; *YWHAZ* probe 1 expression remained associated with survival irrespective of included prognostic variables (P<0.001, hazard ratio = 1.485, 95% confidence interval = 1.204-1.831) (Appendix 3).

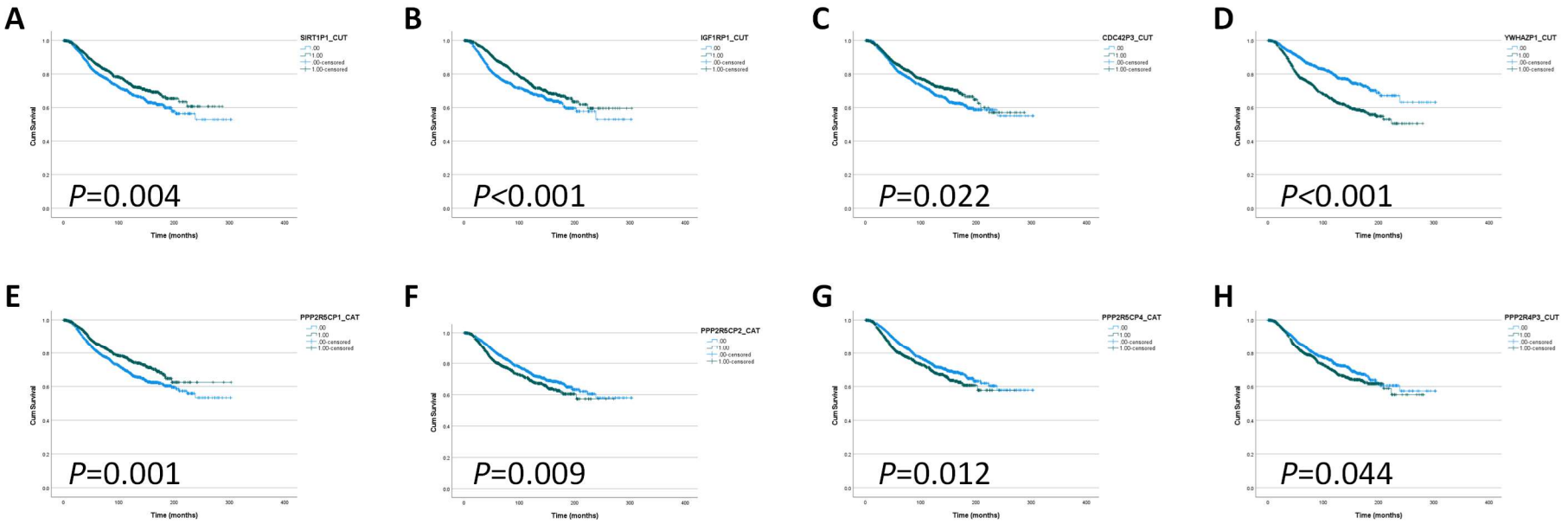


Figure 7-27: Kaplan-Meier breast cancer specific survival curves for gene expression of A: SIRT1 probe 1, B: IGF1R probe 1, C: CDC42 probe 3, D: YWHAZ probe 1, E: PPP2R5C probe 1, F: PPP2R5C probe 2, G: PPP2R5C probe 3 and H: PPP2R4 probe 3. Significance was determined using the log-rank test, 0 denotes low expression, whereas 1 denotes high expression, where expression was categorised around median gene expression.

8 Discussion

We have previously identified that low DARPP-32 expression is associated with poor survival of breast cancer patients, which is particularly apparent in patients with ER positive tumours (6). Despite this observation, we do not know the mechanisms by which DARPP-32 is able to influence breast cancer cell behaviour. This this study sought to understand the transcriptomic changes that occur following changes in DARPP-32 expression, in the presence and absence of oestrogen, in ER positive breast cancer. T47D breast cancer cells were originally derived from the pleural effusion of an infiltrating ductal carcinoma in 1979 (69); the T47D cell line expresses both ER and progesterone receptor, but not HER2, and falls into the luminal A molecular classification of breast cancer (70). The T47D cell line was selected for use within this study as in addition to being ER positive, it demonstrated expression of DARPP-32; DARPP-32 expression is not observed in all ER positive cell lines, such as MCF-7. This study effectively utilised siRNA to reduce DARPP-32 expression in T47D cells, at both the mRNA and protein level. Knockdown of DARPP-32 using siRNA reduced DARPP-32 protein expression by over 95%, and mRNA expression by over 60%. DARPP-32 knockdown and control T47D cells were subject to RNA-Seq to determine transcriptomic changes that occur when DARPP-32 expression is lost in an ER positive breast cancer cell line.

In addition to determining transcriptomic changes resulting from DARPP-32 knockdown in T47D cells, knockdown and control cells were subject to treatment with either E2 or a PKA inhibitor. E2 treatment was performed to determine transcriptomic changes that occur in oestrogen responsive ER positive cells, with the aim of understanding why patients with ER positive breast cancer and low DARPP-32 expression have poor clinical outcomes. The actions of E2, or 17β-estradiol, are mediated by ER, and 10nM E2 treatment in T47D cells has been shown to increase cellular proliferation with significant changes in the transcriptome, including the expression of important cancer associated genes, such as *MYC* (71-74). PKA inhibition with PKA inhibitor fragment (6-22) amide was used determine transcriptomic changes that occur following reduction of PKA mediated DARPP-32 Thr-34 phosphorylation; however, PKA inhibition would also be expected to alter a wide range of cell signalling effects directly through PKA. PKA inhibitor fragment (6-22) amide is a potent inhibitor of PKA that is derived from the active portion of the heat stable PKA inhibitor protein PKI. In T47D cells, 24 hour 3μM PKA inhibitor treatment resulted in a 60% inhibition of PKA, and a 60% decrease in DARPP-32 Thr-34 phosphorylation. Treatment of ER positive MCF-7 breast cancer cells with PKA inhibitor fragment (6-22) amide has been used to demonstrate a link between PKA activity and negative control of E2 action by sex hormone binding globulin (SHBG) (75).

A bioinformatics pipeline that included Trim Galore, Kallisto, Tximport, and DESeq2 was created and differentially expressed transcripts were assessed using

Qiagen IPA. Differentially expressed transcripts identified using DESeq2 demonstrated that the treatment of the ER positive cell line, T47D, was sufficient to elicit large changes in the transcriptome irrespective of DARPP-32 expression, which has been observed in previous publications (74). Interestingly, E2 has been shown to cause differential expression of 7411 genes when comparing T47D breast cancer cells, and another ER positive breast cancer cell line MCF-7 (74). ER is a member of the nuclear receptor superfamily and functions as a transcription factor capable of binding oestrogen response elements and is responsible for the regulation of the expression of genes involved in cell division; over three quarters of all breast cancers express ER. In MCF-7 cells thousands of unique ER binding sites have been identified (2, 3). In this study we identified over 40,000 transcripts when E2 stimulation was compared to non-E2 stimulated cells (both control cells and DARPP-32 knockdown cells); however, many of these transcripts represent multiple isoforms of the same gene. When control cells were compared to control cells stimulated with E2, 40065 transcripts were identified which corresponded to 15258 genes, and when DARPP-32 knockdown cells were compared to DARPP-32 knockdown cells stimulated with E2, 42641 transcripts were identified that corresponded to 15809 genes.

Due to the high number of differentially expressed genes following E2 stimulation, a more stringent fold change and *P* value cut-off was considered; however, as this would be applied to the entire dataset, a cut-off of $P < 0.05$ and a greater than two-fold change, was preferred. This was because one of the primary objectives of this study was not to investigate the role of E2 stimulation in ER positive breast cancer, but to identify changes in the transcriptome that occur when ER positive cells with low DARPP-32 expression are stimulated with E2 when compared with their wild-type counterpart. Interestingly, a number of MT genes were identified when control cells were stimulated with E2, suggesting cells are upregulating metabolism.

Bioinformatics analysis identified differentially expressed transcripts when comparing DARPP-32 knockdown cells to control cells (202), and when DARPP-32 knockdown cells treated with E2 were compared with control cells treated with E2 (193). We were particularly interested to understand how loss of DARPP-32 could affect the transcriptome (DARPP-32 knockdown cells versus control cells analysis), and how that pathway was different in the presence of oestrogen. To determine how oestrogen affects DARPP-32, a number of analyses were performed. Further analyses included DARPP knockdown cells treated with E2 versus control cells treated with E2 to identify transcripts and pathways that were changed next in the presence of oestrogen. Additional analyses of DARPP-32 knockdown cells versus DARPP-32 knockdown cells treated with E2 and control cells versus control cells treated with E2; these analyses demonstrate the effect of oestrogen alone in cells with or without DARPP-32 expression.

The top three significant differentially expressed transcripts identified in the DARPP-32 knockdown cell versus control cell analysis were ENST00000443236.6

(*CPAMD8*), ENST00000521309.5 (*YWHAZ*), and another transcript of *CPAM8*, ENST00000651564.1. Interestingly, one *CPAM8* transcript was reduced, and one was increased in the DARPP-32 knockdown cells, whereas *YWHAZ* expression was reduced in DARPP-32 knockdown cells. In the DARPP-32 knockdown cells, the top 10 downregulated genes by change in log2 fold change in expression were *CLN8*, *GRAMD2B*, *HNRNPC*, *ZCCHC7*, *CMIP*, *OSBPL2*, *TSEN34*, *MAN2C1*, *NDUFS1*, and *MAP2*. Not all genes that fall into the top 10 up and downregulated genes following loss of DARPP-32 expression have been linked with cancer. Focusing on genes that were down regulated when DARPP-32 expression was lost; loss of *HNRNPC* expression has been shown to inhibit breast cancer cellular proliferation *in vitro* (76), and has also been identified as a splice factor involved in aberrant splicing (77). *CMIP* has been shown to regulate triple negative breast cancer growth through a FOXC1 pathway, and reduction in CMIP expression reduces triple negative breast cancer cell proliferation (78), interestingly *NDUFS1*, expression increased in response to FOXQ1, to increase proliferation of MCF7 breast cancer cell lines, MCF7 does not express DARPP-32 (79). Somatic mutations in *OSBPL2* have been identified with poor survival of breast cancer patients (80) and there is evidence that the protein product of *MAN2C1* can attenuate PTEN function in prostate cancer cells (81). High levels of *MAP2* have been shown to increase sensitivity to neoadjuvant taxane based therapy for breast cancer (82).

The top 10 upregulated genes by log2 fold change in expression following DARPP-32 knockdown were *KBTBD11*, *ZNF230*, *BCL2L11*, *ZNF227*, *VKORC1L1*, *C19orf25*, *TSEN35*, *SART3*, *AAGAB* and *CHEK2*. Not all upregulated genes have been linked with breast cancer; however, some have been linked with different tumour types, including *KBTBD11* in colorectal cancer (83). Some of the genes, such as *BCL2L11*, more widely known as BIM, have strong evidence for a role in breast cancer, but typically via pro-apoptotic functions (84), with BIM deficiency *in vivo* causing increased survival of metastatic cells within the lung (85). *CHEK2* is activated by ATM following double strand DNA breaks, and germline mutations in *CHEK2* can lead to hereditary breast cancer (reviewed in (86)). Chk2 expression in breast cancer is not associated with survival of breast cancer patients; however, when low levels of ATM combined with high levels of Chk2 are associated with poor patient survival (87). *VKORC1L1* expression has been shown to be increased in triple negative breast cancer and in advanced stage disease (88). *SART3* has been shown to interact with DNA polymerase η and RAD18 that protects cells from DNA damage (89), but also mediates cross talk between p53 and HIF-1α in hypoxia (90). Finally, *AAGAB* expression has been linked to adverse survival of patients receiving neoadjuvant chemotherapy (91).

Known and putative DARPP-32 interacting partners were identified within differentially expressed gene lists. There was only one known direct interacting partner identified in the DARPP-32 knockdown versus control cell analysis; *MAPK3*. In DARPP-32 knockdown cells, *MAPK3* expression was significantly downregulated. DARPP-32 has been shown to be required for MAPK signalling in thyroid cancer, and similarly to the results observed here, DARPP-32 knockdown resulted in a reduction in the sensitivity of MAPK signalling (92). *MAPK3* was also observed in the DARPP-32

knockdown cell versus DARPP-32 knockdown cell treated with E2 and the control cell versus the control cell treated with E2 analyses. Interestingly, however, a different relationship was observed; *MAPK3* was upregulated in DARPP-32 knockdown cells when treated with E2, when in control cells also treated with E2, a downregulation was observed. This may indicate that *MAPK3* expression can be recovered in the presence of oestrogen when DARPP-32 expression is low. There were a number of differentially expressed genes that were also known or putative partners of PKA within the DARPP-32 knockdown cell versus control cell analysis; *CREM*, *PRKCZ*, *MAPK3*, *MAP2*, *CBFA2T3*.

In the DARPP-32 knockdown cell treated with E2 versus control cell treated with E2 analysis the top 10 downregulated genes were *BCLAF1*, *NEDD4L*, *MAGEA3*, *RBCK1*, *PTBP1*, *GON7*, *PBX3*, *TXLNA*, and *METTL8*. Not all down-regulated genes have a role in breast cancer, with some described in other tumour types, such as *BCLAF1* (reviewed in (93)). *NEDD4L* expression in breast cancer is associated with improved survival and has been shown to be involved in NOTCH1 activation (94). RBCK1 has been shown modulate ER expression and is postulated to act as an ER coactivator (95). *PBX3* has been identified as downregulated during the process of breast cancer metastasis (96). Perhaps surprisingly, *MAGEA3*, *PTBP1* and *METTL8* were identified as downregulated; expression of MAGEA3 has been shown to be associated with ER expression in primary breast tumours, and is associated with poor patient survival (97), expression of PTBP1 has been shown to promote breast cancer cell growth (98) and expression of METTL8 is thought to be up-regulated in breast cancer (99). The top 10 upregulated genes in the same analysis were *CTDSPL*, *ARMC1*, *FGFR3*, *G3BP1*, *TNRC6A*, *EIF3L*, *CDKN1C*, *PUF60*, *BMPR1B*, and *SLC16A7*. Some of the identified transcripts have an established role in breast cancer, such as *FGFR3*, which has been shown to be associated with poor survival of breast cancer patients (100) and *G3BP1* which can promote breast cancer cell proliferation through stabilising β-catenin; interesting in light of the consistent observation of *CTNNB1* changes throughout multiple analyses conducted as part of this study (101). Furthermore, *PUF60*, a component of the spliceosome, has been linked with breast cancer survival (102) and BMPR1B is a pro-migratory protein upregulated in many tumours (103). *SLC16A7,* or MCT2, has been shown to promote breast tumours following β-hydroxybutyrate secretion from mammary gland derived adipocytes (104). *CDKN1C* overexpression was observed in this analysis; however, downregulation of *CDKN1C* has been shown to promote tumourigeneis (105). There are limited reports of some of the top 10 upregulated genes in breast cancer, including *ARMC1*, expression of which is significantly higher in breast tumours compared to normal tissues (106).

In the DARPP-32 knockdown cell treated with E2 versus control cell treated with E2 analysis, *SIRT1*, *CTNNB1* and *IGF1R* were identified as known or putative direct interacting partners using Qiagen IPA. *SIRT1* expression was significantly downregulated in DARPP-32 knockdown cells treated with E2; *SIRT1* (sirtuin-1) is a nicotinamide adenine dinucleotide (NAD+)-dependent histone deacetylase and transcription factor implicated in aging and inflammation, amongst many other

physiological processes. A link between DARPP-32, *SIRT1* and Huntington's disease has been described, and there is accumulating evidence *SIRT1* may play a role in cancer (107, 108). Interestingly, in DARPP-32 knockdown cells, the addition of E2 caused an upregulation of *SIRT1* expression. *SIRT1* and oestrogen signalling have been linked to promote breast cancer progression (reviewed in (109)).

The second gene with a known or direct interaction with *PPP1R1B* was *CTNNB1*; *CTNNB1* expression was significantly downregulated in DARPP-32 knockdown cells treated with E2. *CTNNB1* is the gene that encodes β-catenin, which acts in a complex of proteins that form adherens junctions and transduction of Wnt signals. The DARPP-32 splice variant, t-DARPP, which has lost its Thr-34 phosphorylation site, has been shown to promote activation of β-catenin in gastric cancer (21). Finally, *IGF1R* was identified as significantly upregulated in DARPP-32 knockdown cells stimulated with E2. DARPP-32 has been shown to function in a DARPP-32-IGF1R signalling axis to regulate STAT3 signalling in gastric cancer, through phosphorylation and activation of IGF1R and its downstream effector SRC (110).

Unique transcripts were identified in the DARPP-32 knockdown cell versus DARPP-32 knockdown cell treated with E2 when compared with control cell versus control cell treated with E2 to identify genes associated with changes that happen following E2 stimulation in cells with reduced DARPP-32 expression. This analysis was to aid with understanding why patients with ER positive disease with low DARPP-32 expression have adverse clinical outcome. The top 10 downregulated genes when DARPP-32 knockdown cells were treated with E2 were *TMTC1*, *AMOTL1*, *ANO6*, *NACC2*, *MYO1C*, *ECT2*, *RACGAP1*, *PRRC2A*, *TLE3* and *PIK3C2B*. The top 10 upregulated genes were *RACK1*, *PSMA3*, *SPART*, *NCAM1*, *CLPTM1L*, *KIF20A*, *SERINC2*, *SPATS2L*, *NSMF*, and *RING1*. Not all the up and down regulated genes have had roles described in breast cancer. When focusing on the downregulated genes, *RACGAP1* and *ECT2* have been linked to drive breast cancer metastasis (111), and the absence of TLE3 the basal expression of Erα target genes induced by E2 is increased and is thought to be an important coregulator of the E2 signalling pathway (112). *PIK3C2B* expression has been shown to be associated with the proliferation status of breast tumours (113) and *AMOTL1* has been shown to promote breast cancer progression (114). Genes upregulated in DARPP-32 cells treated with E2 identified upregulation of a number of genes implicated in breast cancer tumourigenesis and disease progression, including RACK1, (reviewed in (115)), which is also induced by E2 stimulation (116); although interestingly RACK1 was a uniquely upregulated gene in the DARPP-32 knockdown cells, not the control cells. *PSMA3* and *KIF20A* expression has been shown to be associated with poor survival of breast cancer patients (117, 118), *NCAM1* with poor prognosis of patients with Luminal A breast cancer (119), and CLPTM1L as an independent risk loci across different cancer types (120). Low expression of *RING1*, however, has been associated with poor prognosis of breast cancer patients (121).

Interestingly, there were more direct known and putative interacting partners in this analysis when compared to the DARPP-32 knockdown cell treated with E2

versus control cell treated with E2 analysis. 33 known or putative direct interacting genes were identified; in the presence of E2 (in DARPP-32 knockdown cells), upregulation of *ITPR1*, *RPS6, BCL2*, *GSK3B*, *CSNK2A1, ATF1*, *HTR2A, MYC*, *MAPT*, *CCK*, *STAT3,* and downregulation of *CREB1*, *ERBB2*, *CDC42, WNT5A*, *BCL2L1*, *PIN1*, *CTNNB1*, *PPP3CA*, *MAPK3*, *FZD3*, *TFCP2*, *CASP3*, *TGFB1*, *FOS*, *HTT*, *ESRRA*, *SRSF3*, *ROBO2*, *PPP1CC*, *GNAS*, *PPP1CA*, and *CASP9* was observed. Some of the genes identified were also identified in the DARPP-32 knockdown cell versus control cell analysis and DARPP-32 knockdown cell treated with E2 versus control cell treated with E2 analysis, including *CTNBB1* and *MAPK3*.

When cells with low levels of DARPP-32 are exposed to E2, upregulation of known or putative DARPP-32 partners, inositol 1,4,5-triphosphate receptor type 1 (*ITPR1*), ribosomal protein S6 (*RPS6*), Bcl-2 apoptosis regulator (*BCL2*), glycogen synthase kinase 3 beta (*GSK3B*), casein kinase 2 alpha 1 (*CSNK2A1*), activating transcription factor 1 (*ATF1*), 5-hydroxytryptamine receptor 2A (*HTR2A*), MYC proto-oncogene (*MYC*), microtubule associate protein Tau (*MAPT*), cholecystokinin (*CCK*), and signal transducer and activator of transcription-3 (*STAT3*) are observed. Many of these are genes are strongly associated with breast cancer. MYC, for example, is an oestrogen responsive gent, and has an important role in ER positive breast cancer; here we show that there is higher increase in *MYC* expression in DARPP-32 knockdown cells treated with E2, than is observed for control cells treated with E2. STAT3 is transcription factor that is overexpressed in breast cancer and has been shown to drive metastasis in ER positive breast cancer, independent of oestrogen (122). In gastric cancer, DARPP-32 has been shown to regulate STAT3 signalling, through a DARPP-32 IGF1R signalling axis (110), with IGF1R identified as upregulated in DARPP-32 knockdown cells in this study.

When cells with low levels of DARPP-32 are exposed to E2, downregulation of known or putative DARPP-32 partners cyclic responsive element binding protein (*CREB1*), HER2/Erb-B2 receptor tyrosine kinase-2 (*ERBB2*), cell division cycle 42/cdc42 (*CDC42*), Wnt family member 5A (*WNT5A*), Bcl-2 like-1 (*BCL2L1*), peptidylprolyl cis/trans isomerase, NIMA-interacting-1 (*PIN1*), *CTNNB1*, protein-phosphatase 3 catalytic subunit alpha (*PPP3CA*), *MAPK3*, frizzled class receptor-3 (*FZD3*), transcription factor CP2 (*TFCP2*), caspase-3 (*CASP3*), transforming growth factor beta-1 (*TGFB1*), Fos proto-oncogene, AP-1 transcription factor subunit (*FOS*), huntingtin (*HTT*), oestrogen-related receptor alpha (*ESRRA*), serine and arginine rich splicing factor-2 (*SRSF3*), roundabout guidance receptor-2 (*ROBO2*), protein phosphatase-1 catalytic subunit (*PPP1CC*), GNAS complex locus (*GNAS*), protein phosphatase 1 catalytic subunit alpha (*PPP1CA*), and caspase-9 (*CASP9*) was observed. As before, many of these genes are associated with breast cancer. In previous publications, we (6), and others had identified a link between *CDC42* and DARPP-32 in breast cancer (32); although this was without E2 stimulation. In breast cancer, links between DARPP-32, *FZD3*, and *Wnt5A* have been described (32). Wnt-5A functions, principally, but not exclusively, in non-canonical Wnt signalling, meaning that signalling does not promote β-catenin mediated transcription and the role of Wnt-5A in cancer is not always clear,

often acting in a context dependent manner (reviewed in (123)). In breast cancer, Wnt5A has been shown to activate frizzled-3 receptors to stimulate the formation of cAMP; ultimately triggering a DARPP-32 and CREM-dependent response to inhibit breast cancer cell migration (32). It is interesting, therefore, that treatment of DARPP-32 knockdown cells with E2, reduces the expression of *WNT5A* and *FZD3* when compared to DARPP-32 knockdown cells alone. DARPP-32

Qiagen IPA was used to perform pathway analysis in response to DARPP-32 knockdown and/or E2 treatment. The DARPP-32 knockdown cell versus control cell analysis and the DARPP-32 knockdown cell treated with E2 versus control cell treated with E2 analysis were used to identify pathways common to the loss of DARPP-32 expression, independent of E2 treatment; these pathways included the tight junction pathway and the CLEAR signalling pathway. The tight junction pathway demonstrated that PP2A was downregulated in DARPP-32 knockdown cells, irrespective of E2 treatment. PP2A can dephosphorylate DARPP-32 on Thr-75, thereby reducing PKA inhibition; PP2A is known to act as a tumour suppressor in general (reviewed in (124)). Different subunits of PP2A were identified as down regulated within the analyses, *PPP2R5C* and *PTPA*. In addition to Qiagen IPA, a number of other programmes were explore differentially expressed genes; Qiagen IPA was favoured, however is associated with licence costs and therefore may be financially restrictive in many projects.

Further analysis was performed of DARPP-32 knockdown cells treated with a PKA inhibitor (PKA inhibitor fragment (6-22) amide) to determine transcriptomic changes. Inhibition of PKA reduces DARPP-32 activity at Thr-34, this is of biological relevance as t-DARPP is lacking Thr-34 and therefore loses the ability to inhibit PP1. Known and putative DARPP-32 interacting partners were identified using Qiagen IPA. The limitation of this assessment is that PKA has a wide range of cellular functions itself, so this assessment was utilised to indicate interesting cellular changes and support previous analysis in overlapping pathway identification. PKA inhibition in DARPP-32 knockdown cells, when compared with DARPP-32 cells with wild type PKA activity demonstrate a decrease in *ADORA2*, *CSNK2A1*, and *AKT* and an increase in *FOS*, *ADCY5*, and *ITPR1*. In control cells treated with a PKA inhibitor, compared with control cells alone induces changes in *ADORA2*, *CSNK2A1, FOS*, *ADCY5*. Numerous more known or putative direct DARPP-32 interacting partners were identified when DARPP-32 knockdown cells treated with a PKA inhibitor were compared with control cells treated with a PKA inhibitor, including *CTNNB1*; interestingly *CTNNB1* was identified in numerous other analyses, including following E2 stimulation, as discussed previously. Qiagen IPA was used for pathway analysis and identified many more overrepresented pathways when PKA was inhibited, than when cells were stimulated with E2; despite the increased number of differentially expressed transcripts observed following E2 stimulation. The tight Junction pathway was commonly identified, in addition to previous identification in all DARPP-32 knockdown groups irrespective of E2 treatment.

The METABRIC data set was explored to identify if the expression of DARPP-32 was directly linked with the expression of known and putative direct DARPP-32 interacting signalling partners identified by Qiagen IPA. DARPP-32 expression significantly correlated with *MAPK3*, *SIRT1* and *IGF1R* mRNA expression in patient specimens. Low *SIRT1*, *IGF1R* and *PPP2R5C* probe 1 mRNA expression, and high *YWHAZ, PPP2R5C* probe 2 and 4, and *PPP2R4* probe 4 were significantly associated with adverse survival of breast cancer patients. Of these genes associated with survival, only *YWHAZ* probe 1 expression remained associated with survival when other prognostic variables were included in the assessment.

YWHAZ expression in tumours has previously linked with patient survival, including overexpression of YWHAZ protein in esophago-gastric junction adenocarcinomas (125) and gastric cancers (126) and breast cancer (127); although our data indicates that low expression of *YWHAZ* mRNA is associated with patient survival. In this study, the expression levels of two probes were available for the assessment of *YWHAZ* expression, with Illumina probe identifiers of ILMN_1801928 and ILMN_1669286. Probe 1 matches 8 *YWHAZ* transcripts (ENST0000395958, ENST00000395957, ENST00000457309, ENST00000395956, ENST00000353245, ENST00000523848, ENST00000521309 and ENST00000522542), whereas probe 2 matches three *YWHAZ* transcripts (ENST00000395957, ENST00000353245 and ENST00000492736); overlapping in two of the transcripts. It is unclear why data differing to that previously published is observed; however, published data is principally using antibodies with undescribed specificity; the results presented here warrant further investigation.

9 Conclusion

The transcriptomic changes resultant from DARPP-32 knockdown in ER positive breast cancer cells have been determined, with and without E2 stimulation and PKA inhibition. These changes identify that DARPP-32 functions as an important partner in many cancer-associated signalling pathways that have been linked with poor prognosis. When DARPP-32 knockdown cells are stimulated with E2 many pathways are altered that are linked with altered cancer cell behaviour, many of which have been previously been associated with patient survival and or oestrogen signalling.

10 Future work

Future work will include expanding the design of this study to multiple cell lines, including further ER positive and ER negative breast cancer cell lines. Further RNA-Seq will be performed on CRISPR-Cas9 DARPP-32 knockout cell lines, which have subsequently been created in the laboratory. Initially, RNA-Seq will be performed on T47D CRISPR-Cas9 DARPP-32 knockout cells compared with both siRNA DARPP-32 knockdown T47D cells and control T47D cells with a full bioinformatic analysis using the methods used for the current study. To understand the importance of DARPP-32 and t-DARPP, constructs will be transfected into T47D CRISPR-Cas9 DARPP-32 knockout cells, which will then be subject to a range of phenotypic assays and RNA-Seq with bioinformatics to identify isoform specific transcriptomic changes that occur in ER positive breast cancer. Other bioinformatics packages, such as IsoformSwitchAnalyzeR will be explored using the current data sets.

Work identifying pathways that may be altered in ER positive breast cancer cell lines with low DARPP-32 expression will be investigated further *in vitro*, to determine how fast interactions occur following E2 stimulation, and understand if similar mechanisms are observed in the presence of t-DARPP following stable transfection.

Further studies will investigate the physical and/or mechanistic interaction between DARPP-32 with differentially expressed transcripts; these experiments will include Bio-ID and proteomics-based studies. Furthermore, tissue microarrays are available for large early-stage invasive breast cancer patients with full clinical outcome and clinicopathological annotation available; preferred genes, identified as associated with survival, will be investigated at the protein level within these tissues to determine links with patient survival.

11 References

1. Carroll JS. Mechanisms of oestrogen receptor (ER) gene regulation in breast cancer. Eur J Endocrinol. 2016;175(1):R41-9.
2. Carroll JS, Meyer CA, Song J, Li W, Geistlinger TR, Eeckhoute J, et al. Genome-wide analysis of estrogen receptor binding sites. Nat Genet. 2006;38(11):1289-97.
3. Welboren WJ, van Driel MA, Janssen-Megens EM, van Heeringen SJ, Sweep FC, Span PN, et al. ChIP-Seq of ERalpha and RNA polymerase II defines genes differentially responding to ligands. EMBO J. 2009;28(10):1418-28.
4. Bjornstrom L, Sjoberg M. Mechanisms of estrogen receptor signaling: convergence of genomic and nongenomic actions on target genes. Mol Endocrinol. 2005;19(4):833-42.
5. Sorlie T, Perou CM, Tibshirani R, Aas T, Geisler S, Johnsen H, et al. Gene expression patterns of breast carcinomas distinguish tumor subclasses with clinical implications. Proc Natl Acad Sci U S A. 2001;98(19):10869-74.
6. Kotecha S, Lebot MN, Sukkarn B, Ball G, Moseley PM, Chan SY, et al. Dopamine and cAMP-regulated phosphoprotein 32 kDa (DARPP-32) and survival in breast cancer: a retrospective analysis of protein and mRNA expression. Sci Rep. 2019;9(1):16987.
7. Hemmings HC, Jr., Nairn AC, Aswad DW, Greengard P. DARPP-32, a dopamine- and adenosine 3':5'-monophosphate-regulated phosphoprotein enriched in dopamine-innervated brain regions. II. Purification and characterization of the phosphoprotein from bovine caudate nucleus. J Neurosci. 1984;4(1):99-110.
8. Walaas SI, Greengard P. DARPP-32, a dopamine- and adenosine 3':5'-monophosphate-regulated phosphoprotein enriched in dopamine-innervated brain regions. I. Regional and cellular distribution in the rat brain. J Neurosci. 1984;4(1):84-98.
9. Ouimet CC, Miller PE, Hemmings HC, Jr., Walaas SI, Greengard P. DARPP-32, a dopamine- and adenosine 3':5'-monophosphate-regulated phosphoprotein enriched in dopamine-innervated brain regions. III. Immunocytochemical localization. J Neurosci. 1984;4(1):111-24.
10. Hemmings HC, Jr., Greengard P, Tung HY, Cohen P. DARPP-32, a dopamine-regulated neuronal phosphoprotein, is a potent inhibitor of protein phosphatase-1. Nature. 1984;310(5977):503-5.
11. Hemmings HC, Jr., Nairn AC, Greengard P. DARPP-32, a dopamine- and adenosine 3':5'-monophosphate-regulated neuronal phosphoprotein. II. Comparison of the kinetics of phosphorylation of DARPP-32 and phosphatase inhibitor 1. J Biol Chem. 1984;259(23):14491-7.
12. Fienberg AA, Greengard P. The DARPP-32 knockout mouse. Brain Res Brain Res Rev. 2000;31(2-3):313-9.
13. Bibb JA, Snyder GL, Nishi A, Yan Z, Meijer L, Fienberg AA, et al. Phosphorylation of DARPP-32 by Cdk5 modulates dopamine signalling in neurons. Nature. 1999;402(6762):669-71.
14. Nishi A, Bibb JA, Matsuyama S, Hamada M, Higashi H, Nairn AC, et al. Regulation of DARPP-32 dephosphorylation at PKA- and Cdk5-sites by NMDA and AMPA receptors: distinct roles of calcineurin and protein phosphatase-2A. J Neurochem. 2002;81(4):832-41.
15. El-Rifai W, Smith MF, Jr., Li G, Beckler A, Carl VS, Montgomery E, et al. Gastric cancers overexpress DARPP-32 and a novel isoform, t-DARPP. Cancer Res. 2002;62(14):4061-4.
16. Beckler A, Moskaluk CA, Zaika A, Hampton GM, Powell SM, Frierson HF, Jr., et al. Overexpression of the 32-kilodalton dopamine and cyclic adenosine 3',5'-monophosphate-regulated phosphoprotein in common adenocarcinomas. Cancer. 2003;98(7):1547-51.
17. Wang MS, Pan Y, Liu N, Guo C, Hong L, Fan D. Overexpression of DARPP-32 in colorectal adenocarcinoma. Int J Clin Pract. 2005;59(1):58-61.

18. Ebihara Y, Miyamoto M, Fukunaga A, Kato K, Shichinohe T, Kawarada Y, et al. DARPP-32 expression arises after a phase of dysplasia in oesophageal squamous cell carcinoma. Br J Cancer. 2004;91(1):119-23.
19. Mukherjee K, Peng D, Brifkani Z, Belkhiri A, Pera M, Koyama T, et al. Dopamine and cAMP regulated phosphoprotein MW 32 kDa is overexpressed in early stages of gastric tumorigenesis. Surgery. 2010;148(2):354-63.
20. Belkhiri A, Dar AA, Zaika A, Kelley M, El-Rifai W. t-Darpp promotes cancer cell survival by up-regulation of Bcl2 through Akt-dependent mechanism. Cancer Res. 2008;68(2):395-403.
21. Vangamudi B, Zhu S, Soutto M, Belkhiri A, El-Rifai W. Regulation of beta-catenin by t-DARPP in upper gastrointestinal cancer cells. Mol Cancer. 2011;10:32.
22. Zhu S, Hong J, Tripathi MK, Sehdev V, Belkhiri A, El-Rifai W. Regulation of CXCR4-mediated invasion by DARPP-32 in gastric cancer cells. Mol Cancer Res. 2013;11(1):86-94.
23. Hong L, Wang J, Han Y, Zhao Y, Gao J, Wang J, et al. Reversal of multidrug resistance of vincristine-resistant gastric adenocarcinoma cells through up-regulation of DARPP-32. Cell Biol Int. 2007;31(9):1010-5.
24. Hong L, Zhao Y, Wang J, Han Y, Guo W, Jin H, et al. Reversal of multidrug resistance of adriamycin-resistant gastric adenocarcinoma cells through the up-regulation of DARPP-32. Dig Dis Sci. 2008;53(1):101-7.
25. Zhu S, Belkhiri A, El-Rifai W. DARPP-32 increases interactions between epidermal growth factor receptor and ERBB3 to promote tumor resistance to gefitinib. Gastroenterology. 2011;141(5):1738-48 e1-2.
26. Belkhiri A, Zhu S, Chen Z, Soutto M, El-Rifai W. Resistance to TRAIL is mediated by DARPP-32 in gastric cancer. Clin Cancer Res. 2012;18(14):3889-900.
27. Varis A, Zaika A, Puolakkainen P, Nagy B, Madrigal I, Kokkola A, et al. Coamplified and overexpressed genes at ERBB2 locus in gastric cancer. Int J Cancer. 2004;109(4):548-53.
28. Maqani N, Belkhiri A, Moskaluk C, Knuutila S, Dar AA, El-Rifai W. Molecular dissection of 17q12 amplicon in upper gastrointestinal adenocarcinomas. Mol Cancer Res. 2006;4(7):449-55.
29. Yun SM, Yoon K, Lee S, Kim E, Kong SH, Choe J, et al. PPP1R1B-STARD3 chimeric fusion transcript in human gastric cancer promotes tumorigenesis through activation of PI3K/AKT signaling. Oncogene. 2014;33(46):5341-7.
30. Chang MJ, Zhong F, Lavik AR, Parys JB, Berridge MJ, Distelhorst CW. Feedback regulation mediated by Bcl-2 and DARPP-32 regulates inositol 1,4,5-trisphosphate receptor phosphorylation and promotes cell survival. Proc Natl Acad Sci U S A. 2014;111(3):1186-91.
31. Hansen C, Greengard P, Nairn AC, Andersson T, Vogel WF. Phosphorylation of DARPP-32 regulates breast cancer cell migration downstream of the receptor tyrosine kinase DDR1. Exp Cell Res. 2006;312(20):4011-8.
32. Hansen C, Howlin J, Tengholm A, Dyachok O, Vogel WF, Nairn AC, et al. Wnt-5a-induced phosphorylation of DARPP-32 inhibits breast cancer cell migration in a CREB-dependent manner. J Biol Chem. 2009;284(40):27533-43.
33. Moasser MM. The oncogene HER2: its signaling and transforming functions and its role in human cancer pathogenesis. Oncogene. 2007;26(45):6469-87.
34. Wang J, Xu B. Targeted therapeutic options and future perspectives for HER2-positive breast cancer. Signal Transduct Target Ther. 2019;4:34.
35. Belkhiri A, Dar AA, Peng DF, Razvi MH, Rinehart C, Arteaga CL, et al. Expression of t-DARPP mediates trastuzumab resistance in breast cancer cells. Clin Cancer Res. 2008;14(14):4564-71.
36. Hamel S, Bouchard A, Ferrario C, Hassan S, Aguilar-Mahecha A, Buchanan M, et al. Both t-Darpp and DARPP-32 can cause resistance to trastuzumab in breast cancer cells and are frequently expressed in primary breast cancers. Breast Cancer Res Treat. 2010;120(1):47-57.

37. Gu L, Waliany S, Kane SE. Darpp-32 and its truncated variant t-Darpp have antagonistic effects on breast cancer cell growth and herceptin resistance. PLoS One. 2009;4(7):e6220.
38. Vangamudi B, Peng DF, Cai Q, El-Rifai W, Zheng W, Belkhiri A. t-DARPP regulates phosphatidylinositol-3-kinase-dependent cell growth in breast cancer. Mol Cancer. 2010;9:240.
39. Hong J, Katsha A, Lu P, Shyr Y, Belkhiri A, El-Rifai W. Regulation of ERBB2 receptor by t-DARPP mediates trastuzumab resistance in human esophageal adenocarcinoma. Cancer Res. 2012;72(17):4504-14.
40. Christenson JL, Denny EC, Kane SE. t-Darpp overexpression in HER2-positive breast cancer confers a survival advantage in lapatinib. Oncotarget. 2015;6(32):33134-45.
41. Denny EC, Kane SE. t-Darpp Promotes Enhanced EGFR Activation and New Drug Synergies in Her2-Positive Breast Cancer Cells. PLoS One. 2015;10(6):e0132267.
42. Murad R, Avanes A, Ma X, Geng S, Mortazavi A, Momand J. Transcriptome and chromatin landscape changes associated with trastuzumab resistance in HER2+ breast cancer cells. Gene. 2021;799:145808.
43. Christenson JL, Kane SE. Darpp-32 and t-Darpp are differentially expressed in normal and malignant mouse mammary tissue. Mol Cancer. 2014;13:192.
44. Martin SG, Zhang S, Yang S, Saidy B, Deen S, Storr SJ. Dopamine and cAMP-regulated phosphoprotein 32kDa (DARPP-32), protein phosphatase-1 and cyclin-dependent kinase 5 expression in ovarian cancer. J Cell Mol Med. 2020;24(16):9165-75.
45. Saidy B, Kotecha S, Butler A, Rakha EA, Ellis IO, Green AR, et al. PP1, PKA and DARPP-32 in breast cancer: A retrospective assessment of protein and mRNA expression. J Cell Mol Med. 2021;25(11):5015-24.
46. Saidy B, Rakha EA, Green AR, Ellis IO, Martin SG, Storr SJ. Retrospective assessment of cyclin-dependent kinase 5 mRNA and protein expression and its association with patient survival in breast cancer. J Cell Mol Med. 2020;24(11):6263-71.
47. Auger AP, Meredith JM, Snyder GL, Blaustein JD. Oestradiol increases phosphorylation of a dopamine- and cyclic AMP-regulated phosphoprotein (DARPP-32) in female rat brain. J Neuroendocrinol. 2001;13(9):761-8.
48. Weiner J, Sun WL, Zhou L, Kreiter CM, Jenab S, Quinones-Jenab V. PKA-mediated responses in females' estrous cycle affect cocaine-induced responses in dopamine-mediated intracellular cascades. Neuroscience. 2009;161(3):865-76.
49. de Leeuw R, Flach K, Bentin Toaldo C, Alexi X, Canisius S, Neefjes J, et al. PKA phosphorylation redirects ERalpha to promoters of a unique gene set to induce tamoxifen resistance. Oncogene. 2013;32(30):3543-51.
50. Al-Dhaheri MH, Rowan BG. Protein kinase A exhibits selective modulation of estradiol-dependent transcription in breast cancer cells that is associated with decreased ligand binding, altered estrogen receptor alpha promoter interaction, and changes in receptor phosphorylation. Mol Endocrinol. 2007;21(2):439-56.
51. Del Rio JP, Alliende MI, Molina N, Serrano FG, Molina S, Vigil P. Steroid Hormones and Their Action in Women's Brains: The Importance of Hormonal Balance. Front Public Health. 2018;6:141.
52. Olesen KM, Auger AP. Dopaminergic activation of estrogen receptors induces fos expression within restricted regions of the neonatal female rat brain. PLoS One. 2008;3(5):e2177.
53. Alam SK, Astone M, Liu P, Hall SR, Coyle AM, Dankert EN, et al. DARPP-32 and t-DARPP promote non-small cell lung cancer growth through regulation of IKKalpha-dependent cell migration. Commun Biol. 2018;1:43.
54. Alam SK, Wang L, Ren Y, Hernandez CE, Kosari F, Roden AC, et al. ASCL1-regulated DARPP-32 and t-DARPP stimulate small cell lung cancer growth and neuroendocrine tumour cell proliferation. Br J Cancer. 2020;123(5):819-32.

55. Alam SK, Zhang Y, Wang L, Zhu Z, Hernandez CE, Zhou Y, et al. DARPP-32 promotes ERBB3-mediated resistance to molecular targeted therapy in EGFR-mutated lung adenocarcinoma. Oncogene. 2022;41(1):83-98.
56. Tiwari A, Tashiro K, Dixit A, Soni A, Vogel K, Hall B, et al. Loss of HIF1A From Pancreatic Cancer Cells Increases Expression of PPP1R1B and Degradation of p53 to Promote Invasion and Metastasis. Gastroenterology. 2020;159(5):1882-97 e5.
57. Televantou D, Karkavelas G, Hytiroglou P, Lampaki S, Iliadis G, Selviaridis P, et al. DARPP32, STAT5 and STAT3 mRNA expression ratios in glioblastomas are associated with patient outcome. Pathol Oncol Res. 2013;19(2):329-43.
58. Edgar R, Domrachev M, Lash AE. Gene Expression Omnibus: NCBI gene expression and hybridization array data repository. Nucleic Acids Res. 2002;30(1):207-10.
59. He B, Zhu R, Yang H, Lu Q, Wang W, Song L, et al. Assessing the Impact of Data Preprocessing on Analyzing Next Generation Sequencing Data. Front Bioeng Biotechnol. 2020;8:817.
60. Bray NL, Pimentel H, Melsted P, Pachter L. Near-optimal probabilistic RNA-seq quantification. Nat Biotechnol. 2016;34(5):525-7.
61. Zhang C, Zhang B, Lin LL, Zhao S. Evaluation and comparison of computational tools for RNA-seq isoform quantification. BMC Genomics. 2017;18(1):583.
62. Anders S, Huber W. Differential expression analysis for sequence count data. Genome Biol. 2010;11(10):R106.
63. Kramer A, Green J, Pollard J, Jr., Tugendreich S. Causal analysis approaches in Ingenuity Pathway Analysis. Bioinformatics. 2014;30(4):523-30.
64. Chowdhury S, Sarkar RR. Comparison of human cell signaling pathway databases--evolution, drawbacks and challenges. Database (Oxford). 2015;2015.
65. Curtis C, Shah SP, Chin SF, Turashvili G, Rueda OM, Dunning MJ, et al. The genomic and transcriptomic architecture of 2,000 breast tumours reveals novel subgroups. Nature. 2012;486(7403):346-52.
66. McShane LM, Altman DG, Sauerbrei W, Taube SE, Gion M, Clark GM, et al. REporting recommendations for tumour MARKer prognostic studies (REMARK). Br J Cancer. 2005;93(4):387-91.
67. Hoadley KA, Yau C, Hinoue T, Wolf DM, Lazar AJ, Drill E, et al. Cell-of-Origin Patterns Dominate the Molecular Classification of 10,000 Tumors from 33 Types of Cancer. Cell. 2018;173(2):291-304 e6.
68. Heberle H, Meirelles GV, da Silva FR, Telles GP, Minghim R. InteractiVenn: a web-based tool for the analysis of sets through Venn diagrams. BMC Bioinformatics. 2015;16:169.
69. Keydar I, Chen L, Karby S, Weiss FR, Delarea J, Radu M, et al. Establishment and characterization of a cell line of human breast carcinoma origin. Eur J Cancer. 1979;15(5):659-70.
70. Neve RM, Chin K, Fridlyand J, Yeh J, Baehner FL, Fevr T, et al. A collection of breast cancer cell lines for the study of functionally distinct cancer subtypes. Cancer Cell. 2006;10(6):515-27.
71. Strom A, Hartman J, Foster JS, Kietz S, Wimalasena J, Gustafsson JA. Estrogen receptor beta inhibits 17beta-estradiol-stimulated proliferation of the breast cancer cell line T47D. Proc Natl Acad Sci U S A. 2004;101(6):1566-71.
72. Dubik D, Dembinski TC, Shiu RP. Stimulation of c-myc oncogene expression associated with estrogen-induced proliferation of human breast cancer cells. Cancer Res. 1987;47(24 Pt 1):6517-21.
73. Katchy A, Edvardsson K, Aydogdu E, Williams C. Estradiol-activated estrogen receptor alpha does not regulate mature microRNAs in T47D breast cancer cells. J Steroid Biochem Mol Biol. 2012;128(3-5):145-53.

74. Yu S, Kim T, Yoo KH, Kang K. The T47D cell line is an ideal experimental model to elucidate the progesterone-specific effects of a luminal A subtype of breast cancer. Biochem Biophys Res Commun. 2017;486(3):752-8.
75. Fortunati N, Fissore F, Fazzari A, Becchis M, Comba A, Catalano MG, et al. Sex steroid binding protein exerts a negative control on estradiol action in MCF-7 cells (human breast cancer) through cyclic adenosine 3',5'-monophosphate and protein kinase A. Endocrinology. 1996;137(2):686-92.
76. Wu Y, Zhao W, Liu Y, Tan X, Li X, Zou Q, et al. Function of HNRNPC in breast cancer cells by controlling the dsRNA-induced interferon response. EMBO J. 2018;37(23).
77. Wen J, Toomer KH, Chen Z, Cai X. Genome-wide analysis of alternative transcripts in human breast cancer. Breast Cancer Res Treat. 2015;151(2):295-307.
78. Zhang P, Long Q, Zeng S, Wen M, Lu Q. FOXC1-induced LINC01123 acts as a mediator in triple negative breast cancer. Cancer Cell Int. 2020;20:199.
79. Kim SH, Singh SV. The FoxQ1 transcription factor is a novel regulator of electron transport chain complex I subunits in human breast cancer cells. Mol Carcinog. 2022;61(3):372-81.
80. Holy P, Hlavac V, Ostasov P, Brynychova V, Kozevnikovova R, Trnkova M, et al. Germline and somatic genetic variability of oxysterol-related genes in breast cancer patients with early disease of the luminal subtype. Biochimie. 2022;199:158-69.
81. He L, Fan C, Kapoor A, Ingram AJ, Rybak AP, Austin RC, et al. alpha-Mannosidase 2C1 attenuates PTEN function in prostate cancer cells. Nat Commun. 2011;2:307.
82. Bauer JA, Chakravarthy AB, Rosenbluth JM, Mi D, Seeley EH, De Matos Granja-Ingram N, et al. Identification of markers of taxane sensitivity using proteomic and genomic analyses of breast tumors from patients receiving neoadjuvant paclitaxel and radiation. Clin Cancer Res. 2010;16(2):681-90.
83. Gong J, Tian J, Lou J, Wang X, Ke J, Li J, et al. A polymorphic MYC response element in KBTBD11 influences colorectal cancer risk, especially in interaction with an MYC-regulated SNP rs6983267. Ann Oncol. 2018;29(3):632-9.
84. Bean GR, Ganesan YT, Dong Y, Takeda S, Liu H, Chan PM, et al. PUMA and BIM are required for oncogene inactivation-induced apoptosis. Sci Signal. 2013;6(268):ra20.
85. Merino D, Best SA, Asselin-Labat ML, Vaillant F, Pal B, Dickins RA, et al. Pro-apoptotic Bim suppresses breast tumor cell metastasis and is a target gene of SNAI2. Oncogene. 2015;34(30):3926-34.
86. Bartek J, Lukas J. Chk1 and Chk2 kinases in checkpoint control and cancer. Cancer Cell. 2003;3(5):421-9.
87. Abdel-Fatah TM, Arora A, Alsubhi N, Agarwal D, Moseley PM, Perry C, et al. Clinicopathological significance of ATM-Chk2 expression in sporadic breast cancers: a comprehensive analysis in large cohorts. Neoplasia. 2014;16(11):982-91.
88. Beaudin S, Kokabee L, Welsh J. Divergent effects of vitamins K1 and K2 on triple negative breast cancer cells. Oncotarget. 2019;10(23):2292-305.
89. Huang M, Zhou B, Gong J, Xing L, Ma X, Wang F, et al. RNA-splicing factor SART3 regulates translesion DNA synthesis. Nucleic Acids Res. 2018;46(9):4560-74.
90. Timani KA, Liu Y, Fan Y, Mohammad KS, He JJ. Tip110 Regulates the Cross Talk between p53 and Hypoxia-Inducible Factor 1alpha under Hypoxia and Promotes Survival of Cancer Cells. Mol Cell Biol. 2015;35(13):2254-64.
91. Bownes RJ, Turnbull AK, Martinez-Perez C, Cameron DA, Sims AH, Oikonomidou O. On-treatment biomarkers can improve prediction of response to neoadjuvant chemotherapy in breast cancer. Breast Cancer Res. 2019;21(1):73.
92. Chocarro-Calvo A, Zaballos MA, Santisteban P, Garcia-Jimenez C. DARPP-32 is required for MAPK/ERK signaling in thyroid cells. Mol Endocrinol. 2012;26(3):471-80.

93. Yu Z, Zhu J, Wang H, Li H, Jin X. Function of BCLAF1 in human disease. Oncol Lett. 2022;23(2):58.
94. Guarnieri AL, Towers CG, Drasin DJ, Oliphant MUJ, Andrysik Z, Hotz TJ, et al. The miR-106b-25 cluster mediates breast tumor initiation through activation of NOTCH1 via direct repression of NEDD4L. Oncogene. 2018;37(28):3879-93.
95. Gustafsson Sheppard N, Heldring N, Dahlman-Wright K. Estrogen receptor-alpha, RBCK1, and protein kinase C beta 1 cooperate to regulate estrogen receptor-alpha gene expression. J Mol Endocrinol. 2012;49(3):277-87.
96. Zheng T, Wang A, Hu D, Wang Y. Molecular mechanisms of breast cancer metastasis by gene expression profile analysis. Mol Med Rep. 2017;16(4):4671-7.
97. Ayyoub M, Scarlata CM, Hamai A, Pignon P, Valmori D. Expression of MAGE-A3/6 in primary breast cancer is associated with hormone receptor negative status, high histologic grade, and poor survival. J Immunother. 2014;37(2):73-6.
98. Wang H, Ma P, Liu P, Guo D, Liu Z, Zhang Z. lncRNA SNHG6 promotes hepatocellular carcinoma progression by interacting with HNRNPL/PTBP1 to facilitate SETD7/LZTFL1 mRNA destabilization. Cancer Lett. 2021;520:121-31.
99. Lee SA, Lee KH, Kim H, Cho JY. METTL8 mRNA Methyltransferase Enhances Cancer Cell Migration via Direct Binding to ARID1A. Int J Mol Sci. 2021;22(11).
100. Chew NJ, Nguyen EV, Su SP, Novy K, Chan HC, Nguyen LK, et al. FGFR3 signaling and function in triple negative breast cancer. Cell Commun Signal. 2020;18(1):13.
101. Zhang CH, Liu H, Zhao WL, Zhao WX, Zhou HM, Shao RG. G3BP1 promotes human breast cancer cell proliferation through coordinating with GSK-3beta and stabilizing beta-catenin. Acta Pharmacol Sin. 2021;42(11):1900-12.
102. An J, Luo Z, An W, Cao D, Ma J, Liu Z. Identification of spliceosome components pivotal to breast cancer survival. RNA Biol. 2021;18(6):833-42.
103. Allison SE, Chen Y, Petrovic N, Zimmermann S, Moosmann B, Jansch M, et al. Activation of the pro-migratory bone morphogenetic protein receptor 1B gene in human MDA-MB-468 triple-negative breast cancer cells that over-express CYP2J2. Int J Biochem Cell Biol. 2016;80:173-8.
104. Huang CK, Chang PH, Kuo WH, Chen CL, Jeng YM, Chang KJ, et al. Adipocytes promote malignant growth of breast tumours with monocarboxylate transporter 2 expression via beta-hydroxybutyrate. Nat Commun. 2017;8:14706.
105. Qiu Z, Li Y, Zeng B, Guan X, Li H. Downregulated CDKN1C/p57(kip2) drives tumorigenesis and associates with poor overall survival in breast cancer. Biochem Biophys Res Commun. 2018;497(1):187-93.
106. Gan Y, Zhong F, Wang H, Li L. The Valuable Role of ARMC1 in Invasive Breast Cancer as a Novel Biomarker. Biomed Res Int. 2022;2022:1740295.
107. Jiang M, Wang J, Fu J, Du L, Jeong H, West T, et al. Neuroprotective role of Sirt1 in mammalian models of Huntington's disease through activation of multiple Sirt1 targets. Nat Med. 2011;18(1):153-8.
108. Jin X, Wei Y, Xu F, Zhao M, Dai K, Shen R, et al. SIRT1 promotes formation of breast cancer through modulating Akt activity. J Cancer. 2018;9(11):2012-23.
109. Liarte S, Alonso-Romero JL, Nicolas FJ. SIRT1 and Estrogen Signaling Cooperation for Breast Cancer Onset and Progression. Front Endocrinol (Lausanne). 2018;9:552.
110. Zhu S, Soutto M, Chen Z, Blanca Piazuelo M, Kay Washington M, Belkhiri A, et al. Activation of IGF1R by DARPP-32 promotes STAT3 signaling in gastric cancer cells. Oncogene. 2019;38(29):5805-16.
111. Ren K, Zhou D, Wang M, Li E, Hou C, Su Y, et al. RACGAP1 modulates ECT2-Dependent mitochondrial quality control to drive breast cancer metastasis. Exp Cell Res. 2021;400(1):112493.

112. Jangal M, Couture JP, Bianco S, Magnani L, Mohammed H, Gevry N. The transcriptional co-repressor TLE3 suppresses basal signaling on a subset of estrogen receptor alpha target genes. Nucleic Acids Res. 2014;42(18):11339-48.
113. Chikh A, Ferro R, Abbott JJ, Pineiro R, Buus R, Iezzi M, et al. Class II phosphoinositide 3-kinase C2beta regulates a novel signaling pathway involved in breast cancer progression. Oncotarget. 2016;7(14):18325-45.
114. Couderc C, Boin A, Fuhrmann L, Vincent-Salomon A, Mandati V, Kieffer Y, et al. AMOTL1 Promotes Breast Cancer Progression and Is Antagonized by Merlin. Neoplasia. 2016;18(1):10-24.
115. Buoso E, Masi M, Long A, Chiappini C, Travelli C, Govoni S, et al. Ribosomes as a nexus between translation and cancer progression: Focus on ribosomal Receptor for Activated C Kinase 1 (RACK1) in breast cancer. Br J Pharmacol. 2022;179(12):2813-28.
116. Buoso E, Masi M, Galbiati V, Maddalon A, Iulini M, Kenda M, et al. Effect of estrogen-active compounds on the expression of RACK1 and immunological implications. Arch Toxicol. 2020;94(6):2081-95.
117. Chiao CC, Liu YH, Phan NN, An Ton NT, Ta HDK, Anuraga G, et al. Prognostic and Genomic Analysis of Proteasome 20S Subunit Alpha (PSMA) Family Members in Breast Cancer. Diagnostics (Basel). 2021;11(12).
118. Chen G, Yu M, Cao J, Zhao H, Dai Y, Cong Y, et al. Identification of candidate biomarkers correlated with poor prognosis of breast cancer based on bioinformatics analysis. Bioengineered. 2021;12(1):5149-61.
119. Jia R, Li Z, Liang W, Ji Y, Weng Y, Liang Y, et al. Identification of key genes unique to the luminal a and basal-like breast cancer subtypes via bioinformatic analysis. World J Surg Oncol. 2020;18(1):268.
120. Wang Z, Zhu B, Zhang M, Parikh H, Jia J, Chung CC, et al. Imputation and subset-based association analysis across different cancer types identifies multiple independent risk loci in the TERT-CLPTM1L region on chromosome 5p15.33. Hum Mol Genet. 2014;23(24):6616-33.
121. Gao S, Wang SY, Zhang XD, Wu H, Pang D. Low Expression of the Polycomb Protein RING1 Predicts Poor Prognosis in Human Breast Cancer. Front Oncol. 2020;10:618768.
122. Siersbaek R, Scabia V, Nagarajan S, Chernukhin I, Papachristou EK, Broome R, et al. IL6/STAT3 Signaling Hijacks Estrogen Receptor alpha Enhancers to Drive Breast Cancer Metastasis. Cancer Cell. 2020;38(3):412-23 e9.
123. McDonald SL, Silver A. The opposing roles of Wnt-5a in cancer. Br J Cancer. 2009;101(2):209-14.
124. Ruvolo PP. The broken "Off" switch in cancer signaling: PP2A as a regulator of tumorigenesis, drug resistance, and immune surveillance. BBA Clin. 2016;6:87-99.
125. Watanabe N, Komatsu S, Ichikawa D, Miyamae M, Ohashi T, Okajima W, et al. Overexpression of YWHAZ as an independent prognostic factor in adenocarcinoma of the esophago-gastric junction. Am J Cancer Res. 2016;6(11):2729-36.
126. Nishimura Y, Komatsu S, Ichikawa D, Nagata H, Hirajima S, Takeshita H, et al. Overexpression of YWHAZ relates to tumor cell proliferation and malignant outcome of gastric carcinoma. Br J Cancer. 2013;108(6):1324-31.
127. Neal CL, Yao J, Yang W, Zhou X, Nguyen NT, Lu J, et al. 14-3-3zeta overexpression defines high risk for breast cancer recurrence and promotes cancer cell survival. Cancer Res. 2009;69(8):3425-32.

12 Acknowledgements

Sarah J Storr is funded through a Nottingham Research Fellowship, with additional funding for RNA-Seq through a Bioscientifica Trust Pilot Grant. Research supervisor was Nigel Mongan, University of Nottingham.

13 Appendix

13.1 Appendix 1

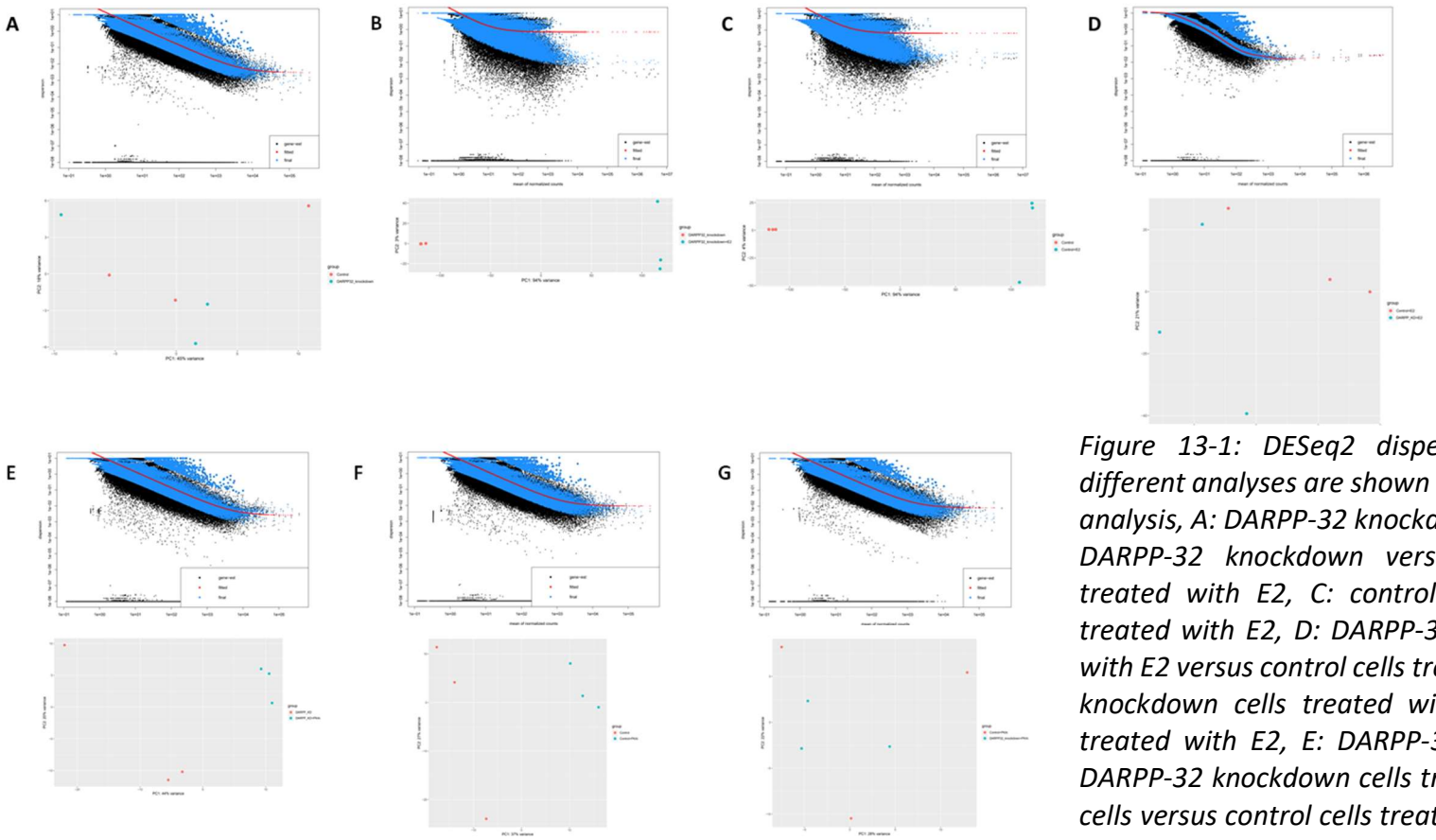


Figure 13-1: DESeq2 dispersion estimates between different analyses are shown above principal component analysis, A: DARPP-32 knockdown versus control cells, B: DARPP-32 knockdown versus DARPP-32 knockdown treated with E2, C: control cells versus control cells treated with E2, D: DARPP-32 knockdown cells treated with E2 versus control cells treated with E2, D: DARPP-32 knockdown cells treated with E2 versus control cells treated with E2, E: DARPP-32 knockdown cells versus DARPP-32 knockdown cells treated with PKAi, F: control cells versus control cells treated with PKAi, G: DARPP-32 knockdown cells treated with PKAi versus control cells treated with PKAi

13.2 Appendix 2

Correlations

			PPP1R1B (p1)	PPP1R1B (p2)	PPP1R1B (p3)	MAPK3 (p1)	MAPK3 (p2)	SIRT1 (p1)	CTNNB1 (p1)	CTNNB1 (p2)	CTNNB1 (p3)	CTNNB1 (p4)	CTNNB1 (p5)	CTNNB1 (p6)	CTNNB1 (p7)	IGF1R (p1)	CDC42 (p1)	CDC42 (p2)	CDC42 (p3)	CDC42 (p4)	TFEB (p1)	YWHAZ (p1)	YWHAZ (p2)	PPP2R5C (p1)	PPP2R5C (p2)	PPP2R5C (p3)	PPP2R5C (p4)	PPP2R4 (p1)	PPP2R4 (p2)	PPP2R4 (p3)	PPP2R4 (p4)
Spearman's rho	PPP1R1B (p1)	Correlation Coefficient	1.000	.390**	.545**	-.096**	-.146**	-.059**	.090**	.095**	-.051*	-.042	-.015	-.030	-.091**	-.148**	.006	.165**	-.032	-.014	.010	.045*	.074**	.061**	.048*	-.013	.025	-.003	-.034	-.010	-.069**
		Sig. (2-tailed)	.	<.001	<.001	<.001	<.001	.009	<.001	<.001	.024	.064	.493	.188	<.001	<.001	.794	<.001	.156	.523	.663	.044	<.001	.007	.032	.567	.266	.893	.136	.650	.003
		N	1980	1980	1980	1980	1980	1980	1980	1980	1980	1980	1980	1980	1980	1980	1980	1980	1980	1980	1980	1980	1980	1980	1980	1980	1980	1980	1980	1980	1980
	PPP1R1B (p2)	Correlation Coefficient	.390**	1.000	.621**	-.156**	-.093**	-.103**	.000	-.001	.063**	-.028	-.040	.010	-.051*	-.125**	-.028	-.067**	-.125**	.010	.001	.105**	.024	.006	.016	.018	.050*	-.017	-.004	.046*	.008
		Sig. (2-tailed)	<.001	.	<.001	<.001	<.001	<.001	1.000	.963	.005	.218	.077	.670	.023	<.001	.209	.003	<.001	.659	.952	<.001	.292	.797	.481	.411	.027	.448	.873	.031	.714
		N	1980	1980	1980	1980	1980	1980	1980	1980	1980	1980	1980	1980	1980	1980	1980	1980	1980	1980	1980	1980	1980	1980	1980	1980	1980	1980	1980	1980	1980
	PPP1R1B (p3)	Correlation Coefficient	.545**	.621**	1.000	-.159**	-.146**	-.079**	.019	.016	.027	-.008	-.009	-.036	-.029	-.221**	-.145**	.004	-.093**	-.030	.041	.041	-.074**	.026	-.002	-.029	.011	-.034	-.008	-.019	-.036
		Sig. (2-tailed)	<.001	<.001	.	<.001	<.001	<.001	.395	.486	.235	.733	.695	.105	.198	<.001	<.001	.875	<.001	.188	.065	.070	<.001	.252	.938	.375	.612	.129	.738	.403	.105

Figure 13-2: Spearman rho correlation between probe level information in the METABRIC patient cohort.

13.3 Appendix 3

A

Variables in the Equation

	B	SE	Wald	df	Sig.	Exp(B)	95.0% CI for Exp(B) Lower	Upper
Age_cat	-.243	.176	1.911	1	.167	.784	.555	1.107
size_cat	.710	.114	38.558	1	<.001	2.034	1.626	2.546
grade	.272	.093	8.533	1	.003	1.313	1.094	1.576
ER status	-.153	.127	1.447	1	.229	.858	.669	1.101
HER2 expression	.468	.127	13.501	1	<.001	1.597	1.244	2.049
PR.Expr	-.315	.115	7.501	1	.006	.729	.582	.914
SIRT1P1_CUT	-.092	.099	.877	1	.349	.912	.752	1.106

B

Variables in the Equation

	B	SE	Wald	df	Sig.	Exp(B)	95.0% CI for Exp(B) Lower	Upper
Age_cat	-.252	.176	2.056	1	.152	.777	.551	1.097
size_cat	.712	.114	38.746	1	<.001	2.039	1.629	2.552
grade	.275	.093	8.703	1	.003	1.317	1.097	1.581
ER status	-.167	.132	1.588	1	.208	.846	.653	1.097
HER2 expression	.471	.128	13.452	1	<.001	1.601	1.245	2.059
PR.Expr	-.324	.116	7.757	1	.005	.724	.576	.909
IGF1RP1_CUT	.015	.111	.017	1	.895	1.015	.817	1.260

C

Variables in the Equation

	B	SE	Wald	df	Sig.	Exp(B)	95.0% CI for Exp(B) Lower	Upper
Age_cat	-.247	.176	1.974	1	.160	.781	.554	1.102
size_cat	.702	.114	37.657	1	<.001	2.017	1.612	2.524
grade	.214	.094	5.126	1	.024	1.238	1.029	1.490
ER status	-.111	.127	.764	1	.382	.895	.697	1.148
HER2 expression	.426	.128	11.112	1	<.001	1.530	1.192	1.965
PR.Expr	-.293	.115	6.504	1	.011	.746	.595	.934
YWHAZP1_CUT	.395	.107	13.620	1	<.001	1.485	1.204	1.831

D

Variables in the Equation

	B	SE	Wald	df	Sig.	Exp(B)	95.0% CI for Exp(B) Lower	Upper
Age_cat	-.254	.176	2.096	1	.148	.775	.550	1.094
size_cat	.708	.114	38.345	1	<.001	2.030	1.623	2.541
grade	.273	.093	8.546	1	.003	1.313	1.094	1.577
ER status	-.154	.127	1.473	1	.225	.857	.668	1.099
HER2 expression	.460	.127	13.026	1	<.001	1.584	1.234	2.033
PR.Expr	-.307	.115	7.088	1	.008	.735	.586	.922
PPP2R5CP1_CAT	-.166	.099	2.792	1	.095	.847	.697	1.029

E

Variables in the Equation

	B	SE	Wald	df	Sig.	Exp(B)	95.0% CI for Exp(B) Lower	Upper
Age_cat	-.252	.176	2.061	1	.151	.777	.551	1.097
size_cat	.711	.114	38.676	1	<.001	2.037	1.628	2.548
grade	.270	.093	8.343	1	.004	1.309	1.091	1.572
ER status	-.152	.128	1.409	1	.235	.859	.669	1.104
HER2 expression	.474	.127	13.817	1	<.001	1.606	1.251	2.061
PR.Expr	-.320	.115	7.750	1	.005	.726	.579	.910
PPP2R5CP2_CAT	.078	.098	.634	1	.426	1.082	.892	1.312

F

Variables in the Equation

	B	SE	Wald	df	Sig.	Exp(B)	95.0% CI for Exp(B) Lower	Upper
Age_cat	-.253	.176	2.065	1	.151	.777	.551	1.096
size_cat	.713	.114	38.833	1	<.001	2.039	1.630	2.552
grade	.272	.093	8.493	1	.004	1.312	1.093	1.575
ER status	-.150	.128	1.377	1	.241	.861	.670	1.106
HER2 expression	.468	.127	13.510	1	<.001	1.596	1.244	2.048
PR.Expr	-.320	.115	7.767	1	.005	.726	.579	.909
PPP2R5CP4_CAT	.089	.098	.825	1	.364	1.093	.902	1.325

G

Variables in the Equation

	B	SE	Wald	df	Sig.	Exp(B)	95.0% CI for Exp(B) Lower	Upper
Age_cat	-.253	.176	2.082	1	.149	.776	.550	1.095
size_cat	.714	.114	39.061	1	<.001	2.043	1.633	2.556
grade	.273	.093	8.597	1	.003	1.314	1.095	1.577
ER status	-.156	.127	1.501	1	.220	.856	.667	1.098
HER2 expression	.471	.127	13.718	1	<.001	1.602	1.248	2.056
PR.Expr	-.322	.115	7.848	1	.005	.724	.578	.908
PPP2R4P3_CUT	.105	.097	1.178	1	.278	1.111	.919	1.342

Figure 13-3: Multivariate survival analysis (cox regression) of genes identified as DARPP-32 partners and prognostic variables, including categorised patient age, tumour size, tumour stage, ER, progesterone receptor (PR) and HER2 receptor status. A: SIRT1 probe 1, B: IGR1R probe 1, C: YWHAZ probe 1, D: PPP2R5C probe 1, E: PPP2R5C probe 2, F: PPP2R5C probe 4, G: PPP2R4 probe 3